CRREL REPORT 90-10

(12)

CRREL

Predicting the Behavior of Asphalt Concrete Pavements in Seasonal Frost Areas Using Nondestructive Techniques

Vincent C. Janoo and Richard L. Berg

November 1990

For conversion of SI metric units to U.S./British customary units of measurement consult ASTM Standard E380, Metric Practice Guide, *published by the American Society for Testing and Materials, 1916 Race St., Philadelphia, Pa. 19103.*

Cover: Falling Weight Deflectometer working in the CRREL Frost Effects Research Facility.

CRREL Report 90-10

U.S. Army Corps of Engineers
Cold Regions Research & Engineering Laboratory

Predicting the Behavior of Asphalt Concrete Pavements in Seasonal Frost Areas Using Nondestructive Techniques

Vincent C. Janoo and Richard L. Berg

November 1990

Prepared for
OFFICE OF THE CHIEF OF ENGINEERS
U.S. DEPARTMENT OF TRANSPORTATION
FEDERAL AVIATION ADMINISTRATION

PREFACE

This report was prepared by Dr. Vincent C. Janoo and Dr. Richard L. Berg, Research Civil Engineers, Civil and Geotechnical Engineering Research Branch, Experimental Engineering Division, U.S. Army Cold Regions Research and Engineering Laboratory. Funding was provided by the Federal Aviation Administration and the U.S. Army Corps of Engineers. The USACE portion was funded through DA Project 4A762784 AT42, *Design, Construction and Operations Technology for Cold Regions;* Mission Area: *Base Support*; Work Unit BS/036, *Improved Pavement Design Criteria in Cold Regions.*

Technical review of the manuscript of this report was provided by E. Chamberlain (CRREL) and L. Irwin (Cornell University). Special thanks to C. Berini, CRREL's FWD operator, for gathering the data.

CONTENTS

ILLUSTRATIONS

Figure

TABLES

Table

Predicting the Behavior of Asphalt Concrete Pavements in Seasonal Frost Areas Using Nondestructive Techniques

VINCENT C. JANOO AND RICHARD L. BERG

INTRODUCTION

Pavements in seasonal frost areas are subject to freezing in the winter and thawing in the spring. In the winter, the pavement structure modulus increases because of ice segregation in the unbound base or subgrade, or both, and because of the influence of temperature on the viscosity of the asphalt. During spring thaw, the pavement foundation can become saturated with water from the thawing ice lenses, thus reducing the structural adequacy of the base or subgrade. With a weakened structure, the pavement can not support the load it was designed for; therefore, one can expect most of the damage to a pavement to occur during the spring thaw period and, to some extent, during the partial winter thaws. The damage to the pavement structure will reveal itself on the surface in the form of fatigue cracking and rutting, owing to deformation in the base or subgrade. The length of time that a pavement structure is subjected to thaw weakening will vary depending on the frost depth, soil type, degree of saturation and drainage conditions.

There are several ways of determining the pavement strength during thaw. Strength can be determined using destructive methods, such as coring and laboratory testing, or using nondestructive testing, such as a Falling Weight Deflectometer (FWD), or existing reduction factors. The reduction factors that are applied in the spring can vary from 50 to 85% of the fall values. Determining pavement strength during thaw periods will then allow the appropriate authorities to impose or remove load restrictions so as to minimize the damage to the pavements. However, using the reduction factors over the entire spring period may be very conservative.

CRREL is developing a nondestructive pavement evaluation procedure for seasonal frost areas using the FWD. One proposed procedure, with some modifications, will be similar to that proposed by the U.S. Army Waterways Experiment Station (WES), which is outlined in Figure 1, with the additional steps or suggested modifications shown as dashed-line boxes. These additional steps include, first, deciding whether or not the three factors essential for frost action to occur are all present (on the left in Fig. 1). These required ingredients are low temperatures, frost-susceptible soils and a nearby source of water. The frost-susceptibility of a soil can either be estimated using Table 1 or can be based upon laboratory frost-susceptibility tests on the soil. Second, during partial winter thaws, and particularly during spring thaw, the subgrade may be considerably weakened for a period of time. Instead of determining a single value of allowable coverages or load, a cumulative damage procedure (on the right in Fig. 1) is proposed that accounts for seasonal variation.

As part of the pavement evaluation process, the moduli of different layers must be determined (Fig. 1). Currently, the Corps of Engineers uses the layered linear elastic theory in the computer program BISDEF for determining layer modulus (back calculation). BISDEF works well when no more than three layers are considered, but during thaw it may be necessary to divide the pavement into six layers (Fig. 2). Rwebangira et al. (1987) found that the back-calculated modulus from BISDEF was sensitive to both the depth of the stiff layer and the layer thicknesses. In seasonal frost areas, as thaw occurs, the depth of the frozen layer (stiff layer) changes with time (changing layer thicknesses). Being able to predict thaw depth is essential in determining thawed layer thicknesses for use in back-calculation procedures. We attempted to estimate the thaw depth with FWD deflection measurements.

We found, however, that FWD deflection measurements during thaw periods were scarce. Therefore, before we tried to modify the back-calculation procedure, we subjected various test sections in CRREL's Frost Effects Research Facility (FERF) to several freeze–thaw cycles. During the thawing period, deflection was measured every day. In this report we present the deflection data and an analysis of the results obtained from the FWD measurements on pavement structures founded on a clay subgrade. In a subsequent report, the results of a comparative study of several back-calculation procedures will be presented.

LITERATURE REVIEW

This section reviews only the thawing period behavior of pavement structures founded on clay subgrades. Using statistical techniques based on Dynaflect data obtained by Scrivner et al. (1969) on pavement structures founded on silty clay and clay loam subgrades,

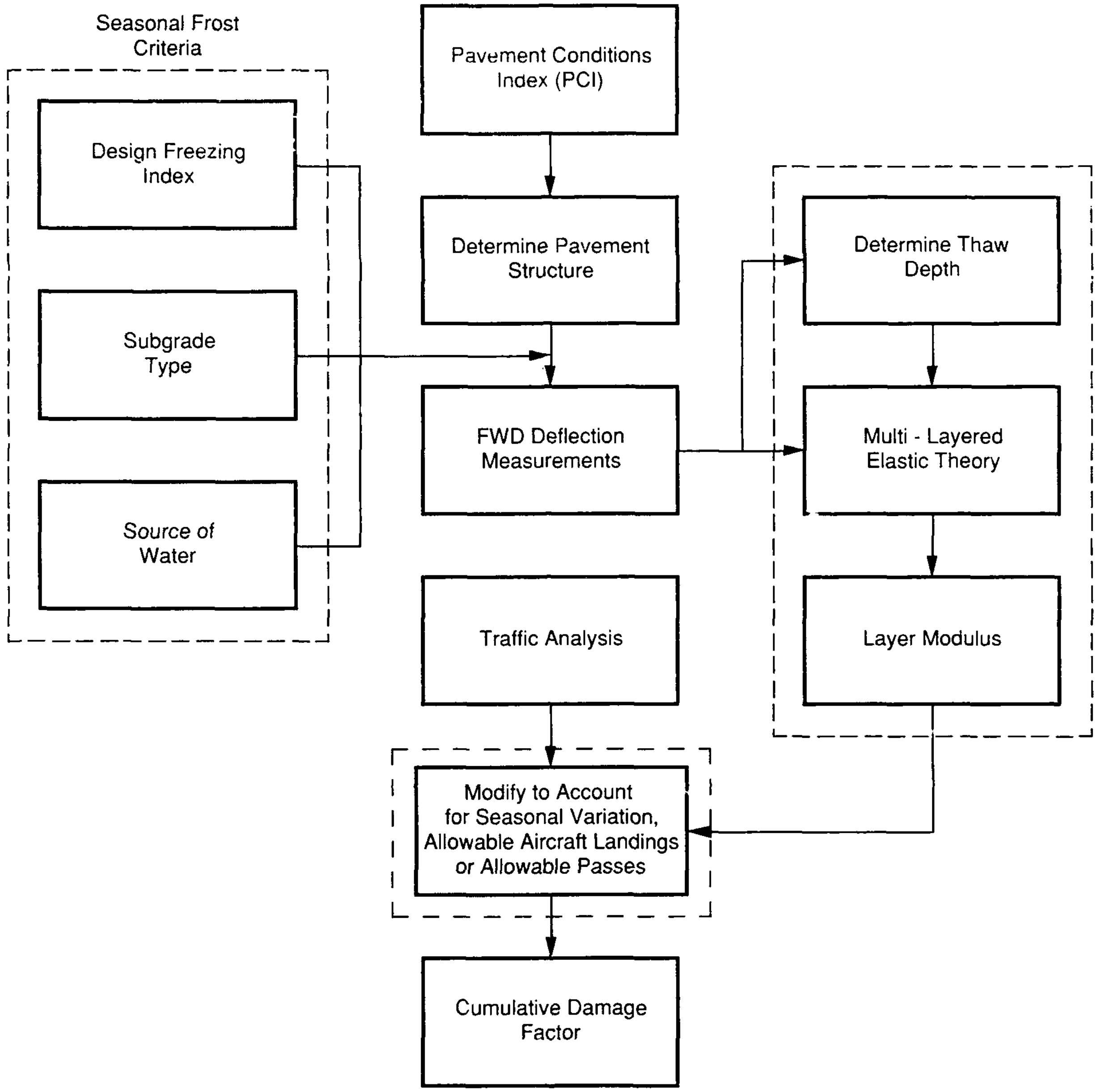

Figure 1. Proposed pavement evaluation procedure in seasonal frost regions. Dashed lines show proposed CRREL modifications to the original WES procedure.

Chamberlain (1981) concluded that the freezing index could not be correlated with the maximum pavement deflection seen during thawing. Chamberlain came to this conclusion because the maximum thaw deflections were nearly the same in areas with freezing indexes of 333°C-days and 1167°C-days. This is shown in Figure 3. Chamberlain also concluded that the recovery time was dependent on the depth of freezing, i.e., the deeper the frost penetration, the slower the recovery.

Nordal (1982) presented Benkelman beam deflection measurements made at the Vormsund Test Road, located 60 km to the northeast of Oslo. A cross section of the test road is shown in Figure 4. The natural subgrade was a lean clay, while the silt subgrade was artificially placed. Deflection measurements were conducted each fall and spring for 6 years (1959–1964).

Nordal's deflection measurements showed that the reduction in bearing capacity was strongly dependent on the type of subgrade soil and the pavement structure. He also found that the length of time that clay subgrades weakened during spring thawing varied from 1.5 to 2 months (Fig. 5). Scrivner et al. (1969), Chamberlain

Table 1. Frost design soil classification.

Frost group		*Kind of soil*	*Percentage finer than 0.02 mm by weight*	*Typical soil types under Unified Soil Classification System*
NFS**	(a)	Gravels Crushed stone Crushed rock	0–1.5	GW, GP
	(b)	Sands	0–3	SW, SP
PFS†	(a)	Gravels Crushed stone Crushed rock	1.5–3	GW, GP
	(b)	Sands	3–10	SW, SP
S1		Gravelly soils	3–6	GW, GP, GW-GM, GP-GM
S2		Sandy soils	3–6	SW, SP, SW-SM, SP-SM
F1		Gravelly soils	6–10	GM, GW-GM, GP-GM
F2	(a)	Gravelly soils	10–20	GM, GW-GM, GP-GM,
	(b)	Sands	6–15	SM, SW-SM, SP-SM
F3	(a)	Gravelly soils	Over 20	GM, GC
	(b)	Sands, except very fine silty sands	Over 15	SM, SC
	(c)	Clays, PI > 12	—	CL, CH
F4	(a)	All silts	—	ML, MH
	(b)	Very fine silty sands	Over 15	SM
	(c)	Clays, PI < 12	—	CL, CL-ML
	(d)	Varved clays and other fine-grained, banded sediments	—	CL, CL-ML CL and ML; CL, ML, and SM; CL, CH, and ML; CL, CH, ML and SM

** Non-frost-susceptible.

† Possibly frost-susceptible, but requires laboratory test to determine frost design soils classification.

(1981) and Berg (1985) found that the critical period ranged from 35 to 60 days for silty and low plasticity clays. Nordal (1982) also reported that, for pavement sections on clay subgrades, the maximum spring thaw deflection correlated well with the freezing index and pavement thickness. The correlation between freezing index and maximum spring thaw deflection is contradictory to Chamberlain's (1981) conclusions. Additional work is required to determine the correlation between freezing index and thaw depth. Nordal's correlations between deflection and both freezing index and pavement thickness are shown in Figure 6.

Berg (1985) reported results from FWD tests conducted on pavement structures founded on a low plasticity clay (CL) subgrade. The test sections (Fig. 7) were subjected to two freeze–thaw cycles. At the end of the first freeze cycle, FWD deflection measurements were taken daily. At the end of the second freeze cycle, besides taking FWD measurements, the researchers trafficked the pavement test sections with a single wheel F15 loading cart (tire pressure = 2.5 Mpa). The

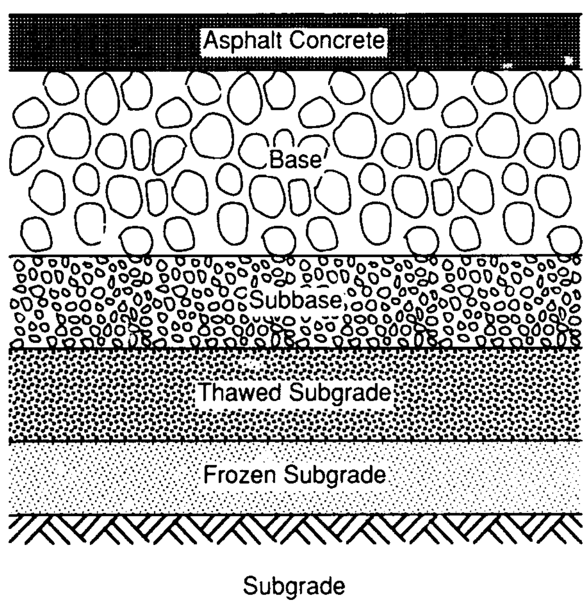

Figure 2. Schematic representation of a partially frozen pavement.

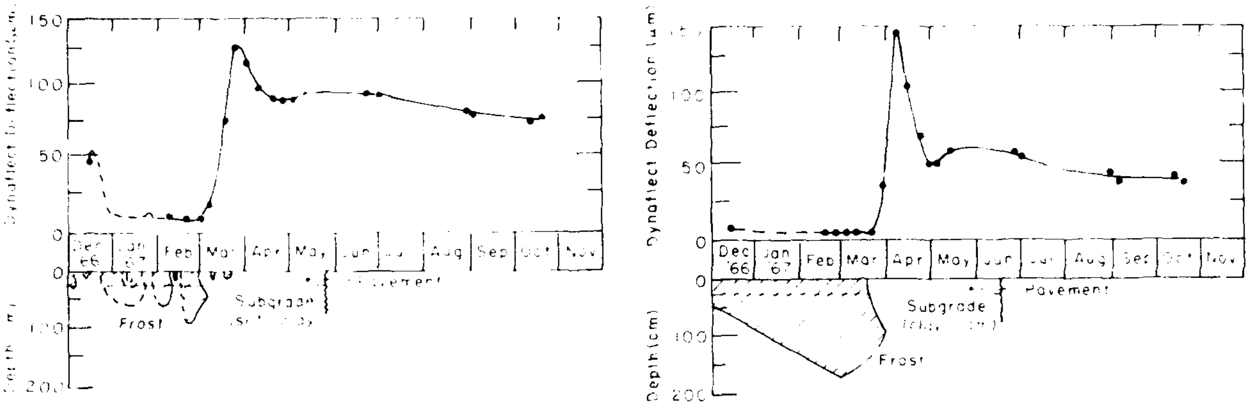

a. 333 °C-days.

b. 1167 °C-days.

Figure 3. Pavement deflection and frost penetration vs time for two freezing indices (after Scrivner et. al 1969).

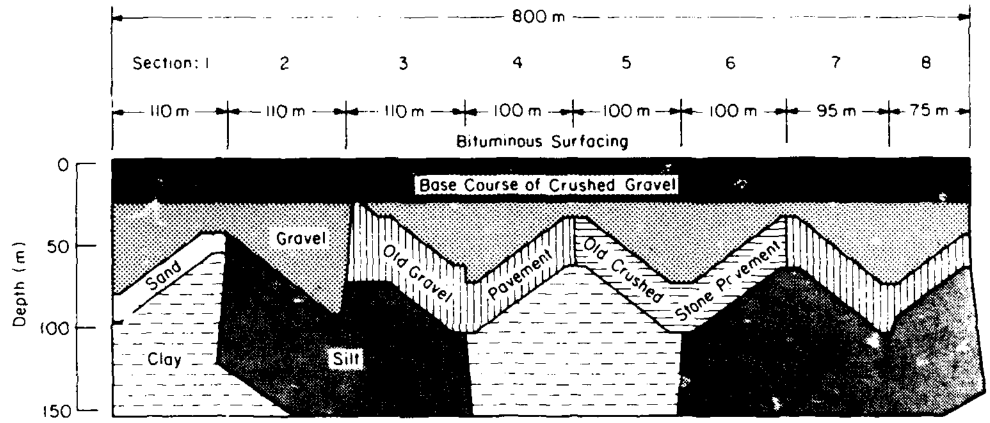

Figure 4. Cross section of the Vormsund test road (after Nordal 1982).

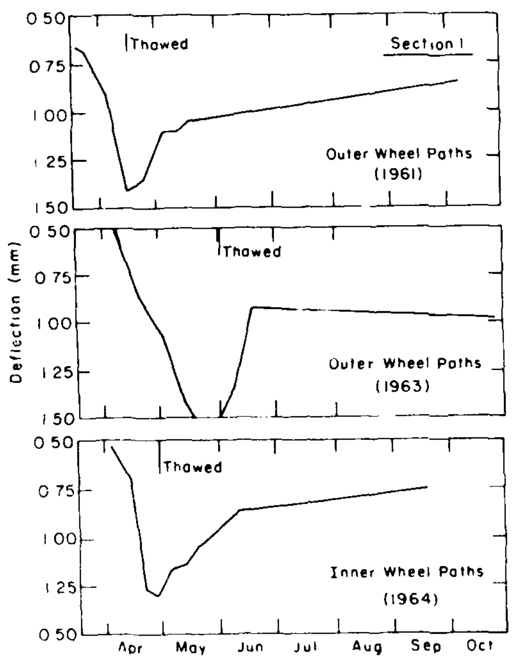

Figure 5. Mean Benkelman beam deflection measurements from 1959 to 1963 (after Nordal 1982).

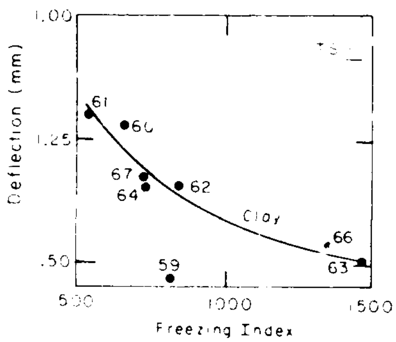

a. As a function of the freezing index

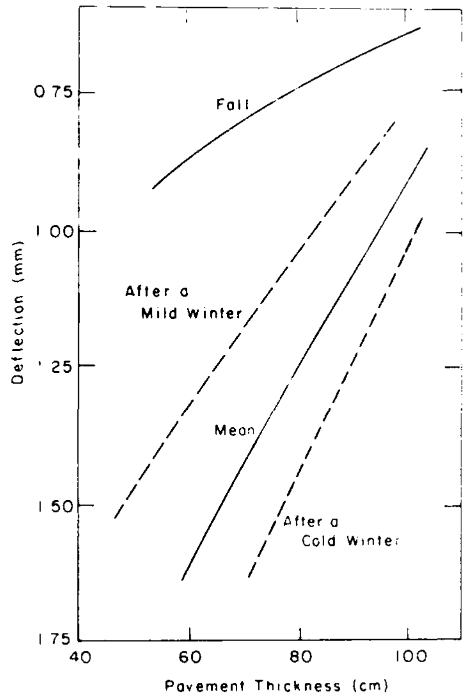

b. As a function of pavement thickness.

Figure 6. Maximum spring deflection (after Nordal 1982).

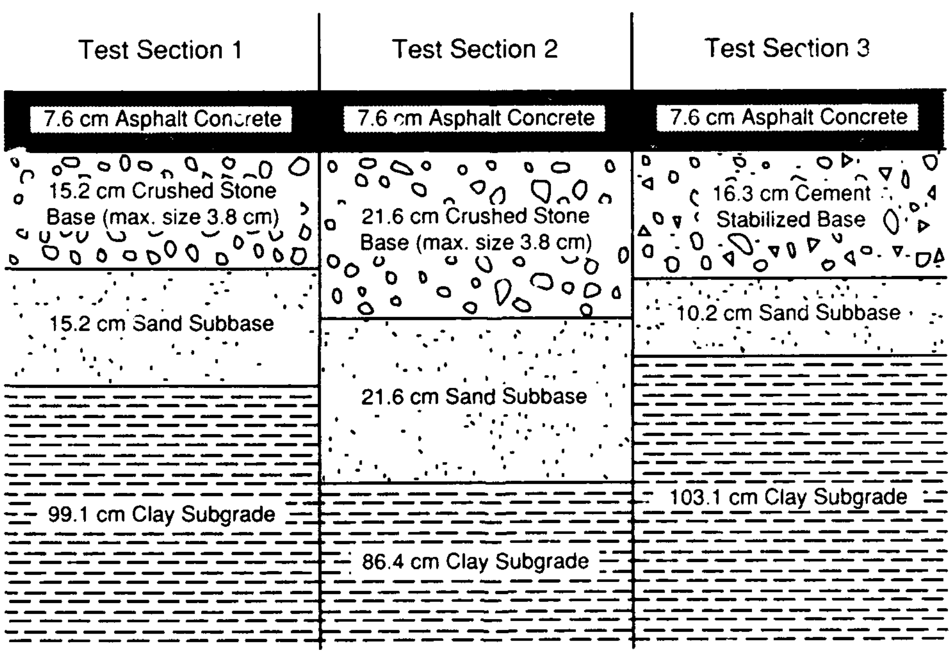

Figure 7. Pavement structure (after Berg 1985).

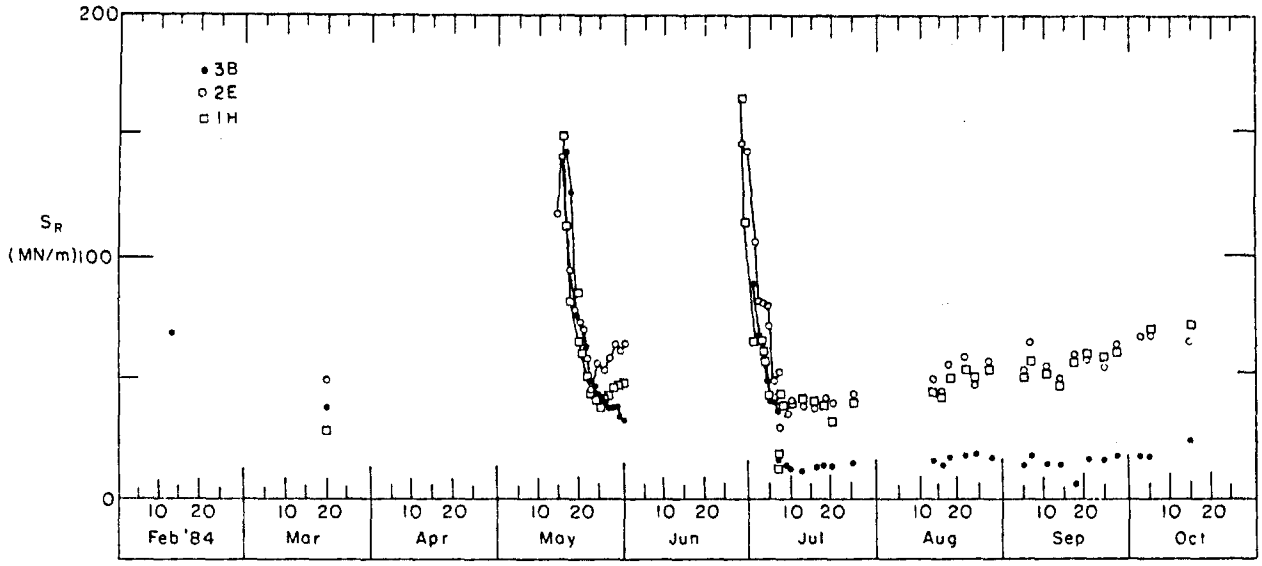

Figure 8. Resilient modulus vs time during thaw of CL subgrade (Berg 1985).

influence of thawing on the clay subgrade is shown in terms of the "resilient stiffness" (applied load/center deflection) in Figure 8. The results suggest that there is a rapid loss of strength when thaw begins; the subgrades in test sections 1 and 2 showed quicker recovery than the one in test section 3. This may be attributable to the frost depth into the clay subgrade in test sections 1 and 2 ranging from only 22.9 to 38.0 cm, whereas in test section 3, it ranged from 73.7 to 78.7 cm. Another possible explanation is that test sections 1 and 2 were constructed with a permeable crushed stone base, whereas test section 3 had a cement-treated base that was only 8.1 cm thick, which was one half of the design requirement (Fig. 7). Similar long recovery periods were reported for clay subgrades by Chamberlain (1981).

To reduce the early deterioration of pavements, many state transportation departments apply a "spring load restriction" to their pavements. Research done in Alaska has shown that the pavement is considered to be the weakest when the thaw depth is between 0.5 to 1 m. The pavement begins to recover its strength when the thaw depth reaches 1.5 m; however, it is difficult to know when this thaw depth is reached and, therefore, when to apply and remove the restriction. Berg (1985) pointed out that our present reduced subgrade strength design procedure based on Frost Area Soil Support Index (FASSI) may be inadequate during the critical thaw period. Depending on the amount of pavement strength required, Berg suggested that consideration be given to reductions of these indices.

In summary, the thaw weakening period is influenced by the subgrade type, depth of frost penetration, number of intermediate thaw periods, pavement thickness, pavement structure and maybe by the freezing index. There are empirical guidelines for determining when the pavement is weakest, but these are usually regionally oriented. The present Corps of Engineers Reduced Subgrade Strength Design for pavements in seasonal frost areas may result in inadequate thickness requirements.

DESCRIPTION OF TEST SECTIONS

Four test sections were constructed in CRREL's Frost Effects Research Facility (FERF). The FERF has an area of 2694 m^2 and incorporates twelve test cells and basins (Fig. 9). All of the test cells and basins are 6.4 m wide. The test basins (TB 9–12) are 11.3 m long and 3.7 m deep and the test cells (TC 1–8) are 7.6 m long and 2.4 m deep. All test cells and test basins have a concrete floor, with the exception of TC 1 and 2. The refrigeration system in the FERF can maintain air temperatures in the building between –4 and 24°C, within a tolerance of ± 3°C. Individual test cells or basins can be cooled using surface freezing panels to a minimum temperature of –38°C and maintained within a tolerance of ± 0.8°C (Eaton 1988).

The four pavement test sections were constructed in three test cells (TC 1, 2 and 3). The test sections were 6.1 × 5.3 m and 1.6 m deep. Test section 1 was extended 1.5 m from TC 1 into the ramp area. Test sections 3 and 4 were designed using the Army Corps of Engineers Reduced Subgrade Strength Method outlined in TM 5-

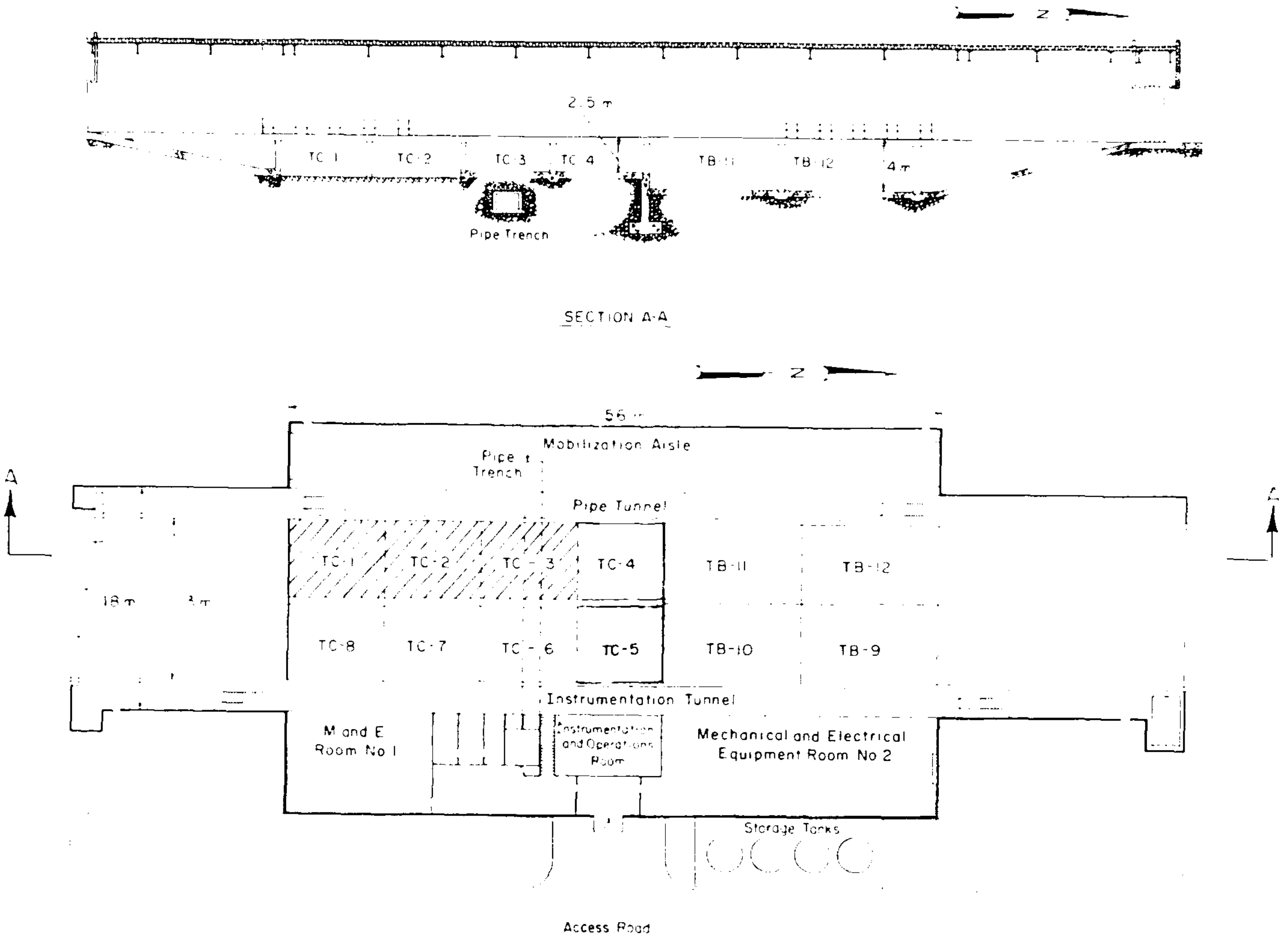

Figure 9. Plan and cross section of CRREL's Frost Effects Research Facility.

818-2 (U.S. Army 1985). This method is used to calculate the total thickness of pavement (including base and subbase) required to accommodate the reduction in bearing capacity of the pavement structure during the frost melting (thaw) period. Test sections 3 and 4 were designed for a Design Index (DI) of 3, which is equivalent to nearly 59,000 passes of an 80-kN Equivalent Single Axle Load (ESAL) over 20 years of pavement life. Based on this performance criterion, the minimum thickness of pavement required was 43.2 cm. As seen in Figure 10, TS 3 consists of a 5.1-cm asphalt concrete pavement on a 17.8-cm base course over a 20.3-cm clean gravel subbase. Test section 4 consists of a 5.1-cm asphalt concrete pavement on a 25.4-cm base course over a 12.7-cm sandy subbase. Test sections 1 and 2 are considered to be full depth asphalt concrete pavements. The thickness design of TS 1 and 2 is based on the following assumptions: the elastic modulus of the asphalt concrete pavement is 2758 MPa and the elastic modulus of the subgrade is 31 MPa. Again, for a de-

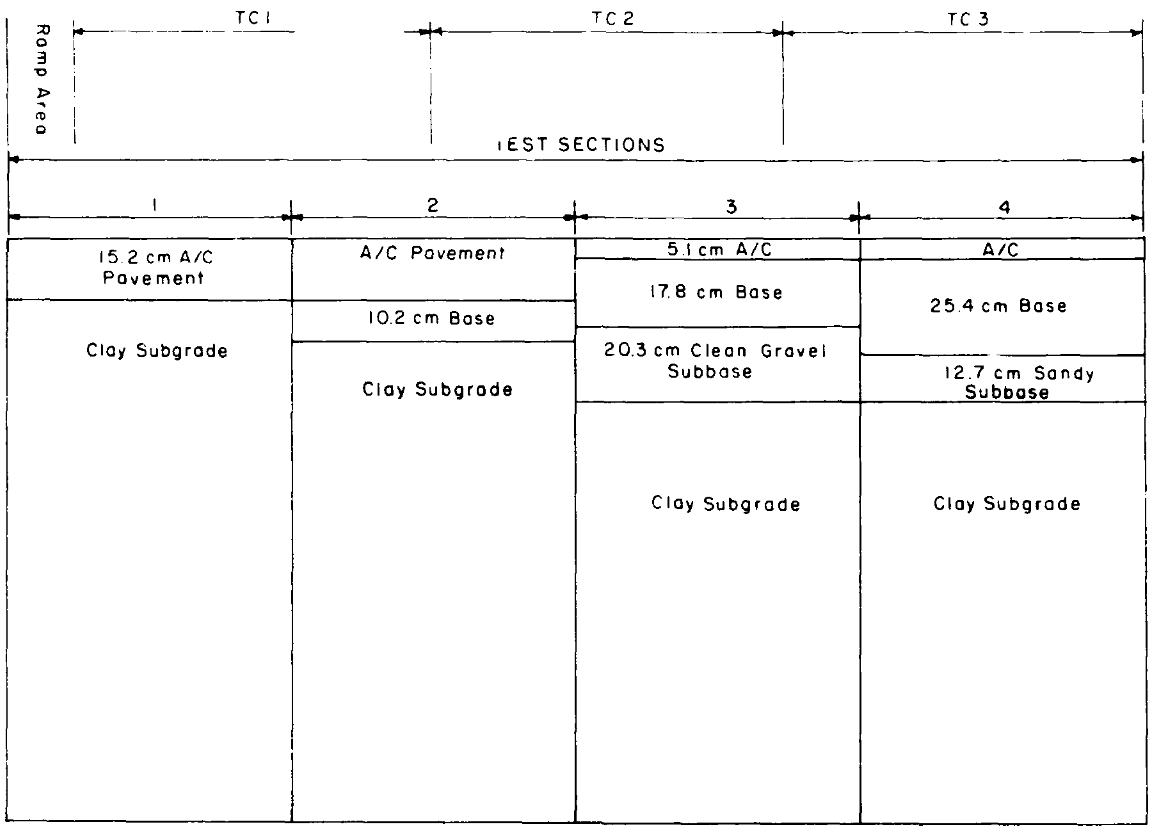

Figure 10. Cross section of test sections.

sign index of 3, the minimum thickness required is 15.2 cm (Brabston et al. 1975). In addition to the 15.2 cm of asphalt concrete pavement in TS 2, the minimum 10.2 cm of free draining base, as required by the Corps of Engineers in seasonal frost areas, was incorporated. A 6.4-mm-thick woven filter fabric was used as a separator between the base course and subgrade in TS 2, 3 and 4.

The grain size distributions for subgrade, base and subbase materials are presented in Figure 11. The subgrade was constructed out of clay obtained near the

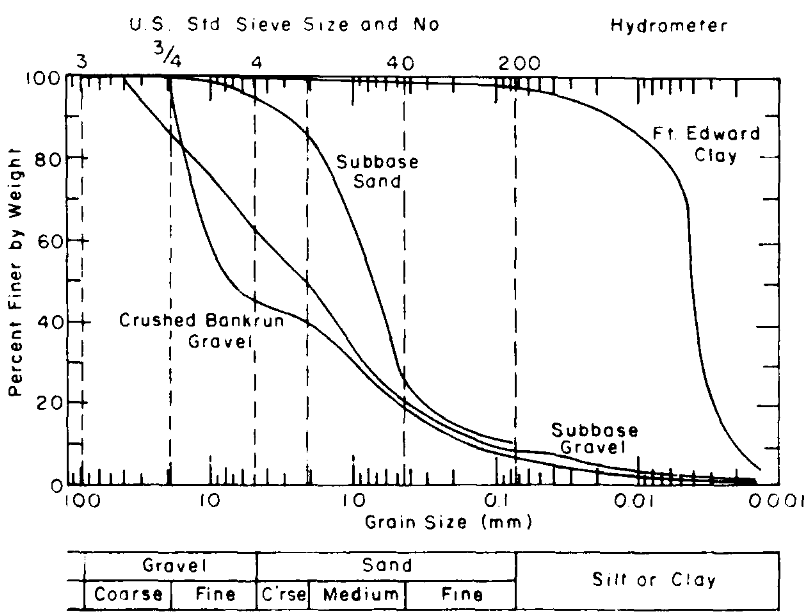

Figure 11. Typical grain size distribution of base, subbase and subgrade material.

Table 2. Properties of Fort Edward clay.

Unified Soil Classification System	CH
Specific Gravity (G_s)	2.79
Liquid Limit (LL)	64
Plastic Limit (PL)	28
Plasticity Index (PI)	36

town of Fort Edward in upstate New York. The in-situ moisture content of the clay was between 38 and 41%. The clay was named Fort Edward clay and classified as an inorganic clay of high plasticity (CH) using the Unified Soil Classification System. The specific gravity of the clay is 2.79, the Liquid Limit (LL) was 64, the Plastic Limit (PL) was 28 and the Plasticity Index (PI) was 36. Based on grain size analysis and Atterberg limits, the clay was classified as a F3 soil with respect to frost-susceptibility. From laboratory frost heave tests, the heave rate was determined to be 0.8 mm/day, which is negligible. The physical properties are presented in Table 2.

Figure 12 shows the compaction and California Bearing Ratio (CBR) test results for the clay. The maximum dry unit weight and optimum water content, based on Corps of Engineers compaction test procedures, are 1.68 g/cm^3 and 21%, respectively, for the CE-55 test procedure and 1.47 g/cm^3 and 27%, respectively, for the CE 12 test procedure.

The clay was delivered to the laboratory at a water content of approximately 40%. We chose the test section density based on the above CE 12 test values. The subgrade was constructed in seven layers, with each layer compacted to the required density using a portable compactor. The thicknesses of the lower four layers ranged from 15 to 17 cm, with the exception of the fifth layer (8 cm), and the upper top three layers ranged from 22 to 27 cm. The overall thickness of the subgrade was 129 cm. We then conducted FWD measurements on the subgrade.

Subgrade material was removed from TS 3 and 4 to bring them to a final thickness of 114 cm and used as a fill in TS 1 and 2, bringing their final subgrade thickness to 142 and 132 cm, respectively, as shown in Figure 10.

The drive cylinder method was used to take a minimum of two density measurements in each test cell for each compacted layer. The variation of density and water content in the test cells is presented in Figures 13 and 14. As can be seen in these figures, the minimum compaction density of 1.47 g/cm^3 was met in the subgrade in most locations, but the water content was higher than required in almost all cases. The clay was compacted at the higher water content because we found it to be difficult to reduce the water content any further by air drying, and winter was setting in. The high densities found were caused by the uncontrolled compaction effort produced by the portable compactor. With respect to Figure 12, the subgrade was compacted to the shaded area shown. Subgrade CBR values ranged from 18 to 27%.

The gradation of the base course used in TS 2, 3 and 4 is shown in Figure 11 as crushed bankrun gravel obtained from a local gravel pit. The specific gravity of the material was 2.8; it had a coefficient of uniformity (C_u) of 47 and a coefficient of curvature (C_c) of 0.5. The amount of material passing the no. 200 sieve was less than 5%. The material is classified as a poorly graded gravel (GP) by the Unified Soil Classification System. The base course was placed in one lift in the three test sections (i.e., 10.2 cm in TS 2, 17.8 cm in TS 3 and 25.4 cm in TS 4) and compacted using a 9070-kg vibratory roller. The material was rolled until no changes in density were seen. Usually, ten passes of the roller compacted the material.

Density measurements were taken using the sand cone method. CBR tests were conducted on the base course; however, the results were low and were considered invalid as there was no correspondence to the field densities measured.

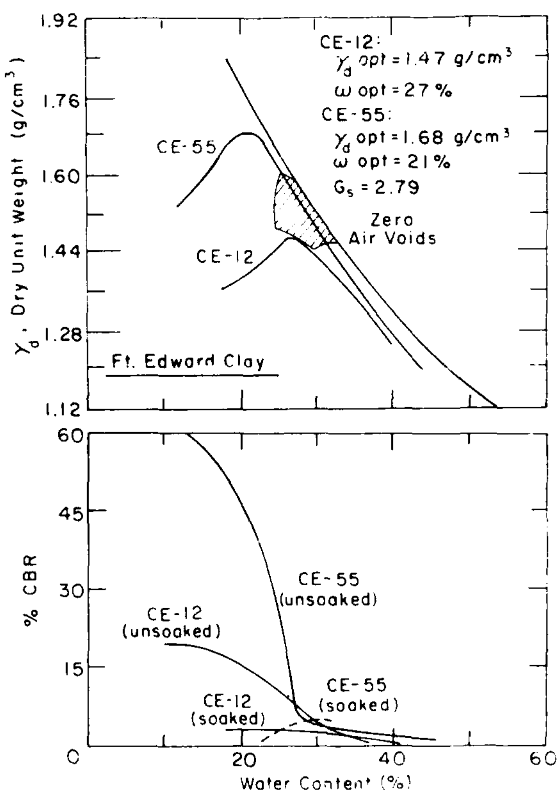

Figure 12. Dry unit weight and CBR vs moisture content (w) for Fort Edward clay (G_s = specific gravity).

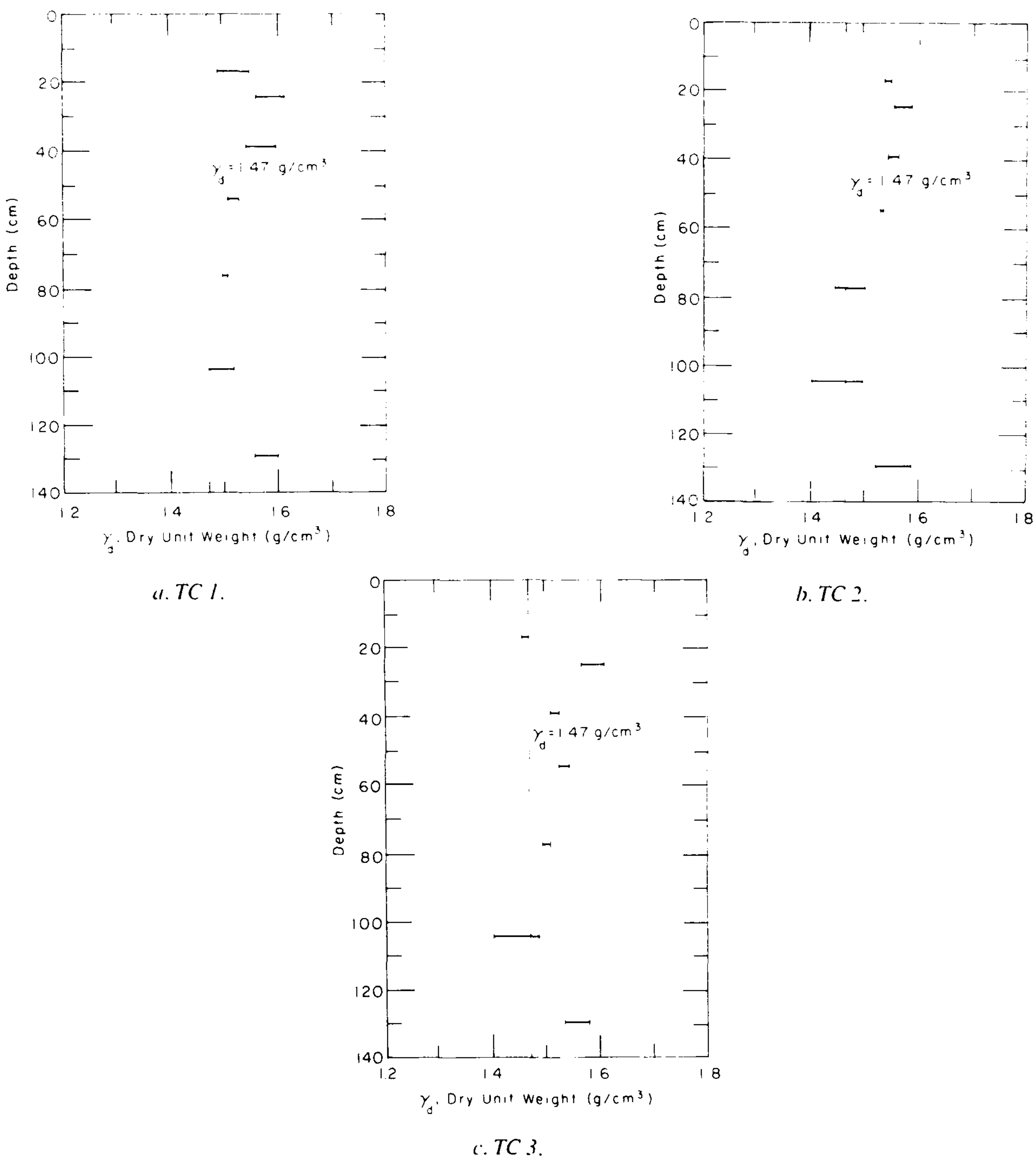

Figure 13. Variation in dry unit weight with depth.

Two subbase materials were used in TS 3 and 4. In TS 3, the subbase had a specific gravity of 2.8, a coefficient of uniformity (C_u) of 30.5 and a coefficient of curvature (C_c) of 1.2. The material had more than 50% passing the no. 4 sieve and 7% passing the no. 200 sieve. The material is classified as a well-graded sand (SW) using the Unified Soil Classification System. However, our examinations of the material led us to classify it as a poorly graded gravel (GP). The gradation for this material is shown in Figure 11 as subbase gravel. In TS 4, the subbase material had a specific gravity of 2.8, a coefficient of uniformity (C_u) of 9 and a coefficient of curvature (C_c) of 2.8. The material had more than 90% passing the no. 4 sieve and 8% passing the no. 200 sieve. This soil is also classified as a well-graded sand (SW) using the Unified Soil Classification

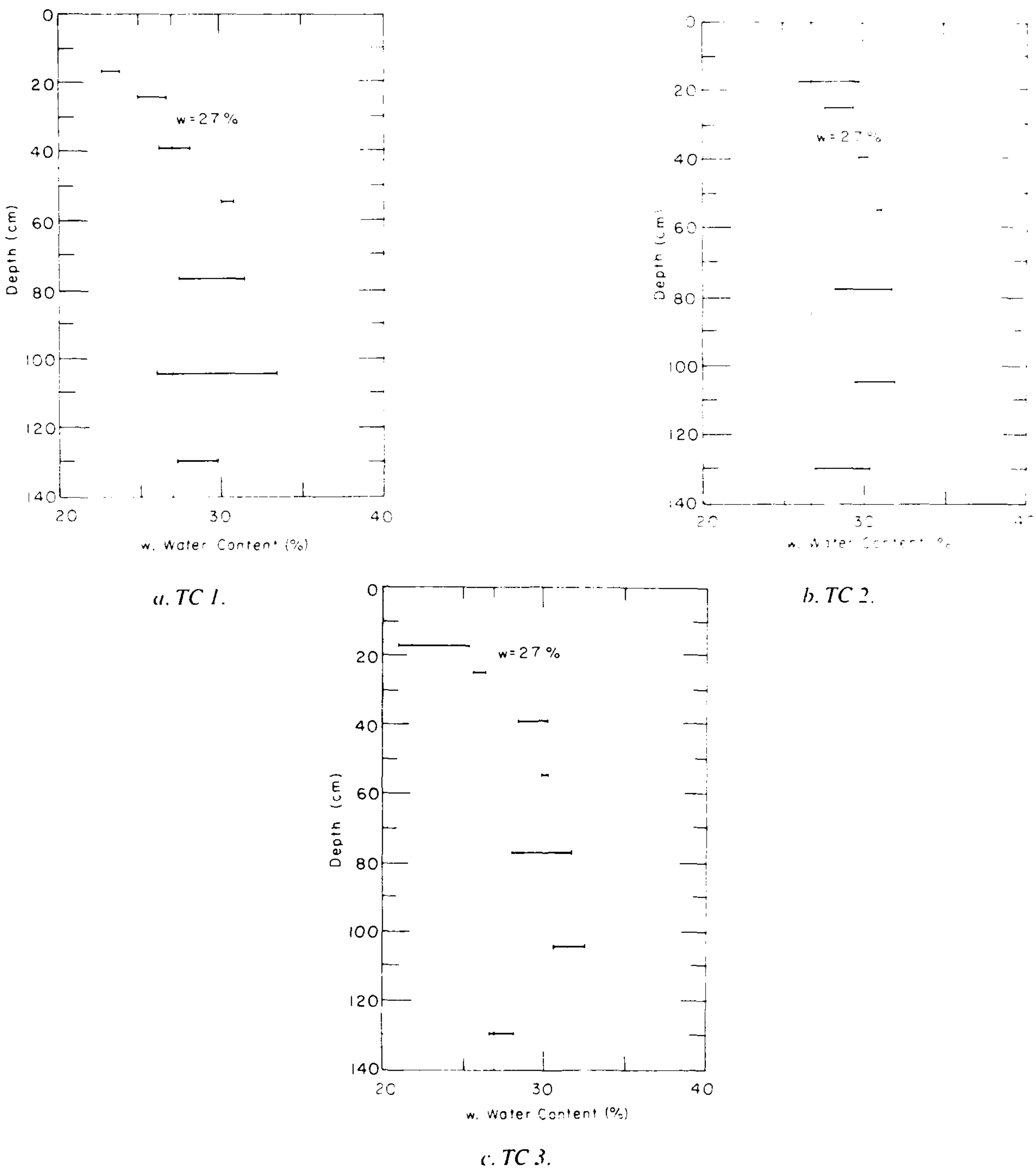

Figure 14. Variation of water content with depth.

System. The gradation of this material is shown in Figure 11 as subbase sand.

Even though both subbase materials are classified as SW, a visual inspection of the gradation curves suggests that the permeability characteristics will be different. The subbase material was placed in a single lift and compacted with one pass of the 9070-kg vibratory roller. We did not measured field densities and water content of the subbase. The subbase is assumed to be compacted at its natural water content of 3.0% in TS 3 and 4.4% in TS 4. A geotextile fabric was placed as a separator between the clay subgrade and the pavement structure in TS 2, 3 and 4. The separator was used to eliminate the migration of clay particles into the subbase or base during compaction and trafficking.

In TS 1 and 2, 15.3-cm Asphalt Concrete (AC)

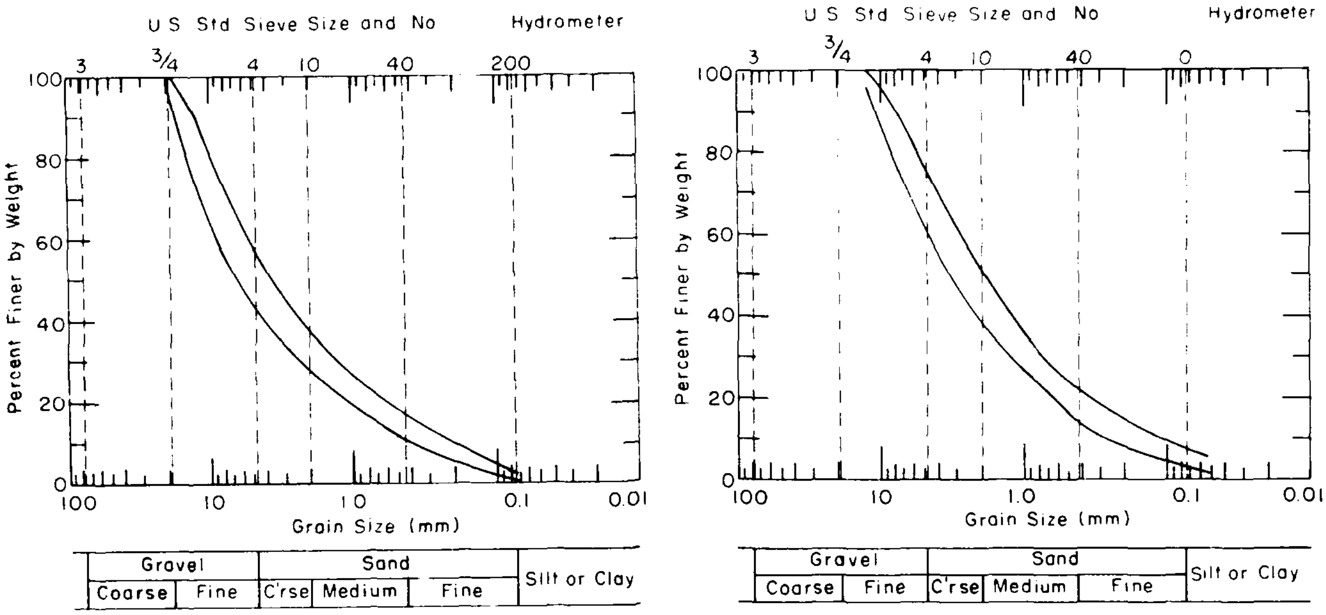

a. Type B base course. *b. Type E wearing course.*

Figure 15. New Hampshire State specifications for the gradation of the AC pavement sections.

pavement sections were constructed. The AC layer consisted of 10.2 cm of black base and 5.1 cm of wearing course. The mix design was provided by the contractor and was based on current New Hampshire state specifications for AC mixtures (the base course is designated as Type B and the wearing course as Type E). The gradation curves for the base and surface course are presented in Figure 15. The liquid asphalt used was an AC 20 (absolute viscosity at 60°C of 206.5 Pa s; kinematic viscosity at 135°C of 400×10^{-6} m^2/s; penetration at 25°C of 0.8 mm; PVN = –0.44); the desired asphalt content for the base course was 5.25% and for the wearing course 6.4%. The base course was laid in 5.1-cm lifts and the wearing course in 2.5-cm lifts. Both the base and wearing courses were compacted with a 2721-kg static roller. In TS 3 and 4, the AC layer was 5.1 cm thick and was laid in two lifts of 2.54-cm thickness and met all the specifications for the New Hampshire Type E wearing course. No density measurements were taken and compaction control was based on the number of passes of the roller.

INSTRUMENTATION

The test sections were instrumented with thermocouples, resistivity gauges and psychrometers; the location of these gauges is shown in Figure 16. The locations of the thermocouples and resistivity gauges in the four test sections are tabulated in Appendix A.

Temperature measurements were made with copper–constantan thermocouples that were placed 15.2 cm apart in the clay subgrade. In the subbase, base and AC, they were placed every 5.1 cm. There were some exceptions to this spacing, as shown in Figure 16. The thermocouples were attached to a Kaye data acquisition system and temperature measurements were taken hourly every day. The data were then transferred via modem and stored on a Prime 9750 minicomputer for further manipulation.

Determining frost penetration using temperature measurements has two disadvantages. First, impurities in the soil–water system tend to depress the freezing point below 0°C. Second, during spring thaw, subsurface temperatures can become nearly isothermal at 0°C. It has been found that water containing small quantities of impurities, such as groundwater, has a volumetric resistivity of approximately 20 kΩ. Frozen groundwater has a volumetric resistivity of 100 kΩ to several megaohms.

With the above in mind, sensors to measure the resistivity of soils during freezing and thawing were developed at CRREL. A detailed description of the sensor and results of performance tests are provided by Atkins (1979). Briefly, the system consisted of a 1.9-cm-diameter wooden dowel approximately 122 cm in length, with 4.0-mm holes drilled through it at 5.1-cm intervals. A bare, solid strand 12-gauge copper wire was

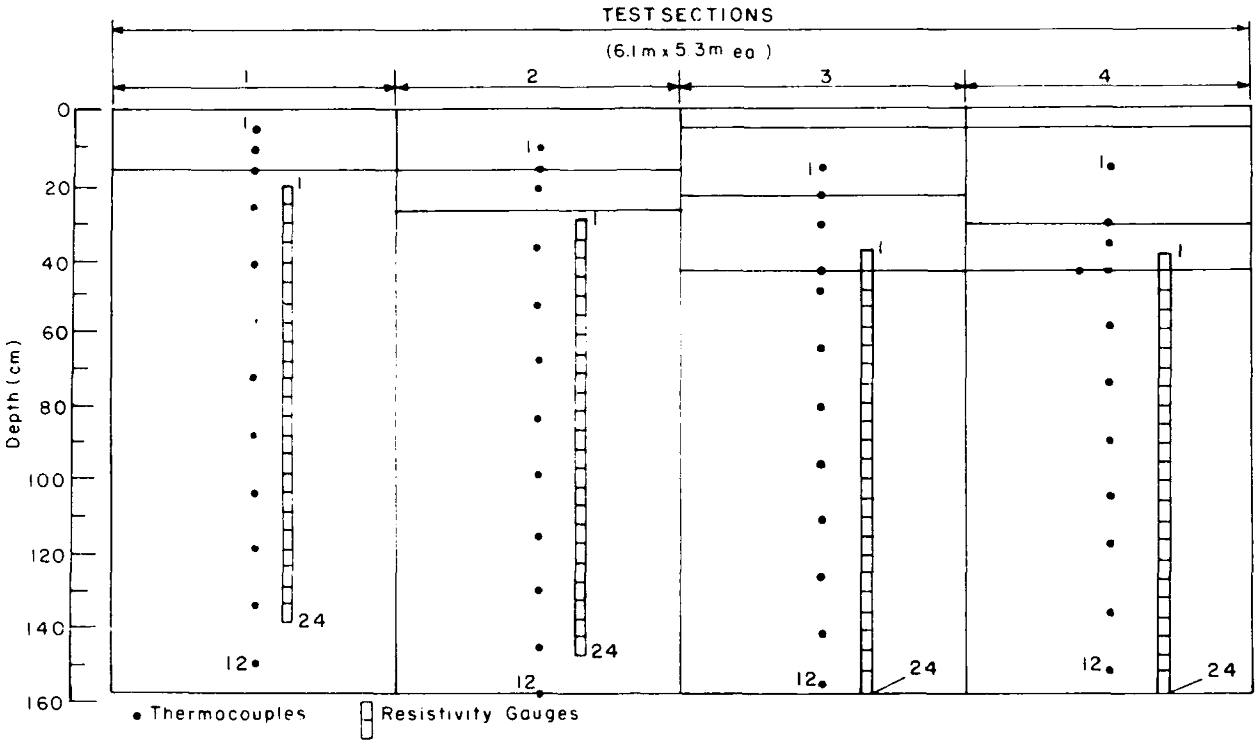

Figure 16. Location of sensors in test sections.

placed through each hole, wrapped tightly around half the circumference and soldered to itself. The wire leading to the 4.0-mm hole was insulated. A schematic of the resistivity probe is shown in Figure 17. The wooden dowel and sensors were then placed in a 7.6-cm-diameter hole to the various depths shown in Figure 16. The holes were then backfilled and compacted in the 15.2-cm lift, with a wooden dowel used as a compactor.

To prevent groundwater polarization, an alternating current source at a frequency of 60 Hz was used. Instead of measuring the actual resistance, the voltage drop across the unknown soil resistance was compared to the voltage drop across a resistor of known value placed in series with it. No absolute resistance measurement is required as the shape of the resistance curve with depth is used to determine frost penetration depths (Atkins 1979). Measurements were taken every 4 hours, every day, and were stored on magnetic tape. They were eventually transferred to the Prime 9750 minicomputer for storage and further manipulation.

Peltier thermocouple psychrometers were the third set of sensors used. A detailed description of these sensors can be found in a paper by Brown and Bartos (1982). Briefly, the thermocouple consists of chromel–constantan wire welded together to form a sensing junction. The sensing junction and reference junctions (copper–chromel and copper–constantan) form the main part of the thermocouple. A 5-mA current is passed through the psychrometer circuit from the constantan to the chromel side for about 30 seconds. The current causes the sensing junction to cool slightly below ambient temperature. If the thermocouple is cooled below

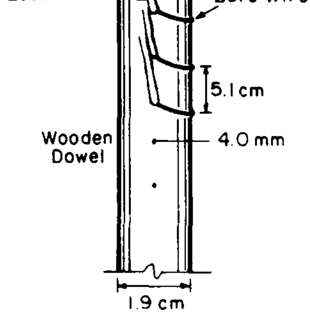

Figure 17. Schematic of resistivity probe.

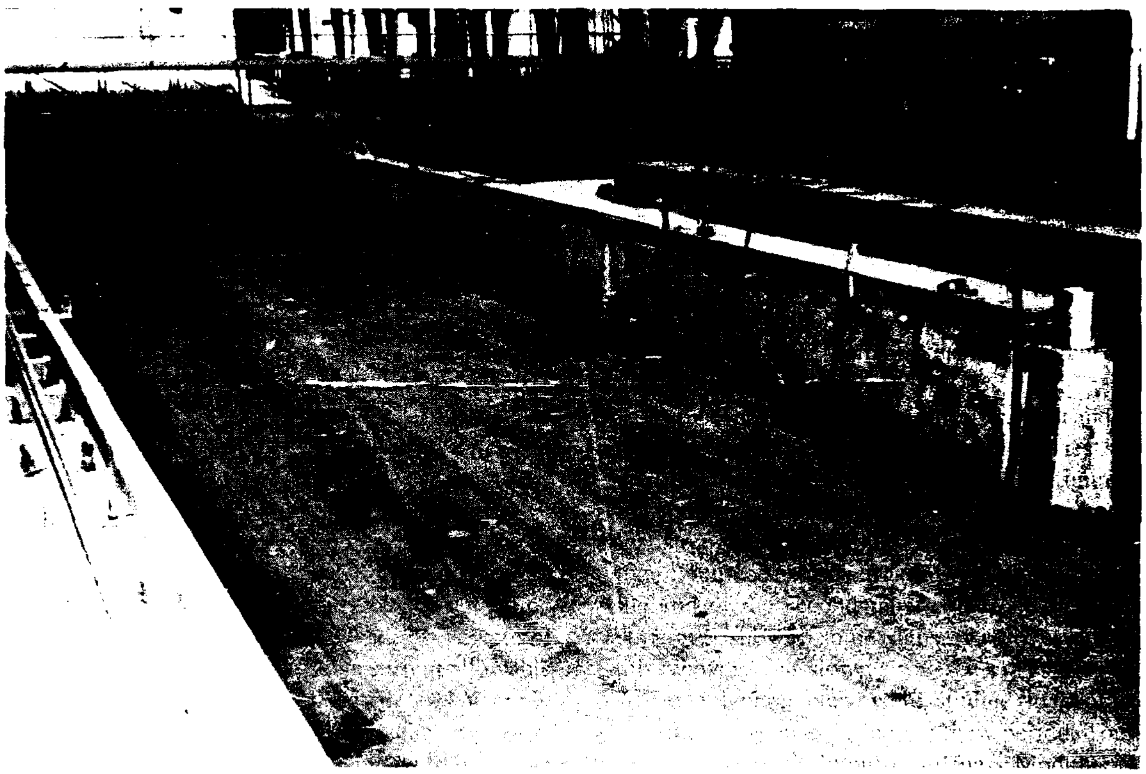

Figure 18. Completed test sections prior to freezing.

the dew-point of the atmosphere surrounding it, water vapor in the air will condense on the sensing junction. After the current is terminated, the condensed water on the junction will evaporate back into the atmosphere. The cooling of the junction by evaporation is a function of the vapor pressure of the atmosphere surrounding the thermocouple. This vapor pressure is the moisture tension on the soil water. The minimum temperature at which the sensors can be used is 0°C.

These sensors were placed horizontally in the clay subgrade at different heights as shown in Figure 16. The sensors were used to determine the feasibility of measuring the moisture tension (negative pore pressure) in the clay subgrade during thawing. Measurements were taken randomly during freezing and thawing until no changes in readings were seen.

The completed test section prior to freezing is shown in Figure 18.

TESTING PROGRAM

After we prepared the subgrade, we measured the deflection of the clay subgrade with the Dynatest 8000 Falling Weight Deflectometer (FWD). At the end of paving, the test sections were subjected to five freeze–thaw cycles. Traffic was applied during the third and fifth thaw cycle. The analysis presented here is primarily concerned with the first two freeze–thaw cycles.

The test sections were frozen from the top down by placing cooling panels on the surface of the pavements (Fig. 19). Freezing of the test sections was begun around mid-March 1987. The temperature profiles in the four test sections during the first and second freeze–thaw cycle are presented in Figure 20. The temperature measurements were taken at a single point and we assumed them to be representative throughout the respective test sections. The freezing rates for the test sections were not controlled. Freezing was stopped when the frost penetration reached the target depths—122 cm for the first cycle and 152.4 cm for the second cycle. The freezing rate in the clay subgrade was found to be around 16.5 mm/day during the first freeze cycle and around 25.4 mm/day during the second freeze cycle. Berg (1985) reported that frost penetration in the field was in the range of 6.35 to 25.4 mm/day. The test sections were thawed by removing the cooling panels and heating the pavement sections with the FERF air. Deflection measurements were taken once a day, around 1000 hours, during the thaw periods.

Resistivity measurements were taken during the freeze and thaw cycles. Figure 21 illustrates the change

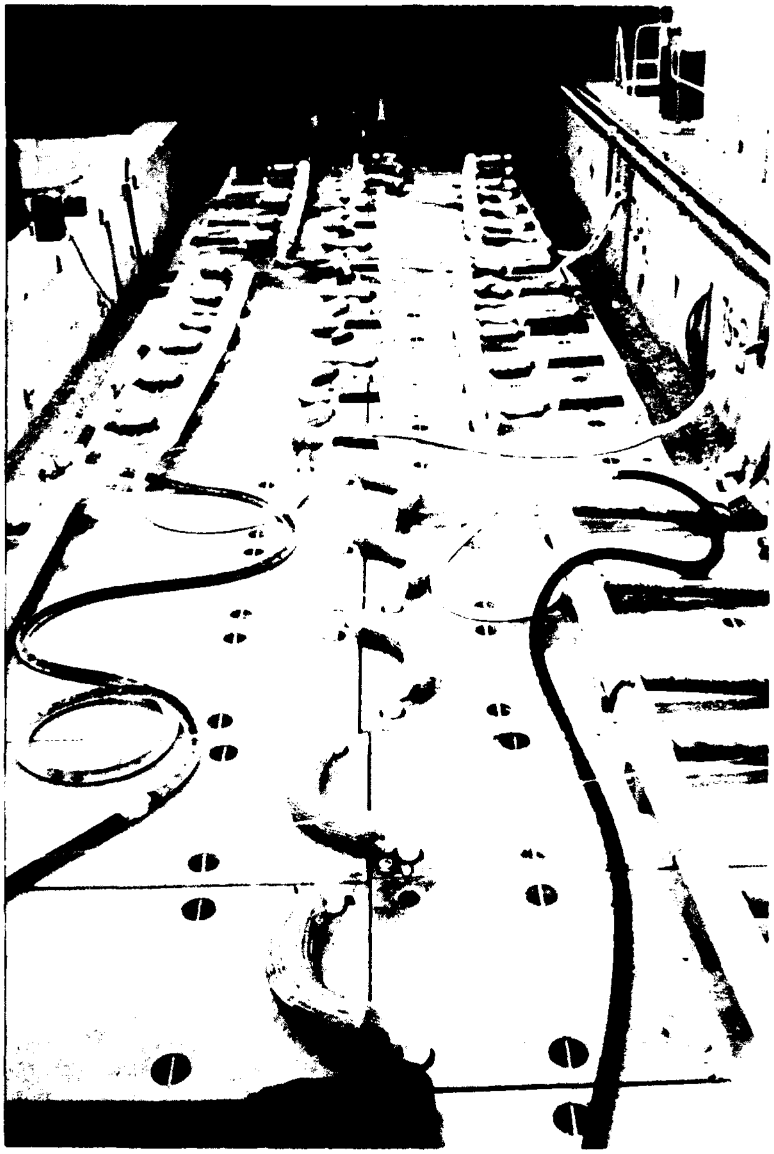

Figure 19. Freezing of test sections.

in resistance with temperature in TS 2. Major changes in resistance are apparent around 0°C. This was typical in all sections. The change in resistance close to 0°C during freezing and thawing is clearly shown in Figure 22. Figures 22a and b show that there is a large change in resistance between 0 and –4°C. This suggests that the phase change from water to ice in the clay subgrade is not instantaneous, but takes place over a 4°C range. Figures 22c and d show that thawing occurs when the temperature in the clay subgrade is slightly below 0°C. The resistance starts to level out when the temperature in the subgrade reaches 2°C. For determining freeze or thaw depths based on the above data, we assumed that freezing and thawing begins at 0°C.

The data obtained from the Peltier thermocouple psychrometers were not evaluated for this report. These data will be evaluated later.

Analysis of FWD deflection data

Deflection measurements were taken with the Dynatest 8000 FWD once a day at four locations per test section (Fig. 23). Four load levels were used during the thaw cycles. The first was in the 27-kN range. The second was in the 40-kN range, one half of an 18-kip single axle load. The third and fourth load levels (50 kN and 67 kN respectively) were used to obtain additional data. At each location, each of the four load levels was applied twice and the corresponding deflection measurements were recorded. Therefore, at each test section we had eight sets of readings for each load level.

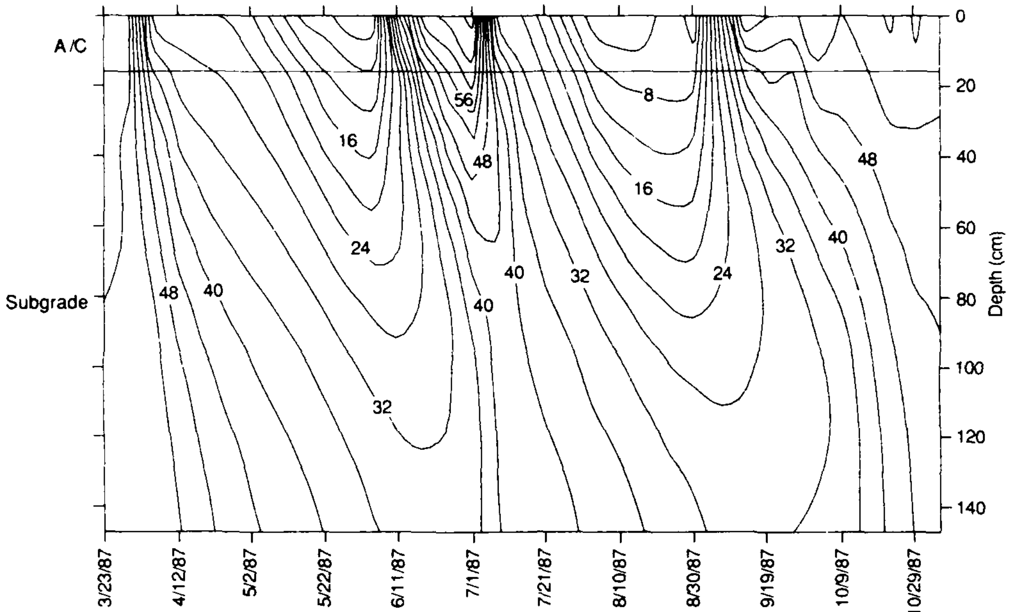

a. TS 1.

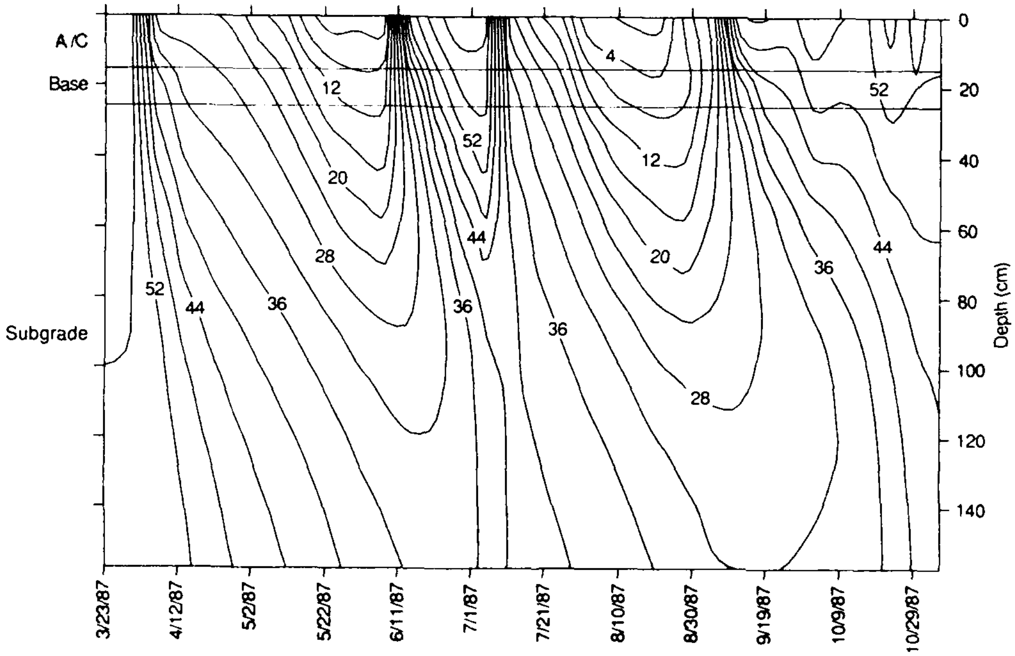

b. TS 2.

Figure 20. Temperature profile during first and second freeze–thaw cycles.

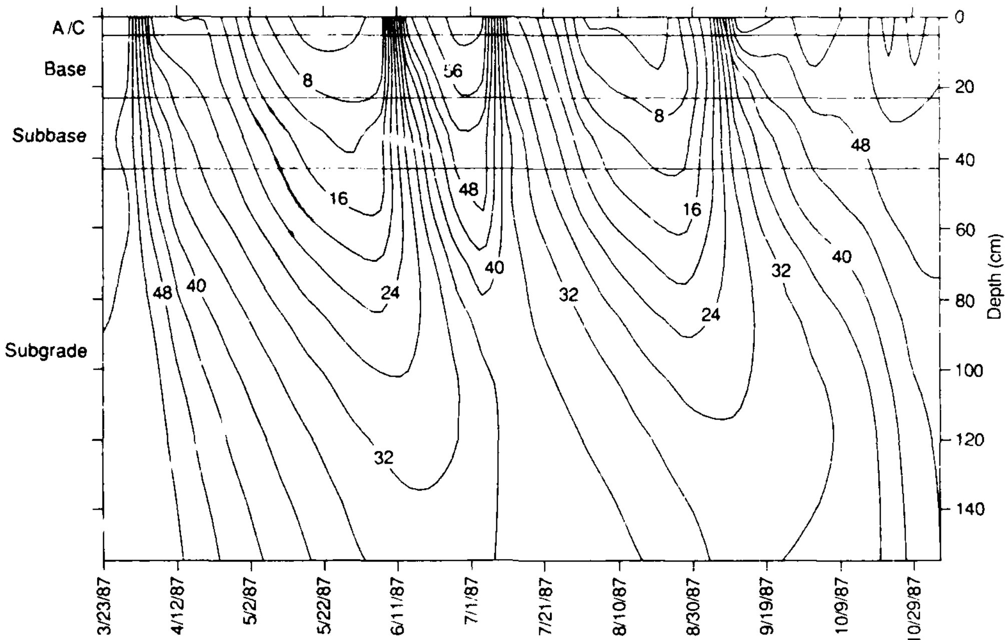

c. TS 3.

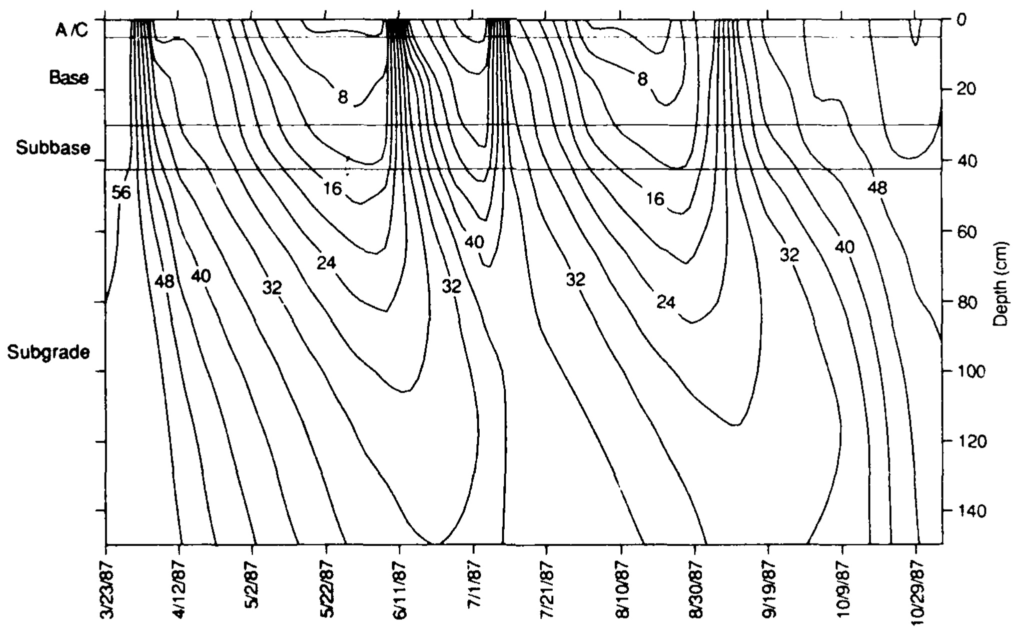

d. TS 4.

Figure 20 (cont'd).

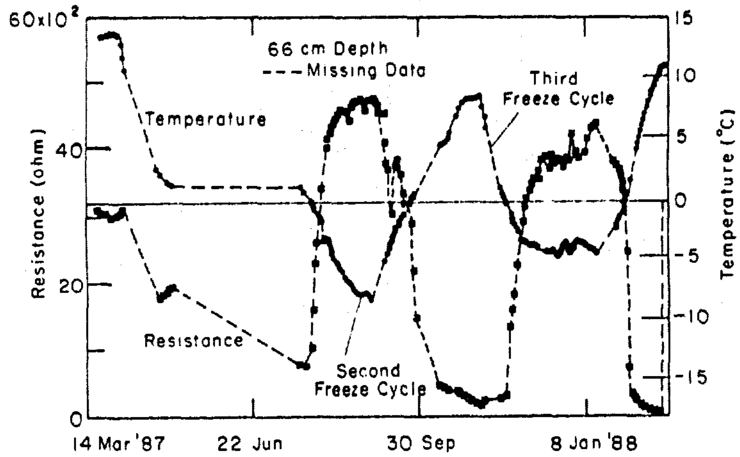

Figure 21. Change in resistance with change in temperature.

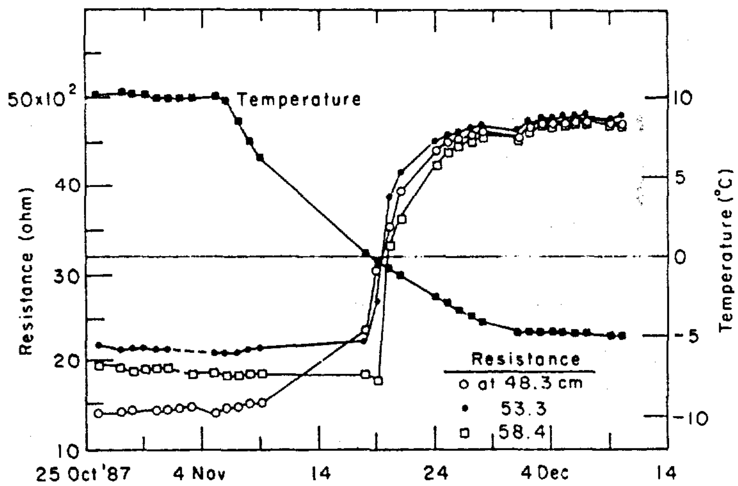

a. Freezing at 56-cm depth in TS 1.

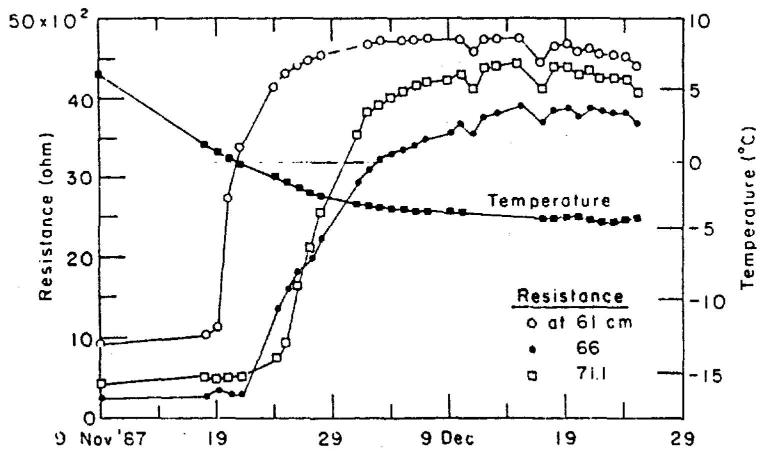

b. Freezing at 66-cm depth in TS 2.

Figure 22. Determination of temperature at two depths in two test sections.

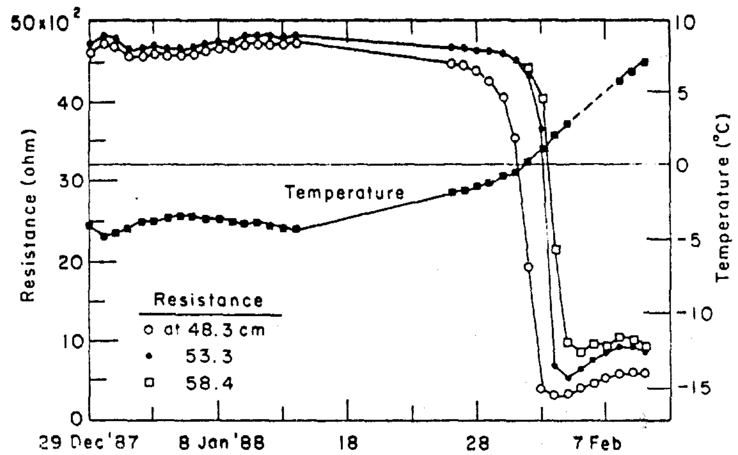

c. Thawing at 56-cm depth in TS 1.

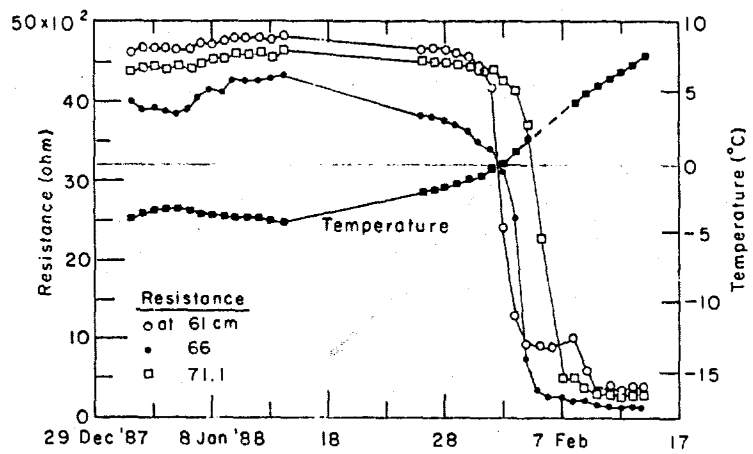

d. Thawing at 66-cm depth in TS 2.

Figure 22 (cont'd).

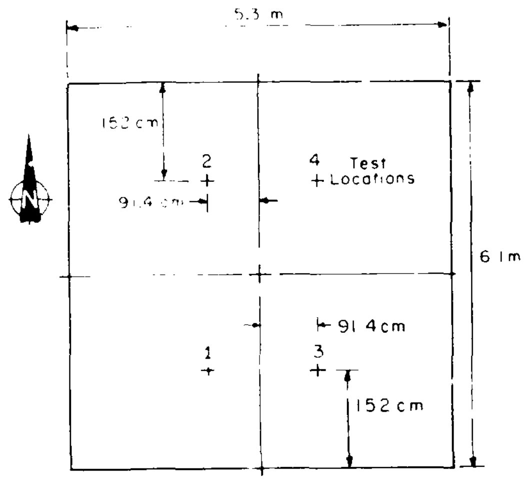

Figure 23. Typical FWD location points in test sections.

A seating load of 27 kN was applied prior to testing. The loading plate was not raised between readings or between the first and second set of measurements. Throughout the first and second thaw cycles, the deflection measurements were taken at the same four locations shown in Figure 23. Deflection measurements were not taken during the freezing cycle. The pavement thaw was induced by changes in the ambient building temperature; the ambient building temperature during the two thaw cycles is shown in Figure 24. During the first cycle, the air temperature in the FERF ranged from 15 to 36°C and, during the second thaw cycle, it ranged from 4 to 19°C. The corresponding thaw depths (located by 0°C isotherm) during the thaw cycles in all test sections are presented in Figure 25. The average thaw rate during the first thaw cycle (12 June–12 October) was 2.7 cm/day. We emphasize that the deflections measured during the first and second thaw periods were attributable only to changing temperature conditions. Traffic, however, was applied during the third and subsequent thaw periods and the results will be reported later.

A small number of FWD measurements were made on the clay subgrade prior to placement of the base–subbase and asphalt layers. The depth of the clay subgrade was 130 cm. The FWD loading plate was 45 cm in diameter, and the sensors were located at distances of 0, 27.5, 40, 70, 110, 150 and 245 cm away from the center of the loading plate. The load level used ranged from 20 to 67 kN. The FWD measurements on the subgrade are presented in Appendix B.

The load and center and second sensor (at 27.5 cm) deflections are shown in Figure 26, which reveals that the center deflections are very variable and, in many cases, exceeded the 2-mm accuracy of the geophones. The average deflection basins from a 40-kN load are shown in Figure 27. For all practical purposes, the subgrade response is considered to be the same.

A representative deflection basin was used to characterize the structural change in the pavements during the thaw periods. This representative basin was selected with the program BASIN developed at the U.S. Army Waterways Experiment Station (WES). The program averages the deflections for a given load (in our case four deflection basins at each load level, as only the second set of deflections from each location was used) and calculates the area of the averaged deflection basin. It then compares the deflection measurements at each location with the averaged values and chooses, as the representative basin, the input deflection basin that is closest to the averaged basin and area. We used BASIN

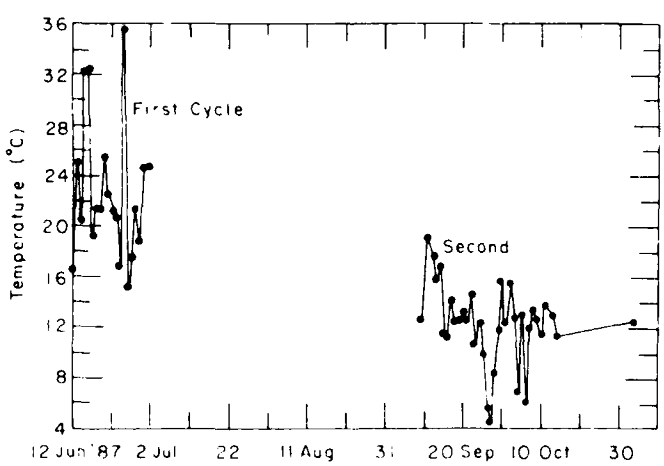

Figure 24. Ambient building temperature during thaw cycles.

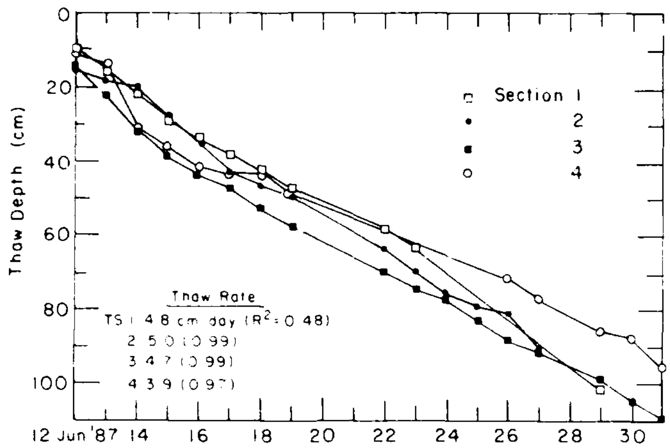

a. During first thaw cycle.

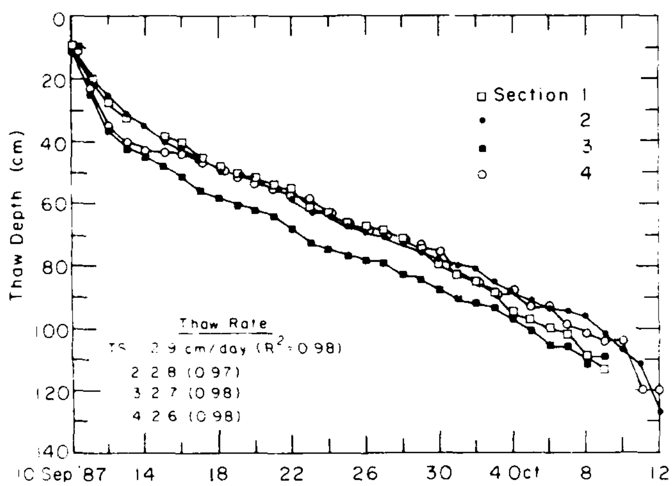

b. During second thaw cycle.

Figure 25. Location of thaw depth.

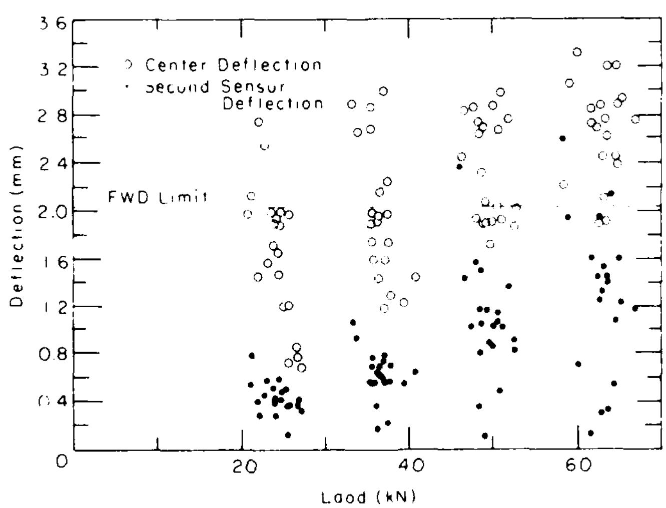

Figure 26. Variation of center and second sensor deflections with applied FWD loads.

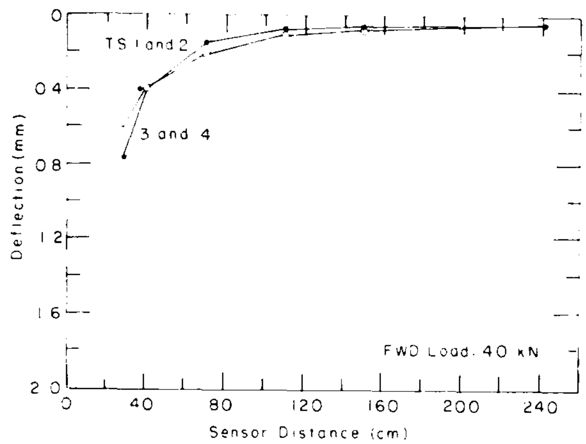

Figure 27. Mean surface deflection (clay subgrade).

to obtain representative 40- and 50-kN load deflection basins for further analysis. These load levels were of interest to us because one represents current allowable loading conditions (40 kN) and the other (50 kN) could represent high tire pressure loadings that are more detrimental to thaw weakened pavements.

Pavement response during thaw

Prior to freezing, FWD measurements were conducted on all the pavement test sections (Fig. 28). It can be seen from this figure that the full depth (TS 1 and TS 2) pavements are structurally stronger than their counterparts (TS 3 and TS 4). Because moisture and density conditions in the subgrade were similar in all test sections and the FWD response of the subgrade was similar (Fig. 27), we concluded that the difference in the mean deflection basins in Figure 28 was caused by the different pavement structures above the subgrade. Higher deflections from the same applied load signifies a lower modulus, which usually signifies lower shear strength (Bjerrum 1972, D'Appolonia et al. 1971). Based on the above conclusions on the subgrade and on inspection of the deflection basins in Figure 28, we further concluded that the fourth sensor (70 cm from the center) apparently measured the deflection of the subgrade attributable to the applied load. The deflection basins in Figure 28 were also used as reference basins during the thaw cycles.

Typical deflection basins during the first and second thaw cycles for the 40-kN load levels for all test sections are presented in Figure 29. Basically, the figures show that as the thaw depth increased, the pavement structure lost strength to its original (before freezing) state and then continued to weaken as thaw progressed deeper. At the end of the second thaw cycle, all the pavement structures showed some signs of recovery; however, this recovery was slow.

Several parameters were studied to characterize pavement response during the thaw period. These parameters were the Impulse Stiffness Modulus (ISM), center deflections, fourth sensor deflections, and deflection basin areas. Bush (1987) suggested using ISM to characterize pavement responses. The ISM is defined as the ratio of the applied FWD load to the corresponding center deflection and is equivalent to the spring constant k in an elastic system. The ISM was found to distinguish different pavement structure types (Fig. 30). The full-depth pavement (TS 1 and TS 2) structures show higher ISM values than their TS 3 and TS 4 counterparts. However, the differentiation in ISM in

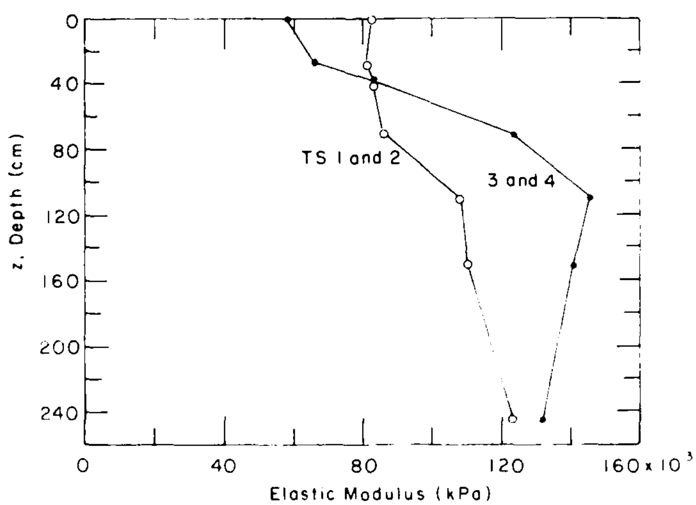

Figure 28. Variation of elastic modulus with depth.

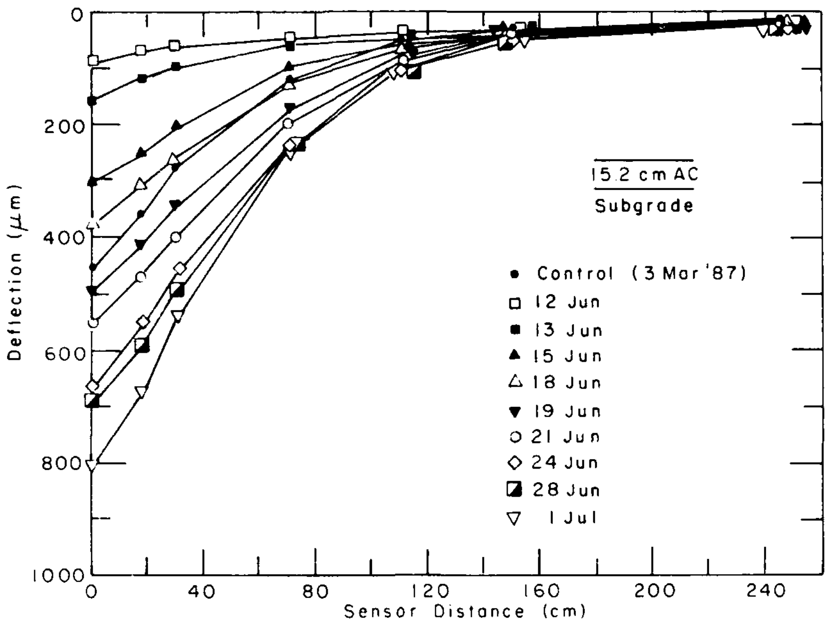

1. TS 1.

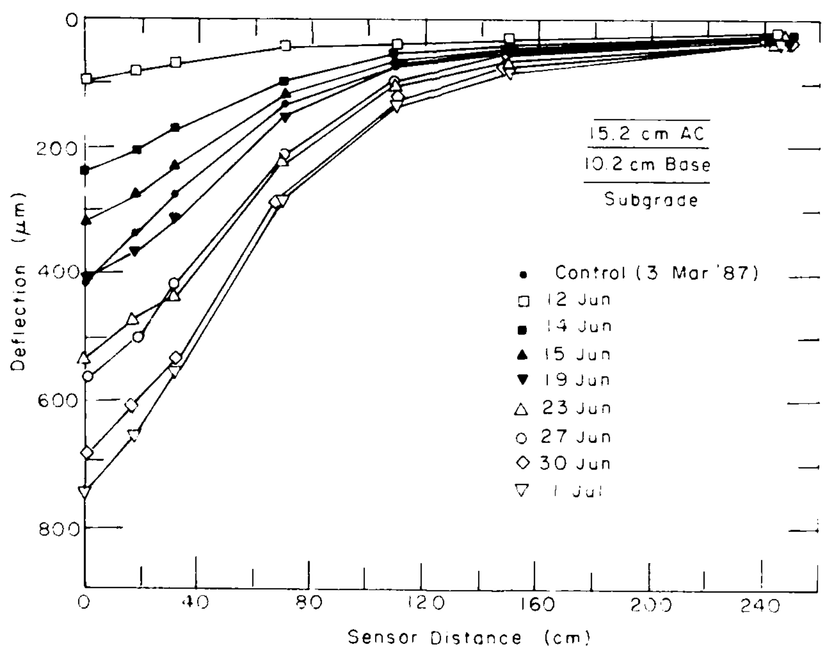

2. TS 2.

a. During the first thaw cycle with a 40-kN FWD load.

Figure 29. FWD deflection measurements.

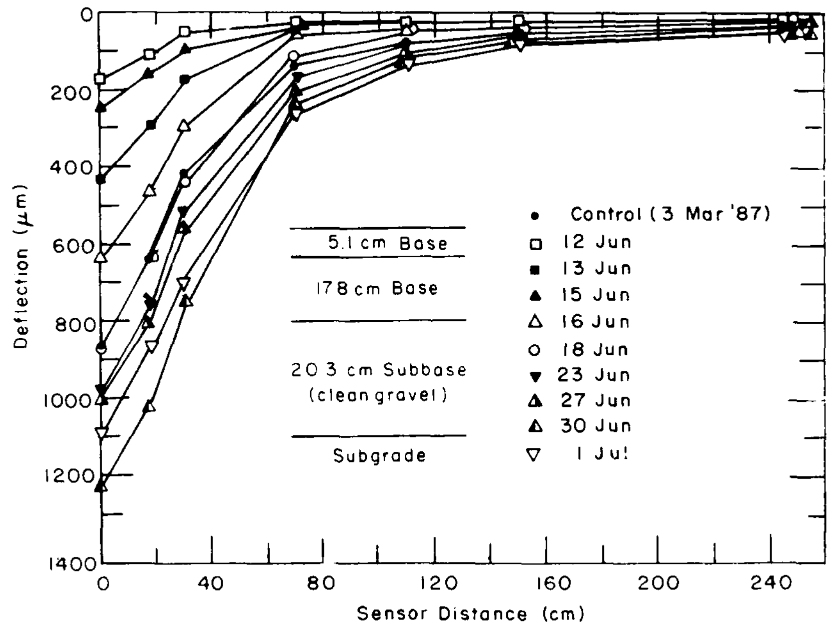

3. TS 3.

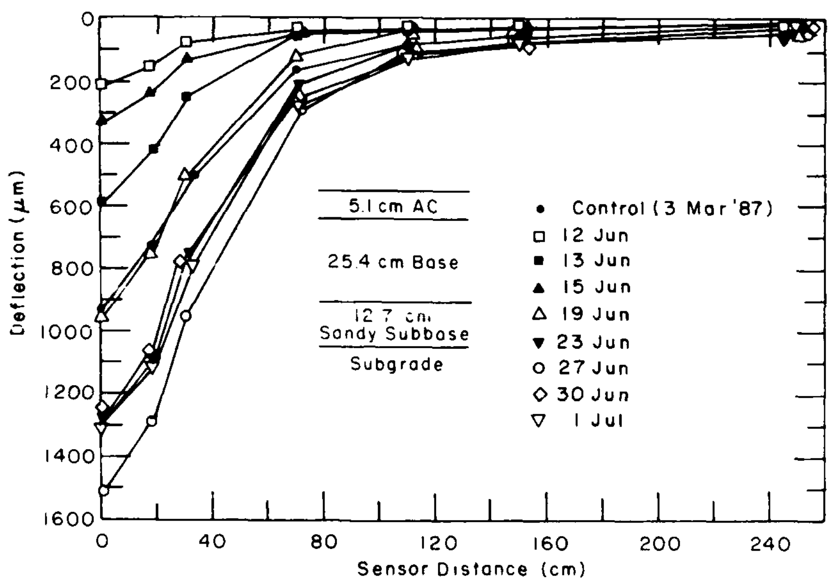

4. TS 4.

a (cont'd). During the first thaw cycle with a 40-kN FWD load.

Figure 29 (cont'd). FWD deflection measurements.

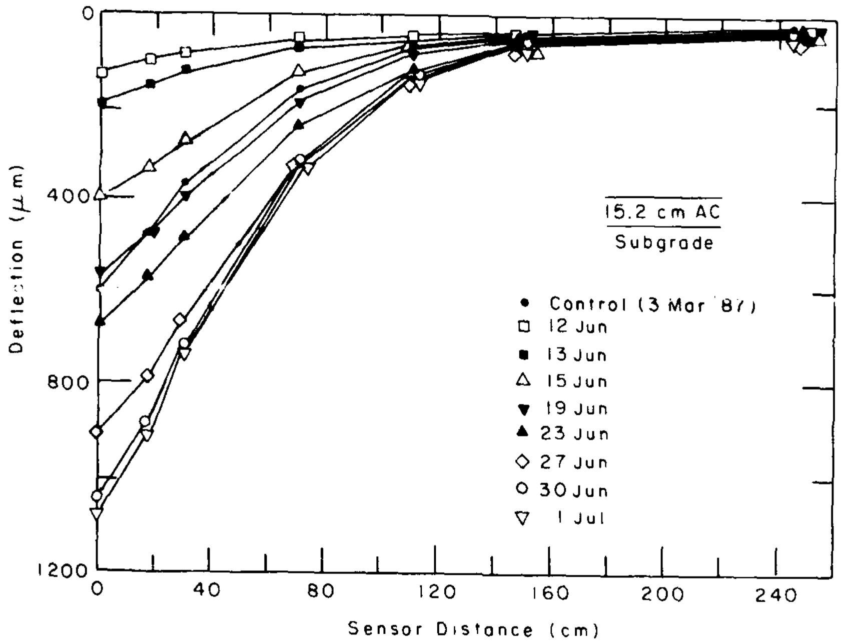

1. TS 1.

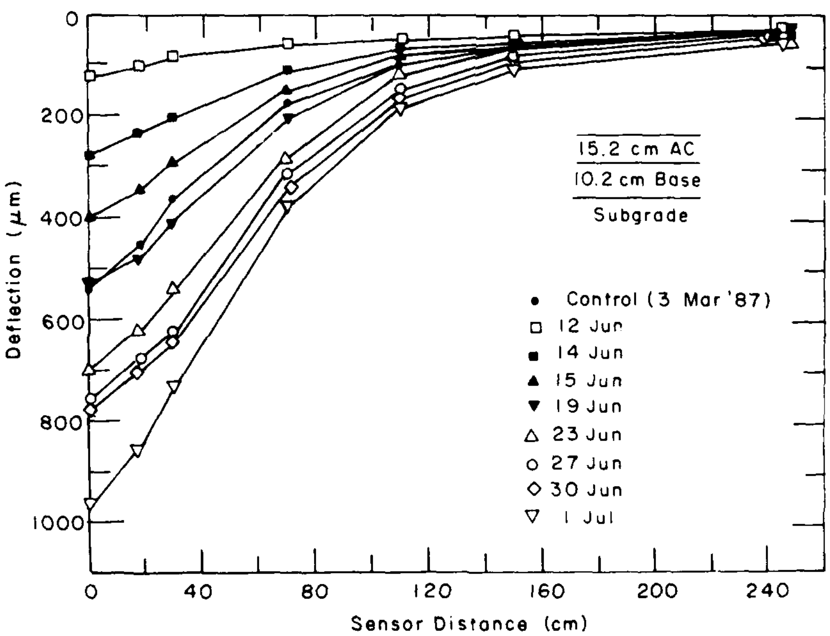

2. TS 2.

b. During the first thaw cycle with a 50-kN FWD load.

Figure 29 (cont'd).

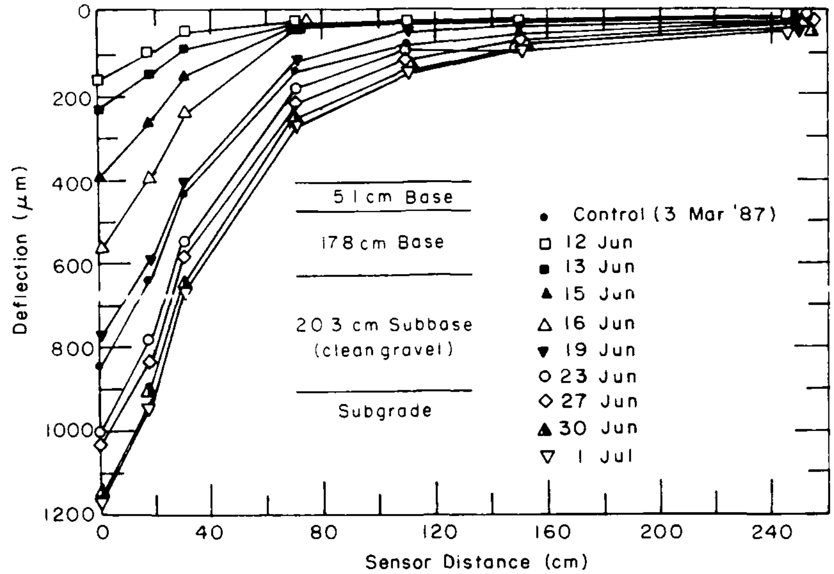

3. TS 3.

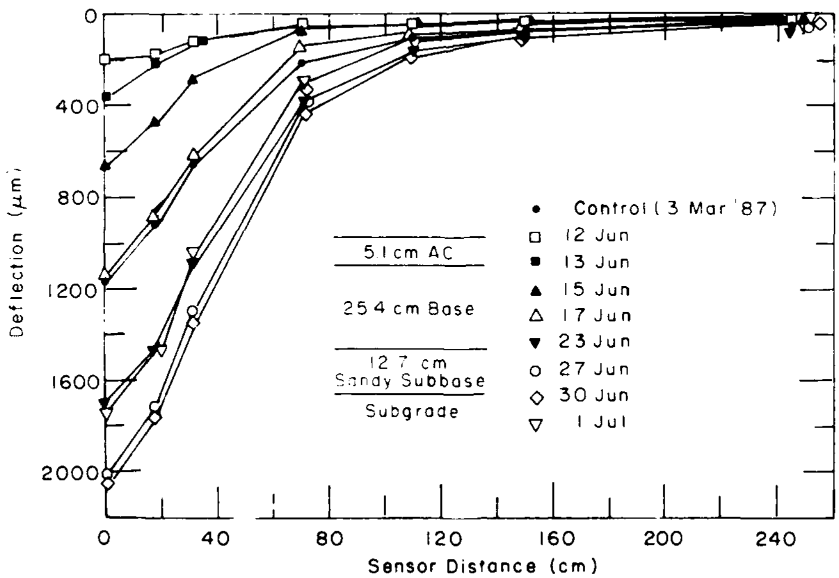

4. TS 4.

b (cont'd). During the first thaw cycle with a 50-kN FWD load.

Figure 29 (cont'd). FWD deflection measurements.

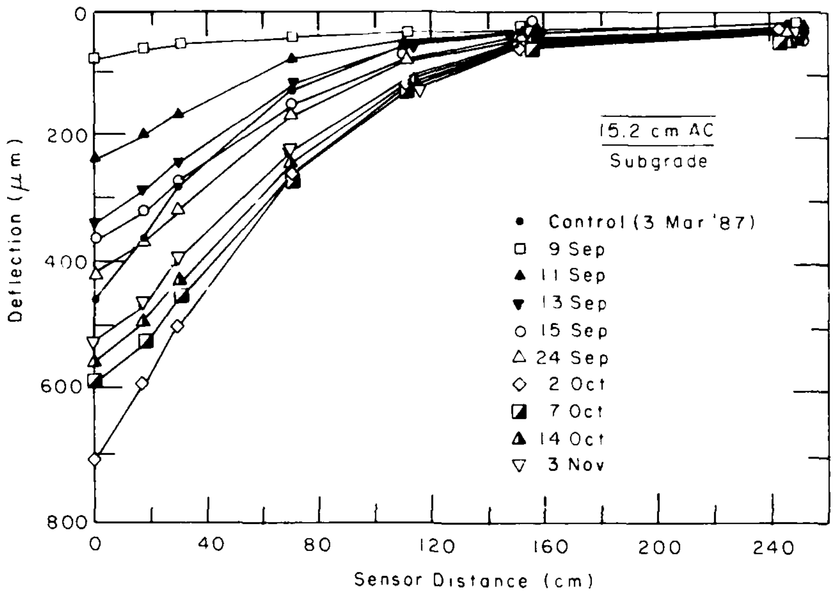

1. TS 1.

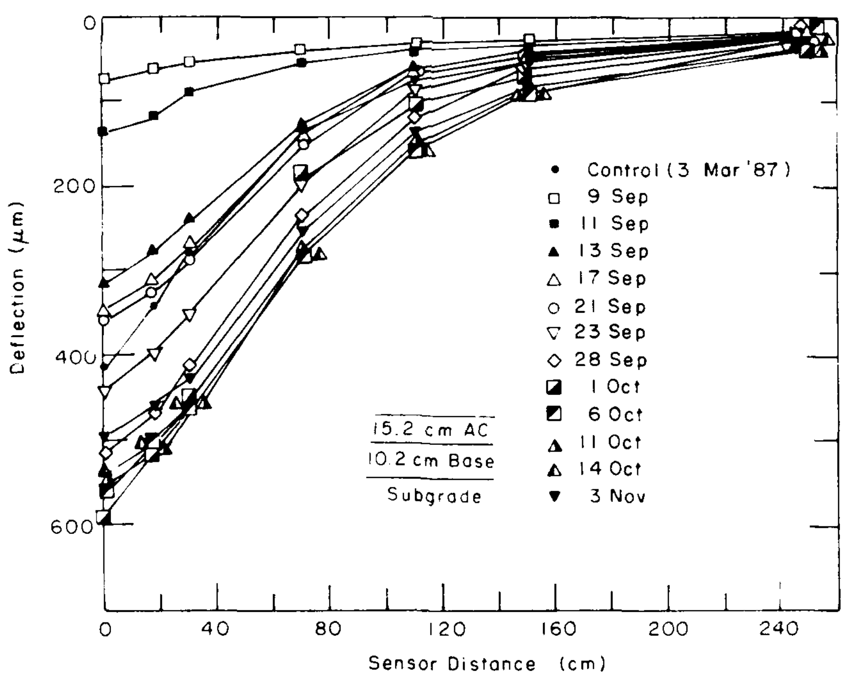

2. TS 2.

c. During the second thaw cycle with a 40-kN FWD load.

Figure 29 (cont'd).

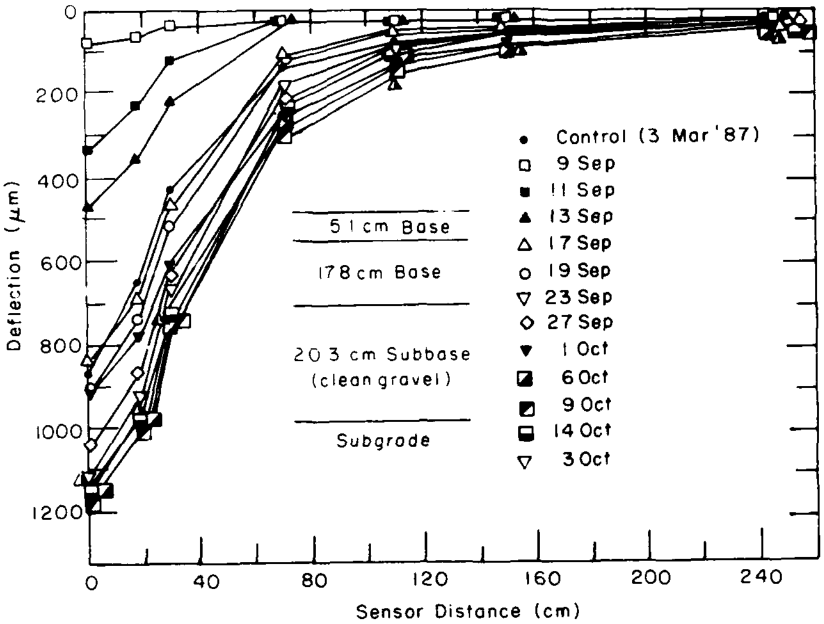

3. TS 3.

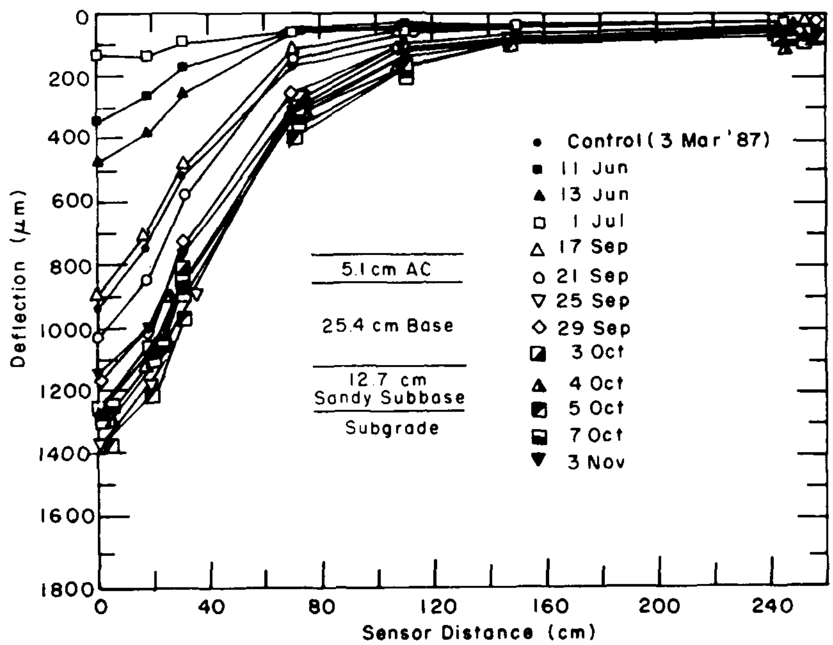

4. TS 4.

c (cont'd). During the second thaw cycle with a 40-kN FWD load.

Figure 29 (cont'd). FWD deflection measurements.

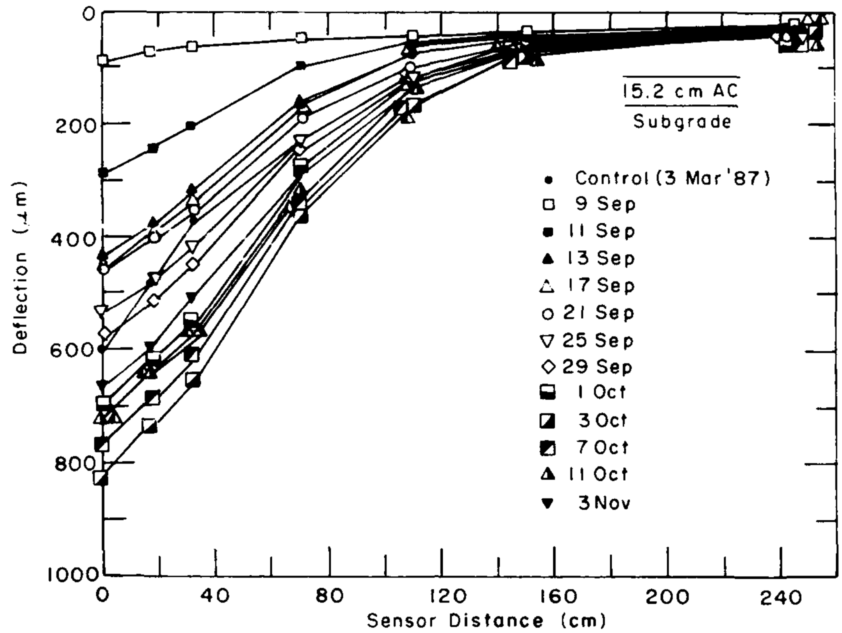

1. TS 1.

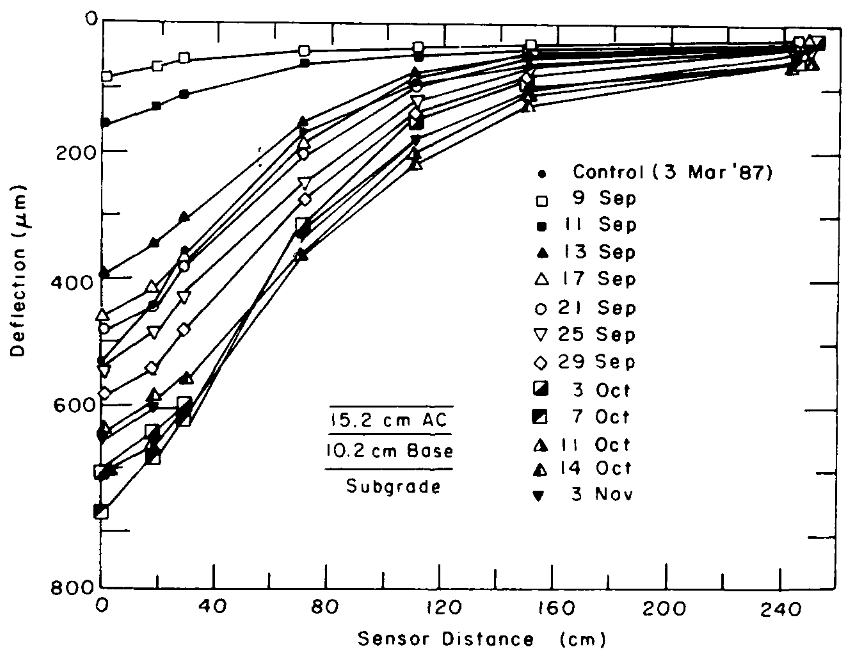

2. TS 2.

d. During the second thaw cycle with a 50-kN FWD load.

Figure 29 (cont'd).

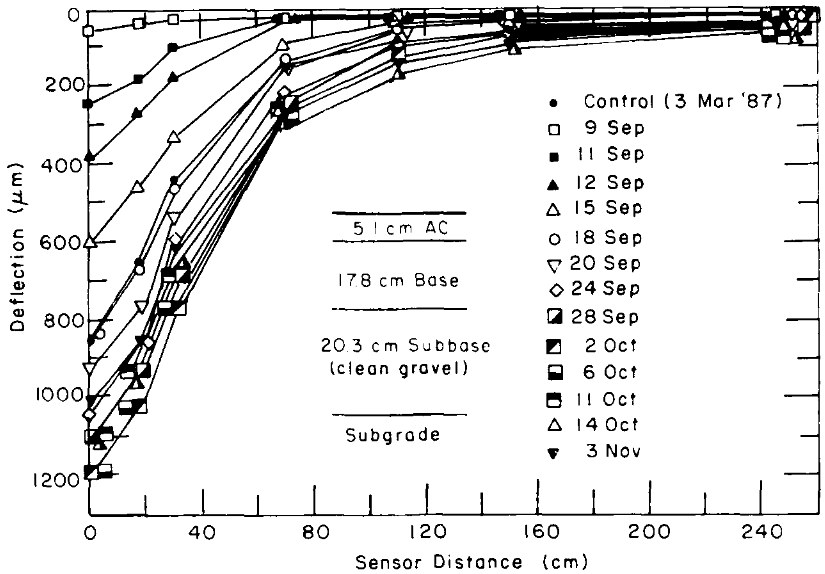

3. TS 3.

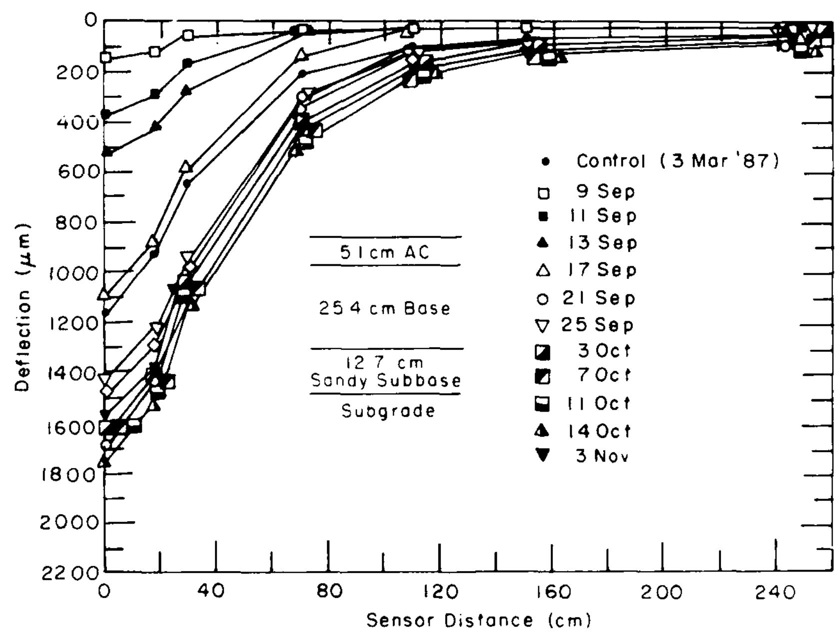

4. TS 4.

d (cont'd). During the second thaw cycle with a 50-kN FWD load.

Figure 29 (cont'd). FWD deflection measurements.

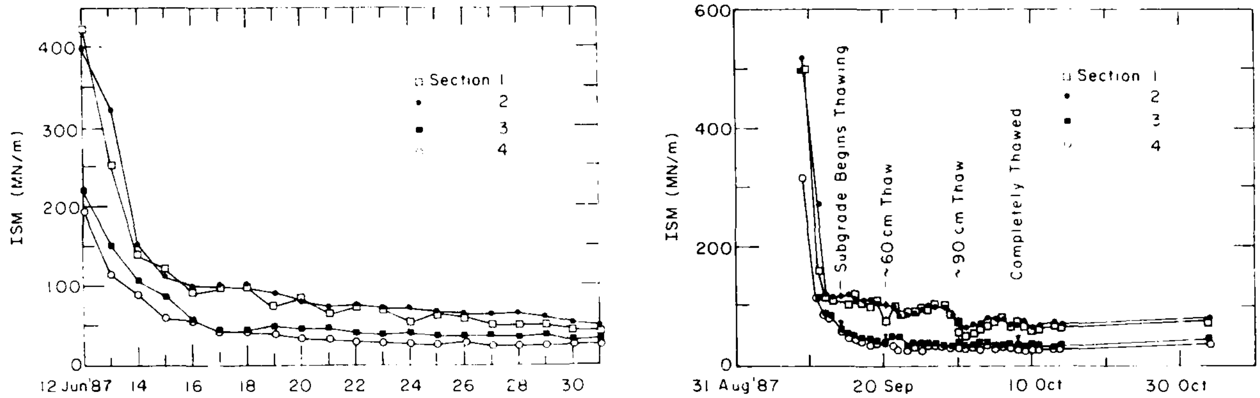

a. During first thaw cycle. *b. During second thaw cycle.*

Figure 30. Variation of ISM in all test sections (40-kN FWD load level).

any one pavement structure during thaw is difficult to discern.

It is common practice to apply a temperature correction to the measured center deflection or ISM to account for the plastic deformation of the AC layer. Thus, we developed a temperature correction factor for the spring thaw period based on the ISM values obtained from the test sections, using a procedure very similar to that used by Bush (1987).

The ISM at 19.5°C was used instead of the ISM at 21.1°C (Bush 1987) because no measurements were made at the pavement temperature of 21.1°C. The results are shown in Figure 31. The mean pavement temperature in Figure 31 is the average of the temperature measured at 5.1- and 10.2-cm depths in the AC layer in TS 2. The calculated correction factors, based on the program FWDTCF developed by Bush (1987), were determined by using the averaged pavement temperature in TS 2. Similar results were found with TS 1. No attempts were made to determine correction factors for TS 3 and TS 4 because the asphalt concrete was only 5.1 cm thick. Bush (1987) found that, for pavement thicknesses less than 7.6 cm, other factors such as moisture conditions, accuracy of FWD load and deflections had a greater influence on the measured deflection than temperature.

As shown in Figure 31, the correlation between the observed and calculated temperature correction factors is poor. This is because Bush's (1987) correction factors were developed under the assumption that changes in temperature affected only the asphalt layer and not the base, subbase or the subgrade. This assumption may be legitimate in regions that have no frost and during the late summer and fall in seasonal frost areas, but during the seasonal frost-affected periods, correction factors developed on the basis of temperature effects on the asphalt layer only will produce incorrect results.

To see if we needed to correct the center deflection measurements during the spring thaw period for temperature effects, a computer simulation was conducted using BISAR on a 15.2-cm full-depth pavement structure with different subgrade moduli. The results of that simulation are presented in Figure 32, which shows that the influence of the AC layer deflection (at temperatures less than 20°C) on the total deflection is small. Therefore, during the spring thaw period there is no need to correct center deflection for temperature effects since almost 90% of the deflection is from the base/subbase and subgrade.

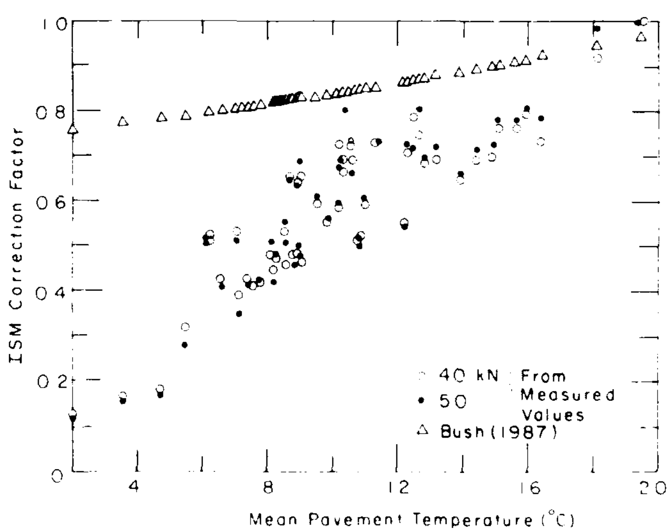

Figure 31. Comparison of measured and calculated ISM correction factors.

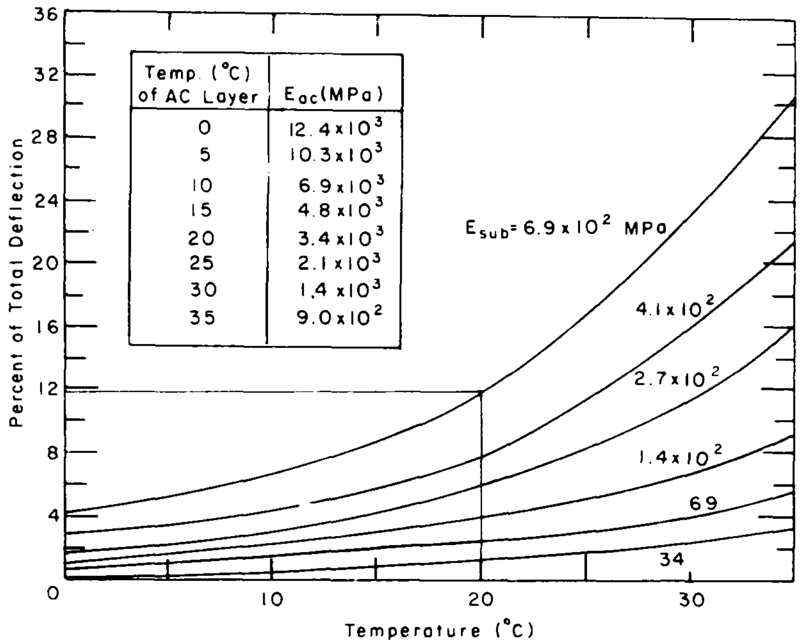

Figure 32. Influence of AC deflection on the total center deflection.

Since ISM was found ill-suited for characterizing pavement response during thaw, measured deflections were used to characterize pavement response. The basin area, center deflections and fourth sensor deflections were used to characterize the pavement structure during thaw weakening periods.

Two basin areas (A_{TOT} and A_{D4}), as shown in Figure 33, were used to characterize the strength of the subgrade during thaw. This concept is similar to that developed by Hoffman and Thompson (1981), who used the center deflection and a normalized deflection basin area bounded by the first four sensors to characterize pavement performance. We calculated the basin area as a ratio of the respective areas prior to freezing. This would be similar to comparing springtime deflections to, say, fall deflections. The change of these ratios with time are shown in Figures 34 and 35. It is interesting to note that both the 40- and 50-kN load levels fall along the same line. The change in the A_{D4} ratio with time is more linear. However, using either A_{TOT} or A_{D4} ratios clearly shows the changes occurring in the pavement structure during thaw weakening periods.

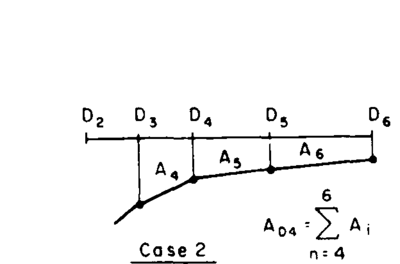

Figure 33. Schematic of basin area calculations.

We also compared deflection measurements during thawing with deflection measurements prior to thawing. As mentioned earlier, we found that the fourth sensor (70 cm from the center plate) was measuring the response of the subgrade. We propose that the ratio of the fourth sensor deflection during thaw to the same sensor deflection measured prior to freezing is an indicator of the subgrade strength. This ratio, called the Subgrade Strength Index (SSI), was used to characterize the subgrade strength during thaw. The use of the deflections 70 cm from the center is similar in concept to using the last sensor deflection from the Dynaflect device (placed at 124 cm from the center) to characterize the subgrade response.

The variations of SSI with time for TS 1, 2, 3 and 4 are shown in Figure 36. The data presented in this fashion clearly show the reduction in the subgrade

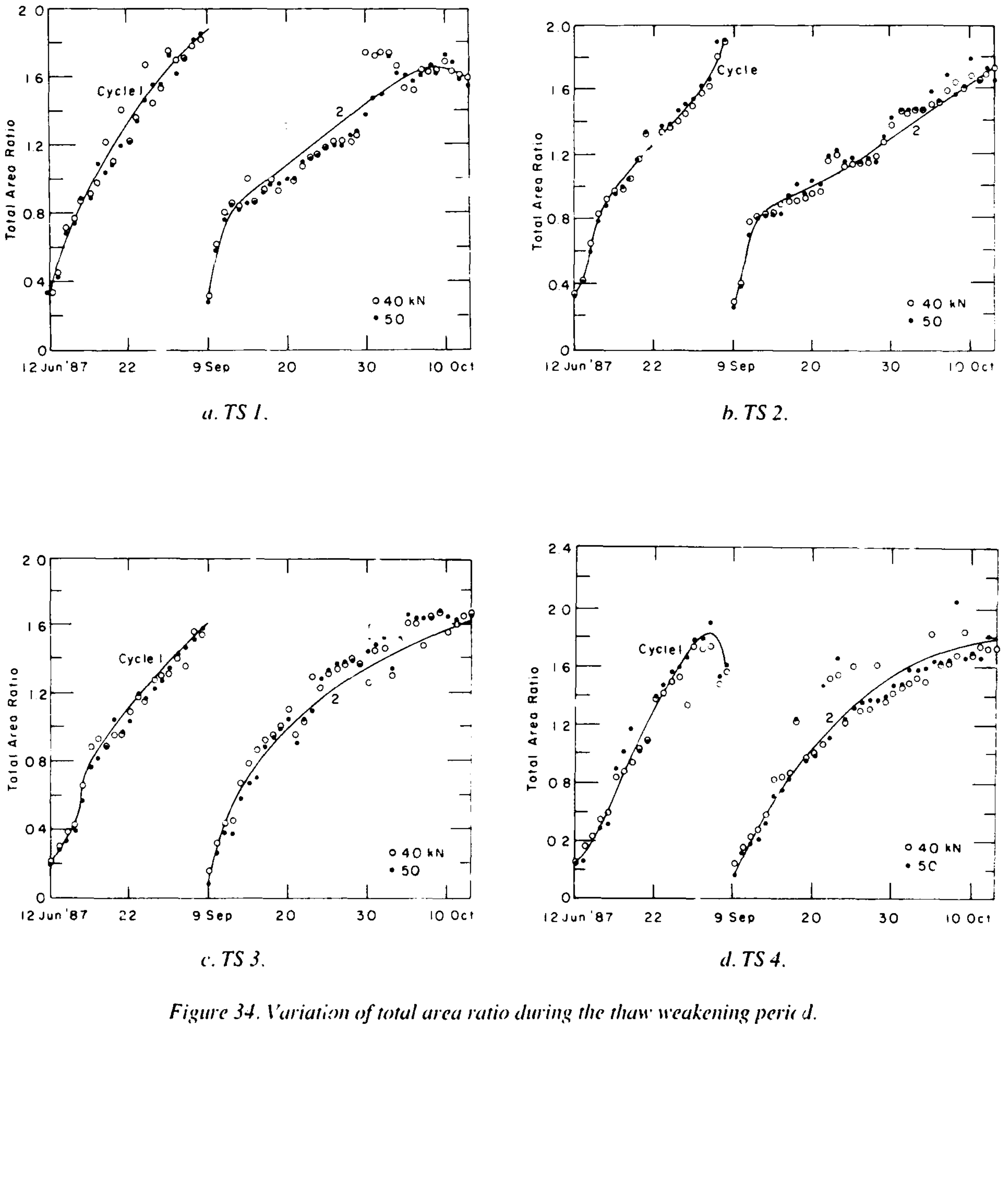

Figure 34. Variation of total area ratio during the thaw weakening period.

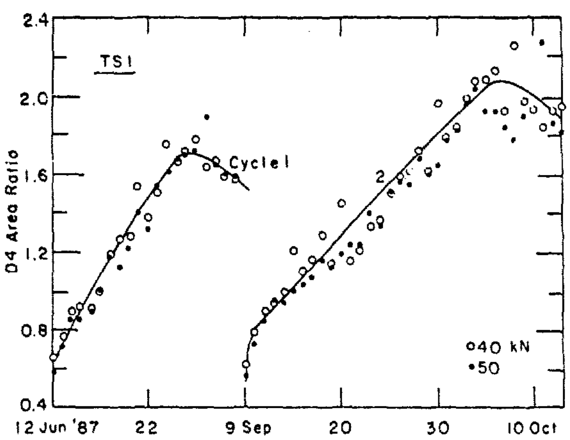

a. TS 1.

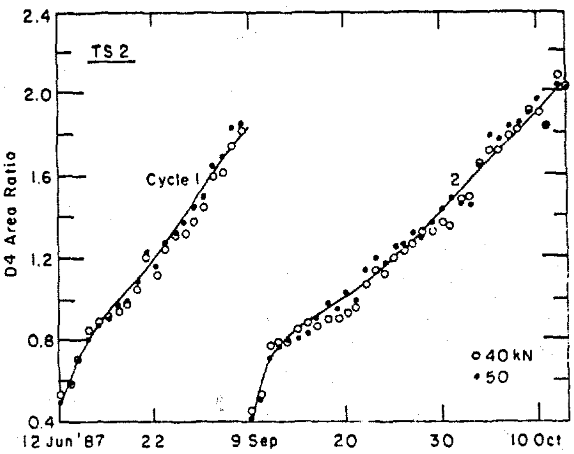

b. TS 2.

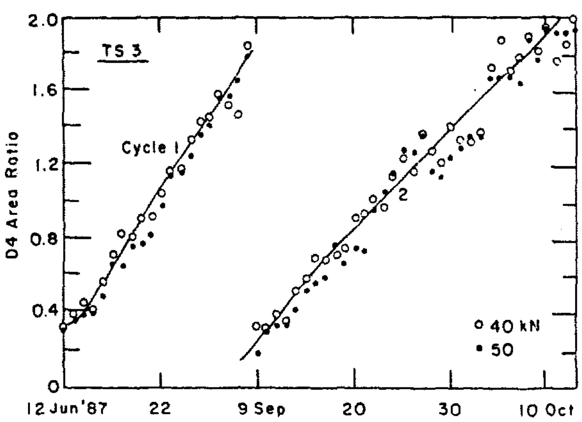

c. TS 3.

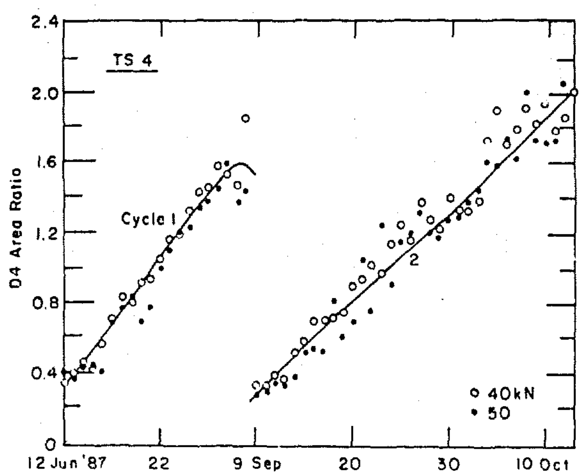

d. TS 4.

Figure 35. Variation of D4 area ratio during the thaw weakening period.

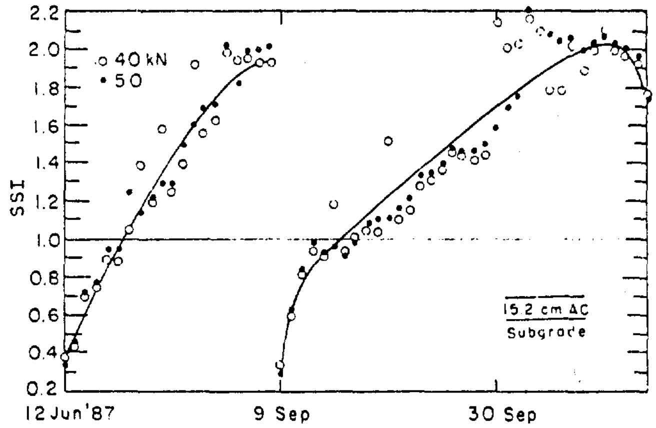

a. TS 1.

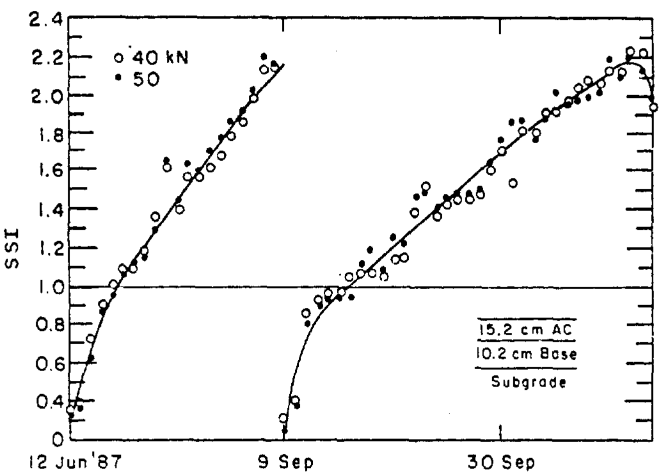

b. TS 2.

Figure 36. Variation of the fourth sensor deflection ratio (SSI) during the thaw weakening period.

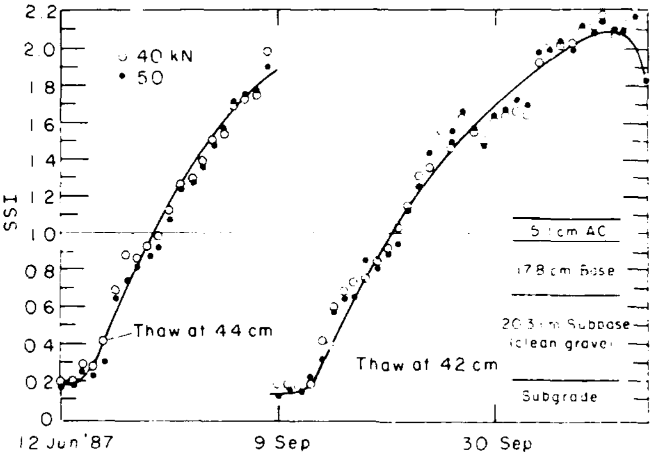

c. TS 3.

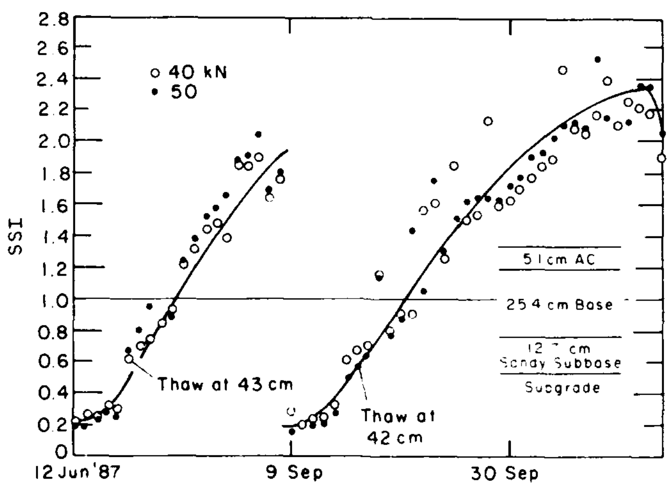

d. TS 4.

Figure 36 (cont'd).

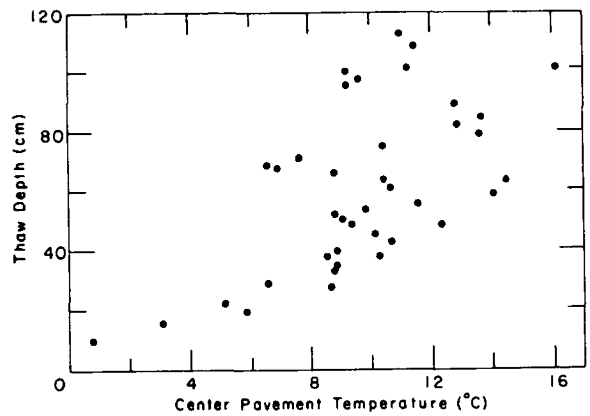

a. TS 1.

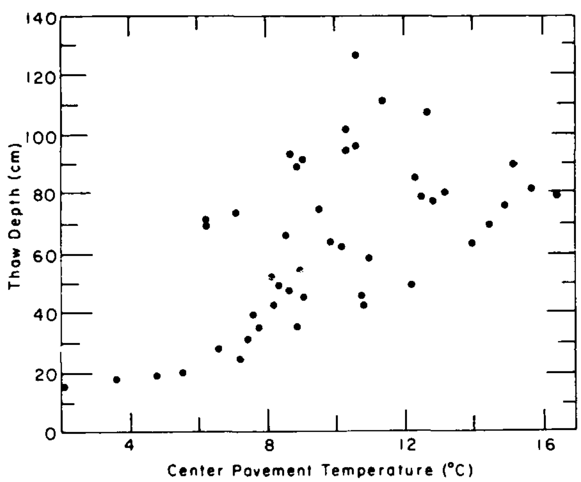

b. TS 2.

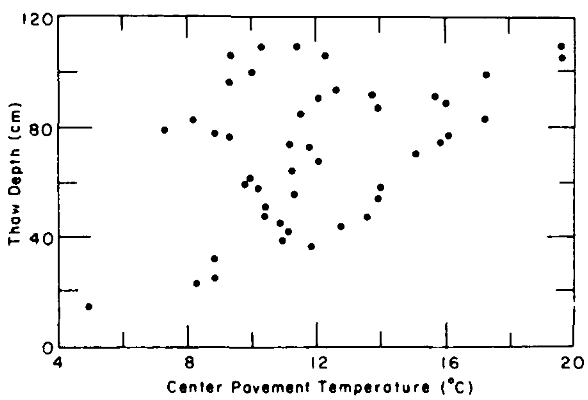

c. TS 3.

Figure 37. Variation of thaw depth with center pavement temperature.

strength (a factor ranging between 2 to 2.2) during thaw. It can also be seen in Figure 36 that the SSI does not change until the thaw depth reaches the bottom of the subbase, i.e., 42 cm from the surface. Further, the results also suggest that recovery from thaw takes time and is not rapid as suggested by some models.

It is apparent from this investigation that, for pavement evaluation in seasonal frost areas, either the fourth sensor deflection ratio or the basin area, or both, can be used to characterize pavement performance during thaw weakening periods. We also found that the ISM was inadequate for characterizing pavements during thaw weakening.

Estimation of thaw depth

We investigated the possibility of using only the temperature and deflection measurements to estimate thaw depth. We looked at using parameters such as pavement temperature, ISM, basin area, center deflection, fourth sensor deflection or a combination of the above for estimating thaw depth. A discussion of the results is presented below.

Pavement temperature

Bush (1987) found good correlation between measured mid-pavement temperature and the Kentucky procedure (Southgate and Deen 1969), which predicts the temperature at some depth in the AC pavement by adding the measured surface temperature and the mean of the previous 5 days air temperature. We attempted to see if there might be any correlation between thaw depth and pavement temperature. Figure 37 shows the variation of thaw depth with mid-depth pavement temperature in TS 1, 2 and 3. In all test sections there is a poor correlation between pavement temperature and thaw depth.

Impulse Stiffness Modulus

As mentioned earlier, the ISM was introduced by Bush (1987) and is defined as the FWD load divided by the center deflection. He used the ISM as an indicator of the bearing capacity of different pavement structures. The ISM vs thaw depth for TS 1–4 is shown in Figure 38.

When the subgrade thaws, the ISM varies between 50 and 100 MN/m in TS 1 and 2. The ISM drops rapidly from about 300 to 100 MN/m, a factor of 3, when the thaw depth is between 15 to 30 cm.

In TS 3 and 4, once thaw reaches the subgrade, the ISM remains fairly constant at approximately 30 MN/m. The ISM changes most rapidly when thaw is in the base and subbase layer, approximately 200 to 30 MN/m, a factor of nearly 7.

With respect to the subgrade, the ISM remains fairly

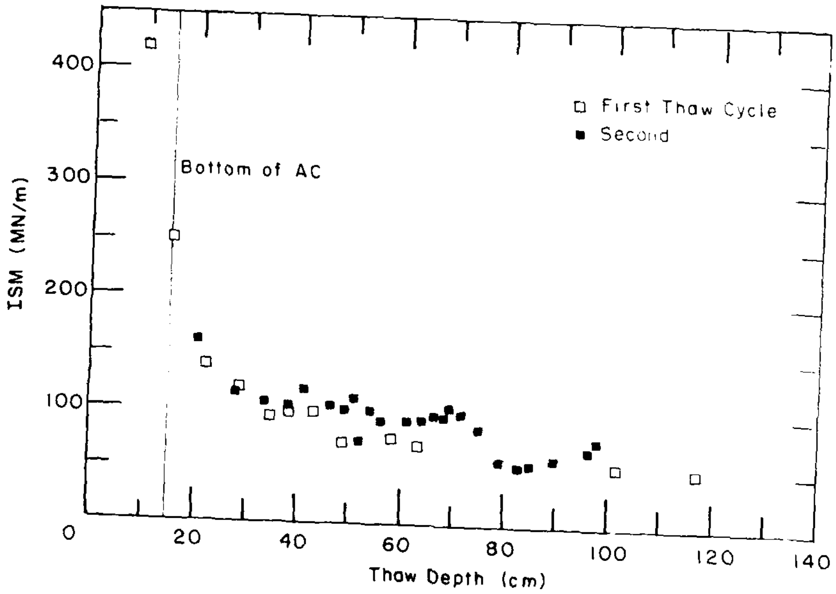

a. TS 1.

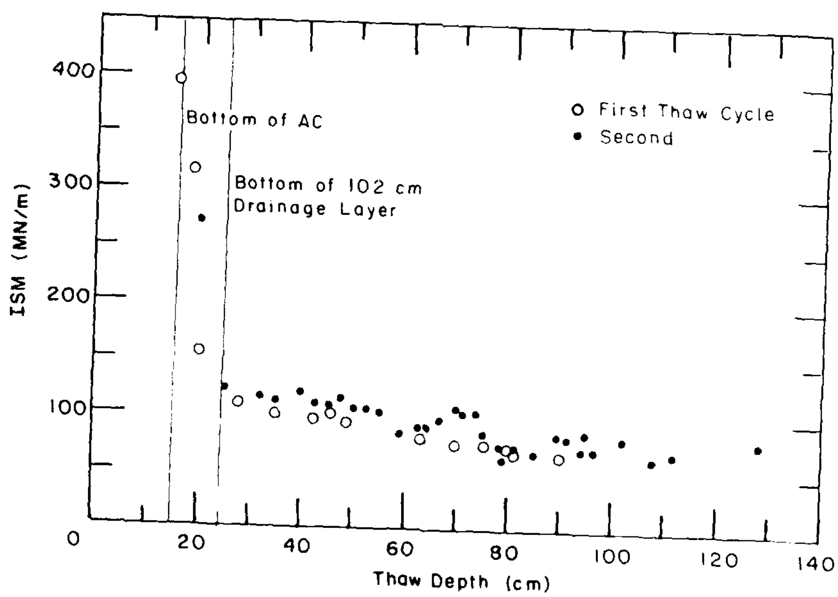

b. TS 2.

Figure 38. Change in ISM with thaw depth.

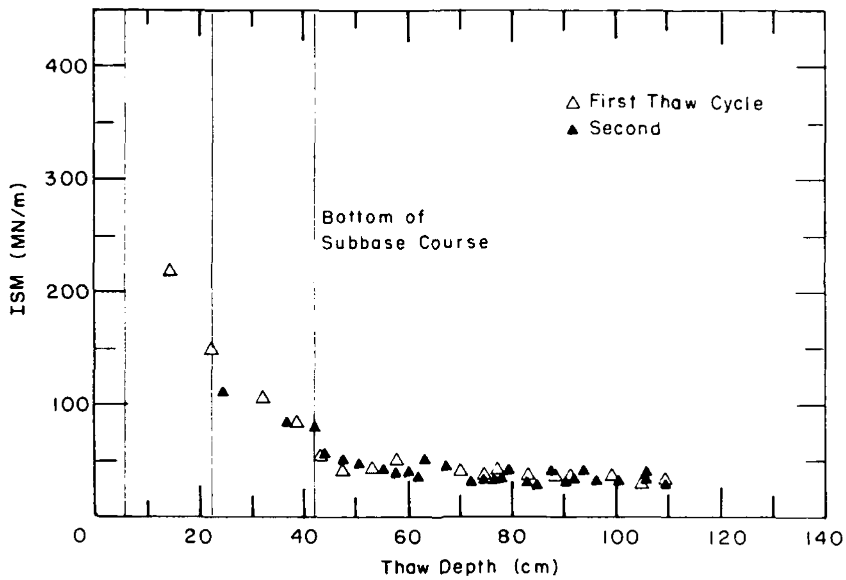

c. TS 3.

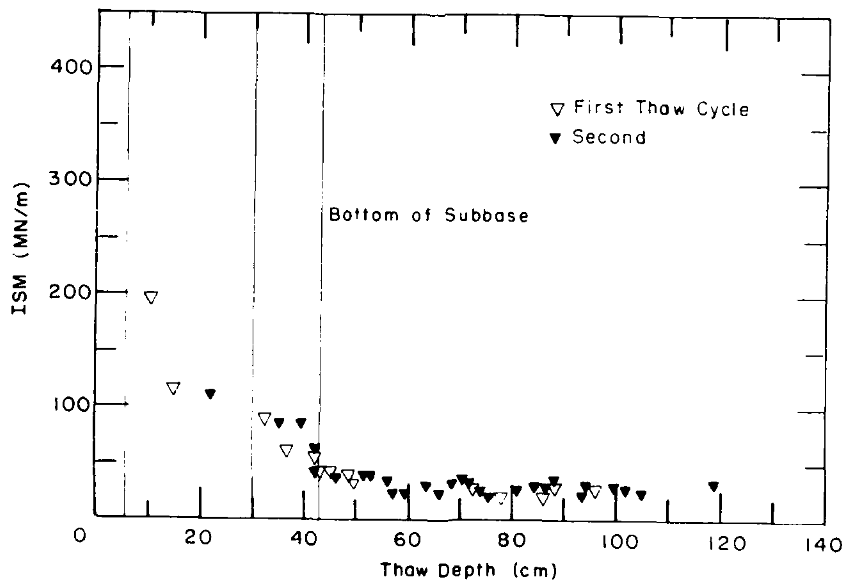

d. TS 4.

Figure 38 (cont'd).

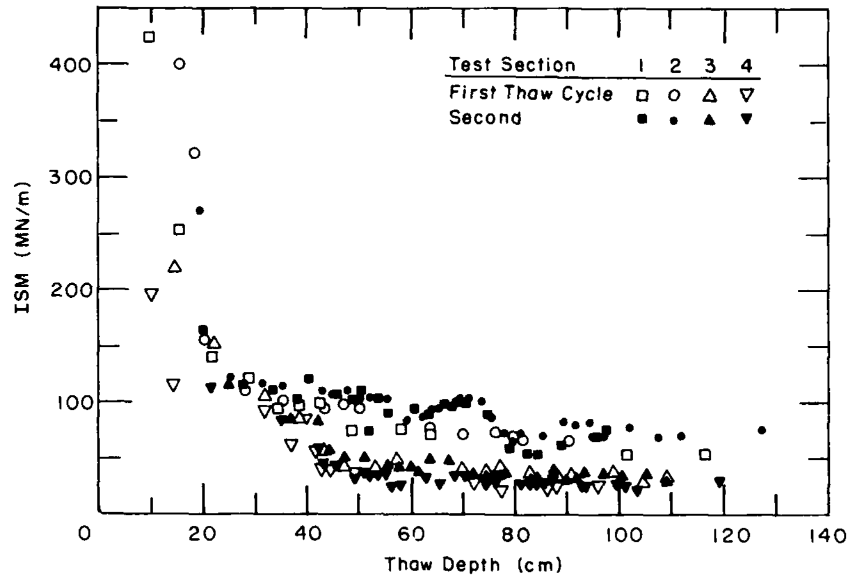

Figure 39. Change in ISM with thaw depth in all test sections.

Table 3. Equations for predicting thaw depth (cm).

TS 1	(23.35 × Area) – 17.33	$R^2 = 0.88$
TS 2	(27.52 × Area) – 32.50	$R^2 = 0.94$
TS 3	(14.82 × Area) – 7.29	$R^2 = 0.92$
TS 4	(11.60 × Area) – 6.30	$R^2 = 0.70$

Area = cm^2.

constant with thaw depth when the subgrade is thawing (Fig. 39).

Area of deflection basin

We also looked at whether the area of the deflection basin could be used as an indicator of thaw depth. The area was determined by summing the trapezoid enclosed by the sensor positions and the measured deflection in the vertical plane (Fig. 33). The relationship between the deflection basin area and thaw depth for TS 1–4 is shown in Figure 40. The figures show a strong correlation between thaw depth in the subgrade and basin area in TS 1,2 and 3. A similar trend is seen in TS 4, but the correlation between area and thaw depth in TS 4 was not as good as those in the other three test sections. The linear equations for predicting the thaw depth in the subgrade are presented in Table 3.

The thaw depth can be estimated in the critical upper 60 cm in TS 1 to within 5 cm. In TS 2 the estimation can also be made to within 5 cm. In TS 4 the thaw depth can be estimated to within 5 cm to a depth of 80 cm.

For TS 3 and 4, there is a distinct break in the relationship between area and thaw depth in the base–subbase courses and in the subgrade (Fig. 40b and c). Similar equations can be developed for predicting thaw depth in the base–subbase courses.

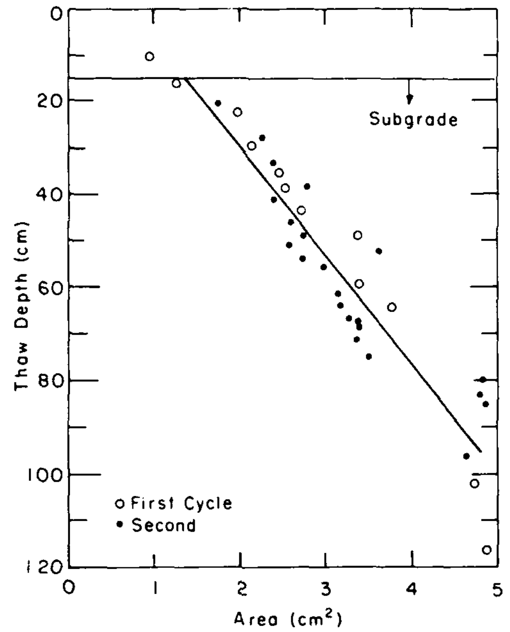

a. TS 1.

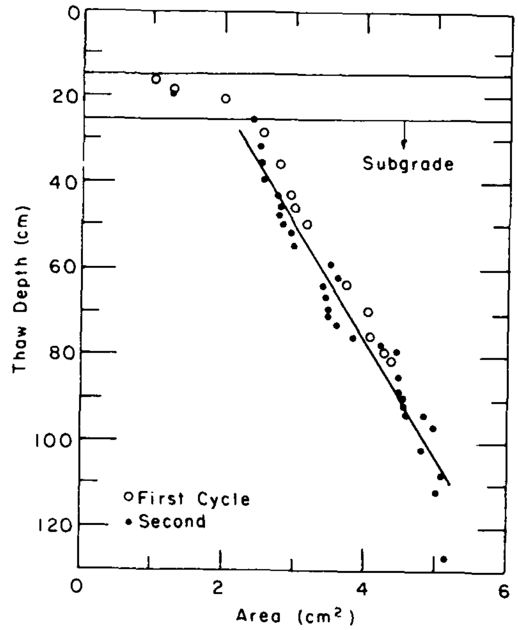

b. TS 2.

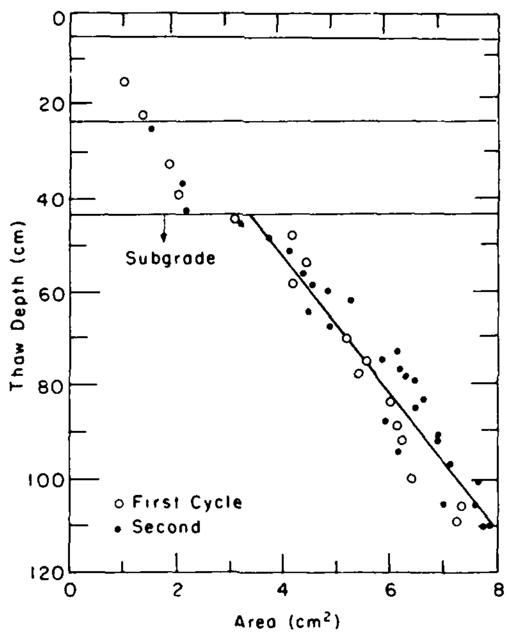

c. TS 3.

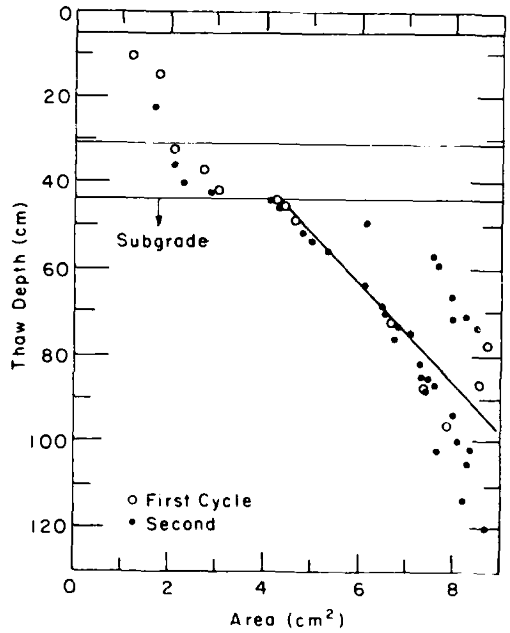

d. TS 4.

Figure 40. Variation of deflection basin area with thaw depth.

Deflection ratio

Finally, we looked at the possibility of using deflection ratios to predict thaw depth. Comparisons between the center (D0) and fourth sensor (SSI) (27.6 cm) deflection ratios and thaw depths in the four test sections are presented in Figures 41 and 42. From these figures, several observations can be made: 1) the center deflection ratios (D0) tend to level off towards the end of the thaw period (this leveling may suggest that the base–subbase courses have drained and are recovering their strength); 2) the variation of the thaw depth with D0 in the base–subbase can be considered to be linear; 3) the deflection ratios from the fourth sensor (SSI) tend to increase with increasing thaw depth; 3) the fourth

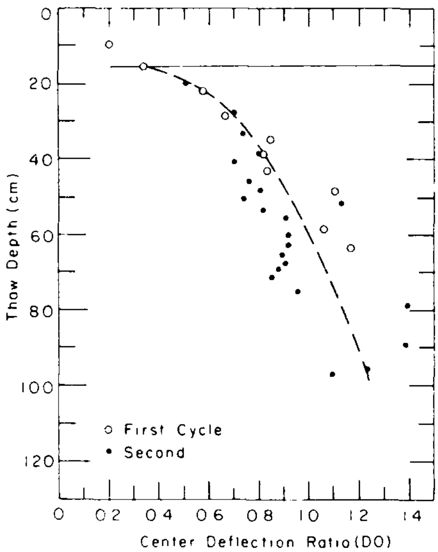

a. TS 1.

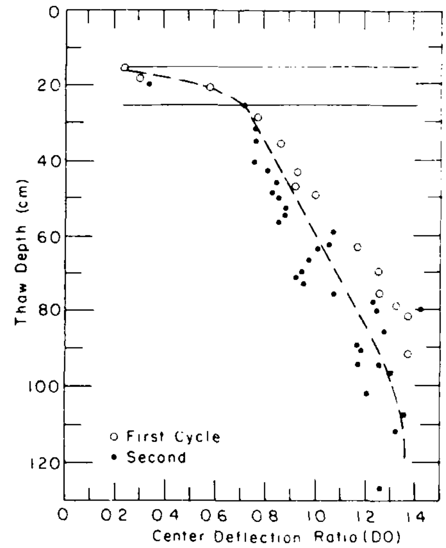

b. TS 2.

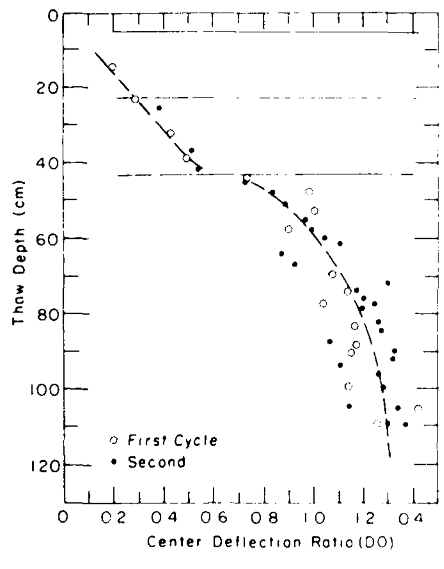

c. TS 3.

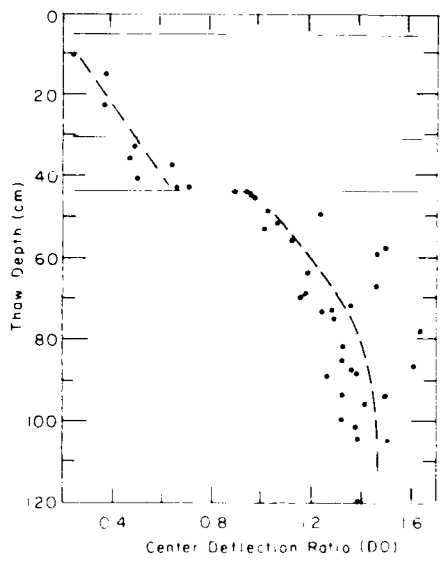

d. TS 4.

Figure 41. Variation of center deflection ratio with thaw depth.

sensor deflection ratios (SSI) remain constant at 0.2 while thawing is occurring within the base and subbase (Fig. 42b and c).

The equations in Table 4, which are derived from a linear regression, can be used to predict thaw depth in the subgrade based on the fourth sensor deflection ratio (SSI). With deflection ratios or basin areas, or both, easy comparison can be made of the strength of the pavements during spring thaw. Again, thaw depth estimation is similar to that shown by the area.

A graph was developed for relating thaw depth to FWD measurements using the deflection basin area and fourth deflection ratio (SSI). Thaw depth contours were generated on a total basin area versus deflection ratio

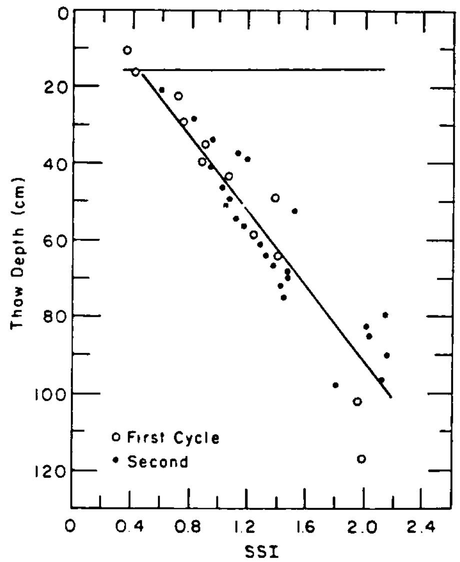

a. TS 1.

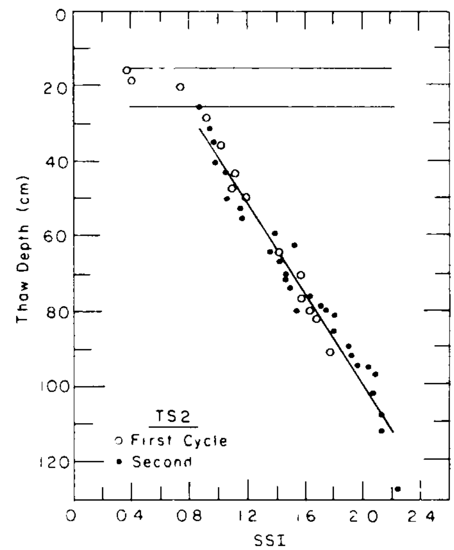

b. TS 2.

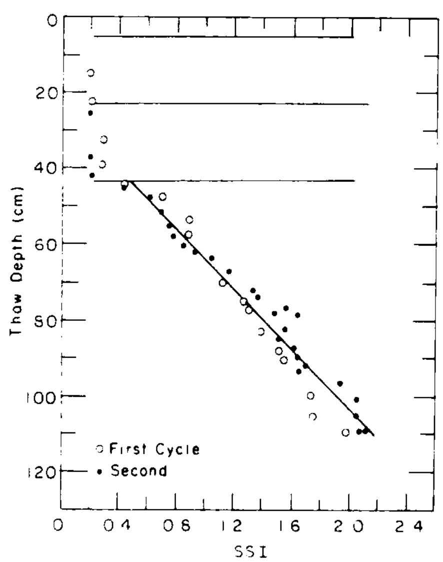

c. TS 3.

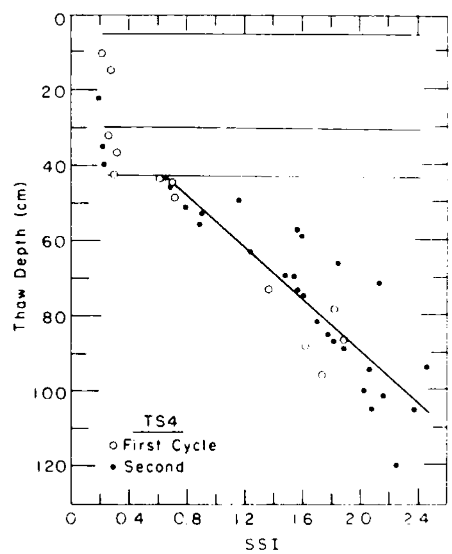

d. TS 4.

Figure 42. Variation of fourth sensor deflection ratio with thaw depth.

Table 4. Equations for predicting thaw depth (cm) based on SSI.

TS 1	$49.33 \times D3 - 6.45$	$R^2 = 0.85$
TS 2	$60.00 \times D3 - 20.27$	$R^2 = 0.96$
TS 3	$39.91 \times D3 + 24.25$	$R^2 = 0.95$
TS 4	$34.34 \times D3 + 20.33$	$R^2 = 0.81$

graph. Two graphs were prepared, one for the full depth pavements, TS 1 and 2 (Fig. 43a), and the other for the conventional pavement sections, TS 3 and 4 (Fig. 43b). When the basin area was calculated between the fourth and the seventh sensors (rather than the total basin area), one graph was sufficient to characterize this relationship (Fig. 43c).

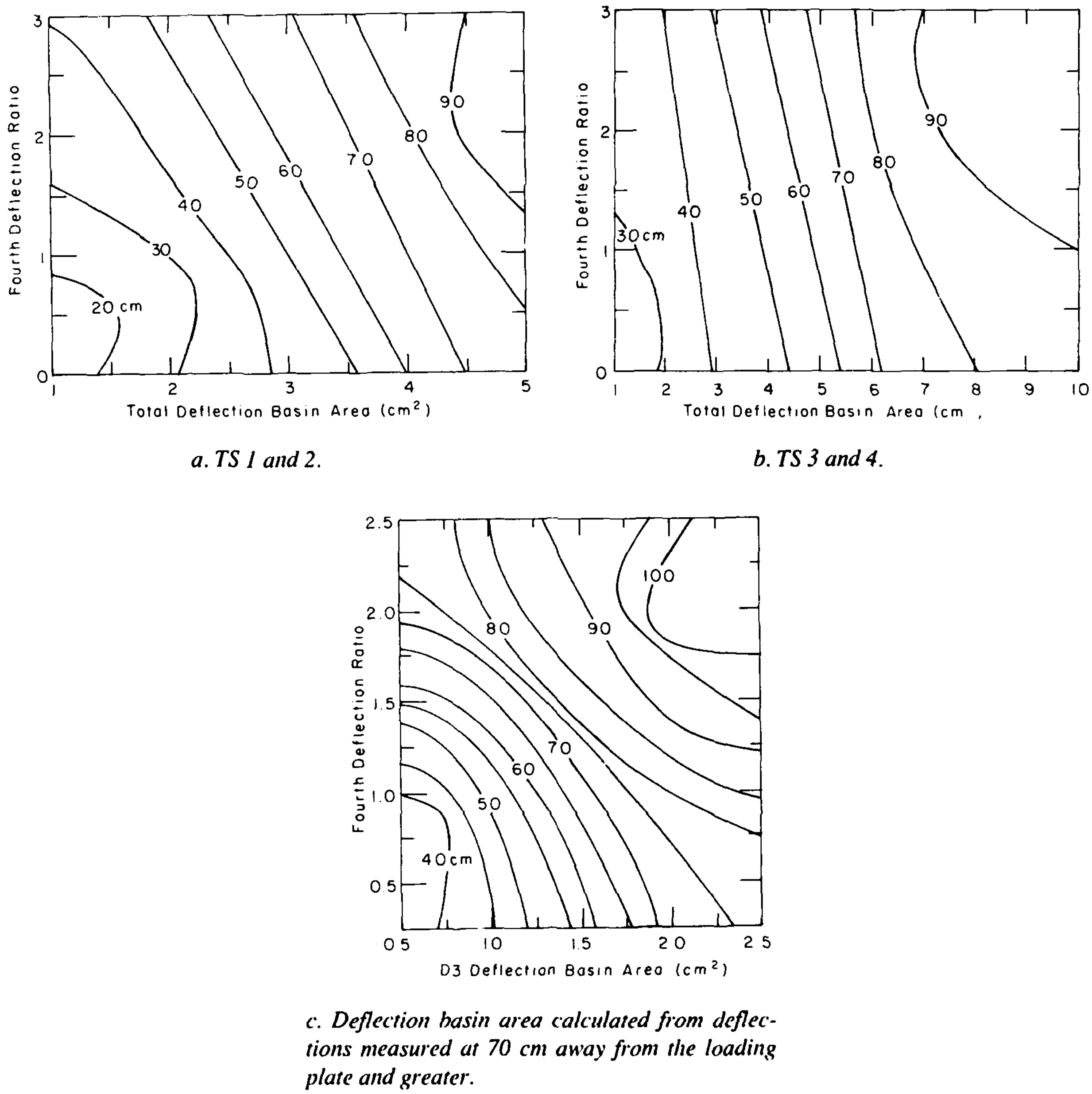

a. TS 1 and 2.

b. TS 3 and 4.

c. Deflection basin area calculated from deflections measured at 70 cm away from the loading plate and greater.

Figure 43. Thaw depth contours.

SUMMARY AND RECOMMENDATIONS

Four flexible pavement test sections were constructed in the FERF and subjected to several freeze–thaw cycles. The subgrade was a clay classified as CH by the Unified Soil Classification System. Two sections were 15.2-cm, full-depth AC pavements and the other two were 5.1-cm-thick AC pavements over a total of 38.1 cm of base and subbase course.

The test sections were instrumented with thermocouples and resistivity gauges that were used to determine the location of the 0°C isotherm and the location of the freezing or thawing front respectively. The resistivity gauges were found to complement the temperature measurements as they indicated the dramatic change in resistance when the soil water changes from a frozen to a thawed state or vice versa.

We found that the clay subgrade was weakened by a factor ranging between 2 and 2.4 when subjected to freeze–thaw. This implies that one could use a 50 to 60% reduction in the "normal period" modulus of a CH subgrade in any mechanistic design procedure for determining the thawing period damage to the pavement in terms of vertical strains. This reduction factor is similar to that proposed by the Asphalt Institute (Shook and Burton 1987) for heavily loaded pavements during thaw.

Since the prediction of thaw depth is considered a critical element in back-calculation procedures for determining layer moduli, we attempted to develop equations for predicting thaw depths in the subgrade based on FWD deflection measurements. We found that we were able to predict the thaw depth reasonably well for a CH subgrade by using the area of the deflection basin or the fourth sensor deflection ratio, or both.

A graph was developed that can be used to predict thaw depth using both the fourth sensor ratio and the basin area.

We recommend that the equations developed in this study be validated in the field; this suggestion also applies to the graph for predicting thaw depth based on FWD measurements.

We also recommend that similar studies be conducted with other fine-grained subgrades. This may lead to development of a thaw depth prediction model for all frost-susceptible soils. Such a prediction model would be incorporated into any mechanistic design procedure.

The analytical procedures developed from this experiment will be used in validating the existing back-calculation procedures for pavement layer moduli in seasonal frost areas. The procedures will make use of any available freeze–thaw deflection data.

Although we would like to see these analytical procedures tried by others, we caution that there currently is only a sparse data base and that it would be premature to make generalizations at this time.

LITERATURE CITED

Atkins, R.T. (1979) Determination of frost penetration by soil resistivity measurements. USA Cold Regions Research and Engineering Laboratory, Special Report 79-22.

Berg, R.L. (1985) Optimize freeze-thaw design of ALRS. Report for Air Force Engineering and Service Center, Tyndall Air Force Base, Florida, 32403.

Bjerrum, L. (1972) Embankment on soft ground. In *Proceedings of the ASCE Specialty Conference on Performance of Earth and Earth Supported Structures, Purdue University*. New York: American Society of Civil Engineers, p. 1–54.

Brabston, W.N., W.R. Barker and G.G. Harvey (1975) Development of a structural design procedure for all bituminous concrete pavements for military roads. Vicksburg, Mississippi: USA Waterways Experiment Station, Technical Report 5-75-10.

Brown, R.W., and D.L. Bartos (1982) A calibration model for screen-cages Peltier thermocouple psychrometers. U.S. Forest Service, Research Paper INT-293.

Bush III, A.J. (1987) Development of a pavement evaluation method for low volume airfield pavements. Ph.D Dissertation, University of Illinois at Urbana-Champaign (unpublished).

Chamberlain, E.J. (1981) A statistical evaluation of soil and climate parameters affecting the change in pavement deflection during thawing of subgrade. USA Cold Regions Research and Engineering Laboratory, CRREL Report 81-15.

D'Appolonia, D.J., H.G. Boulous and C.C. Ladd (1971) Initial settlement of structures on clay. *Journal of the Soil Mechanics and Foundation Division, ASCE*, **97**(SN10):1359–1377.

Eaton, R. A. (1988) A unique new cold weather testing facility. In *Proceedings, Test Technology Symposium, May*. U.S. Army Materiel Command..

Hoffman, M.S., and M.R. Thompson (1981) Nondestructive testing of flexible pavements—field testing program summary. Transportation Engineering Series No. 31, Illinois Cooperative Highway and Transportation Research Program Series No. 188, University of Illinois at Urbana-Champaign.

Nordal, R.S. (1982) Detection and prediction of seasonal changes of the bearing capacity at the Vormsund test road. In *Proceedings, International Symposium on Bearing Capacity of Roads and Airfields, 23–25 June, Trondheim, Norway*, vol. 1 (R.S. Nordal and R. Sortevsdal, Ed.). p. 374–382.

Rwebangira, T., R.G. Hicks and M Truebe (1987) Sensitivity analysis of selected backcalculation procedures. Transportation Research Board Record 117, p. 25–37.

Scrivner, F.H., R. Peohl, W.M. More and M.B. Philips (1969) Detecting seasonal changes in load-carrying capabilities of flexible pavements. National Cooperative Highway Research Program, NCHRP Report No. 67.

Shook, J.F., and J.A. Burton (1987) Structural design of asphalt pavements for heavy loads. In *Proceedings, 6th International Conference on Structural Design of Asphalt Pavements, 13–17 July, Ann Arbor, Michigan*, vol. 1. University of Michigan, p. 3–87.

Southgate, H.F. and R.C. Deen (1969) Temperature distribution within asphalt pavements and its relationship to pavement deflection. Highway Research Board Record 291.

U.S. Army (1985) Pavement design for seasonal frost conditions. Departments of the Army and the Air Force, TM 5-818-2/AFM 88-6, Chap. 4.

APPENDIX A: LOCATION OF INSTRUMENTS IN TEST SECTIONS

Table A1. Test section 1.

Thermocouples			Resistivities		
Channel no.	TC no.	Depth below surface (cm)	Channel no.	Resistivity ring no.	Depth below surface (cm)
201	0	5.1	000	open	--
202	1	10.2	001	1-2	22.9
203	2	10.2	002	2-3	27.9
204	3	15.2	003	3-4	33.0
205	4	25.4	004	4-5	38.1
206	5	40.6	005	5-6	43.2
207	6	55.9	006	6-7	48.3
208	7	71.1	007	7-8	53.3
209	8	86.3	008	8-9	58.4
210	9	101.6	009	9-10	63.5
211	10	116.8	010	10-11	68.6
212	11	132.1	011	11-12	73.7
213	12	147.3	012	12-13	78.7
214	13	surface E	013	13-14	83.8
215	14	surface W	014	14-15	88.9
216	open	---	015	15-16	94.0
			016	16-17	99.1
			017	17-18	104.1
			018	18-19	109.2
			019	19-20	114.3
			020	20-21	119.4
			021	21-22	124.5
			022	22-23	129.5
			023	23-24	134.6

Table A2. Test section 2.

Thermocouples			Resistivities		
Channel no.	TC no.	Depth below surface (cm)	Channel no.	Resistivity ring no.	Depth below surface (cm)
			024	OPEN	--
301	0	5.1	025	1-2	30.5
302	1	10.2	026	2-3	35.6
303	2	15.2	027	3-4	40.6
304	3	20.3	028	4-5	45.7
305	4	35.6	029	5-6	50.8
306	5	50.8	030	6-7	55.9
307	6	66.0	031	7-8	61.0
308	7	81.3	032	8-9	66.0
309	8	96.5	033	9-10	71.7
310	9	111.8	034	10-11	76.2
311	10	127.0	035	11-12	81.3
312	11	142.2	036	12-13	86.3
313	12	157.5	037	13-14	91.6
314	13	Surface E	038	14-15	96.5 E
315	14	Surface W	039	15-16	open
36	open	---	040	16-17	106.7
			041	17-18	111.8
			042	18-19	116.8
			043	19-20	121.9
			044	20-21	127.0
			045	21-22	132.1
			046	22-23	137.2
			047	23-24	142.2

Table A3. Test section 3.

Thermocouples			Resistivities		
Channel no.	TC no.	Depth below surface (cm)	Channel no.	Resistivity ring no.	Depth below surface (cm)
401	0	5.1	100	open	--
402	1	10.2	101	1-2	43.2
403	2	22.9	102	2-3	48.3
404	3	open	103	3-4	53.3
405	4	43.2	104	4-5	58.4
406	5	48.3	105	5-6	63.5
407	6	63.5	106	6-7	68.6
408	7	78.7	107	7-8	73.7
409	8	94.0	108	8-9	78.7
410	9	109.2	109	9-10	83.8
411	10	124.5	110	10-11	88.8
412	11	139.7	111	11-12	94.0
413	12	155.0	112	12-13	99.1
414	13	surface E	113	13-14	104.1
415	14	surface W	114	14-15	109.2
416	open	--	115	15-16	114.3
			116	16-17	119.4
			117	17-18	124.5
			118	18-19	129.5
			119	19-20	134.6
			120	20-21	139.7
			121	21-22	144.8
			122	22-23	149.9
			123	23-24	155.0

Table A4. Test section 4.

Thermocouples			Resistivities		
Channel no.	TC no.	Depth below surface (cm)	Channel no.	Resistivity ring no.	Depth below surface (cm)
601	0	5.1	124	open	--
602	1	15.2	125	1-2	43.2
603	2	30.5	126	2-3	48.3
604	3	35.6	127	3-4	53.3
605	4	43.2	128	4-5	58.4
606	5	43.2	129	5-6	63.5
607	6	58.4	130	6-7	68.6
608	7	73.7	131	7-8	73.7
609	8	88.9	132	8-9	78.7
610	9	104.1	133	9-10	83.8
611	10	119.4	134	10-11	88.9
612	11	134.6	135	11-12	94.0
613	12	149.9	136	12-13	99.1
614	13	surface E	137	13-14	104.1
615	14	surface W	138	14-15	109.2
616	open	--	139	15-16	114.3
			140	16-17	119.4
			141	17-18	124.5
			142	18-19	129.5
			143	19-20	134.6
			144	20-21	139.7
			145	21-22	144.8
			146	22-23	149.9
			147	23-24	155.0
			148	open	--

APPENDIX B: FWD MEASUREMENTS

TEST SECTION 1

LOC	DATE	AIR TEMP(C)	LOAD (kN)	D0	D1	D2	D3	D4	D5	D6
				DEFLECTION (microns)						
110	24-Nov-86	10.0	37.35	2235.2	223.5	325.1	157.5	71.1	55.9	40.6
110	27-Feb-87	18.3	37.05	353.1	287.0	231.1	106.7	50.8	33.0	15.2
130	03-Mar-87	12.8	37.52	426.7	335.3	259.1	116.8	50.8	30.5	15.2
140	12-Jun-87	16.6	38.26	86.4	66.0	55.9	43.2	33.0	27.9	15.2
120	13-Jun-87	25.1	38.46	147.3	109.2	91.4	50.8	40.6	30.5	17.8
120	14-Jun-87	20.4	36.71	243.8	205.7	170.2	81.3	43.2	30.5	17.8
120	15-Jun-87	32.2	35.90	269.2	226.1	182.9	83.8	43.2	30.5	17.8
130	16-Jun-87	32.4	35.56	340.4	271.8	215.9	99.1	43.2	25.4	15.2
120	17-Jun-87	19.0	35.97	330.2	276.9	223.5	99.1	48.3	30.5	17.8
140	18-Jun-87	21.4	36.57	345.4	281.9	236.2	119.4	58.4	38.1	20.3
130	19-Jun-87	21.3	36.17	452.1	375.9	309.9	154.9	66.0	33.0	15.2
140	20-Jun-87	25.6	36.44	391.2	327.7	271.8	134.6	66.0	38.1	20.3
130	21-Jun-87	22.4	35.70	492.8	416.6	353.1	175.3	78.7	38.1	25.4
120	22-Jun-87	21.3	36.24	436.9	370.8	304.8	139.7	66.0	40.6	27.9
120	23-Jun-87	20.7	36.78	490.2	414.0	353.1	160.0	76.2	45.7	25.4
130	24-Jun-87	16.6	36.10	604.5	505.5	421.6	215.9	96.5	43.2	20.3
140	25-Jun-87	35.7	36.03	497.8	421.6	353.1	175.3	83.8	48.3	27.9
120	26-Jun-87	15.2	36.71	546.1	467.4	391.2	185.4	86.4	50.8	30.5
130	27-Jun-87	17.6	35.90	627.4	530.9	454.7	221.0	96.5	43.2	20.3
130	28-Jun-87	21.4	35.29	612.1	525.8	436.9	213.4	86.4	38.1	15.2
130	29-Jun-87	18.8	35.97	624.8	530.9	449.6	218.4	88.9	38.1	20.3
130	30-Jun-87	24.7	34.82	683.3	569.0	459.7	208.3	78.7	33.0	20.3
130	01-Jul-87	24.7	35.49	718.8	602.0	480.1	213.4	81.3	35.6	15.2
120	09-Sep-87	12.7	37.65	71.1	55.9	48.3	38.1	30.5	25.4	15.2
140	11-Sep-87	19.0	36.71	210.8	177.8	147.3	68.6	35.6	27.9	17.8
140	12-Sep-87	17.7	35.97	284.5	243.8	205.7	91.4	43.2	25.4	17.8
110	13-Sep-87	15.7	35.70	297.2	254.0	213.4	104.1	48.3	25.4	15.2
140	14-Sep-87	16.9	35.29	276.9	236.2	200.7	99.1	48.3	27.9	17.8
110	15-Sep-87	11.6	36.44	330.2	287.0	246.4	134.6	66.0	33.0	17.8
120	16-Sep-87	11.1	37.52	297.2	248.9	213.4	109.2	55.9	33.0	25.4
120	17-Sep-87	14.2	36.17	309.9	261.6	223.5	114.3	58.4	35.6	20.3
140	18-Sep-87	12.6	36.37	330.2	276.9	231.1	119.4	55.9	38.1	35.6
120	19-Sep-87	12.4	36.84	312.4	266.7	228.6	119.4	55.9	38.1	17.8
130	20-Sep-87	13.3	36.17	462.3	391.2	322.6	170.2	73.7	35.6	25.4
140	21-Sep-87	12.6	37.05	337.8	292.1	246.4	127.0	55.9	35.6	20.3
140	22-Sep-87	14.6	36.17	370.8	317.5	269.2	129.5	61.0	35.6	20.3
140	23-Sep-87	10.7	37.59	391.2	340.4	287.0	149.9	71.1	38.1	22.9
140	24-Sep-87	12.4	36.78	378.5	332.7	284.5	149.9	71.1	40.6	20.3
140	25-Sep-87	10.0	39.00	396.2	348.0	304.8	165.1	78.7	50.8	25.4
140	26-Sep-87	5.6	38.87	396.2	348.0	302.3	175.3	81.3	53.3	27.9
140	27-Sep-87	4.4	39.54	396.2	353.1	312.4	177.8	91.4	53.3	27.9
120	28-Sep-87	8.3	38.67	375.9	330.2	289.6	170.2	94.0	53.3	38.1
140	29-Sep-87	11.8	37.45	403.9	358.1	309.9	167.6	83.8	48.3	30.5
110	30-Sep-87	15.7	35.97	566.4	500.4	436.9	241.3	109.2	48.3	20.3
130	01-Oct-87	12.4	36.24	629.9	530.9	442.0	226.1	94.0	43.2	22.9
130	02-Oct-87	15.6	36.30	635.0	530.9	447.0	228.6	94.0	43.2	30.5
110	03-Oct-87	12.8	36.64	574.0	508.0	436.9	246.4	114.3	48.3	22.9
110	04-Oct-87	6.8	37.25	518.2	464.8	411.5	243.8	121.9	53.3	27.9
140	05-Oct-87	13.1	36.91	459.7	406.4	358.1	205.7	111.8	66.0	33.0
140	06-Oct-87	6.1	38.40	459.7	408.9	363.2	213.4	116.8	71.1	38.1
110	07-Oct-87	12.0	35.90	523.2	462.3	396.2	226.1	106.7	48.3	22.9
140	08-Oct-87	13.3	37.18	490.2	429.3	378.5	218.4	119.4	71.1	43.2
110	09-Oct-87	12.7	36.84	530.9	467.4	406.4	228.6	109.2	53.3	25.4
110	10-Oct-87	11.3	35.97	561.3	482.6	416.6	236.2	106.7	48.3	20.3
110	11-Oct-87	13.8	36.37	538.5	475.0	411.5	226.1	104.1	45.7	20.3
110	13-Oct-87	13.1	37.32	530.9	467.4	398.8	228.6	114.3	50.8	22.9
110	14-Oct-87	11.3	36.84	508.0	449.6	391.2	221.0	106.7	48.3	35.6
110	03-Nov-87	12.6	38.80	505.5	447.0	375.9	213.4	99.1	48.3	20.3
140	24-Nov-86	10.0	50.71	1899.9	1010.9	533.4	233.7	129.5	96.5	48.3

TEST SECTION 1

LOC	DATE	AIR TEMP(C)	LOAD (kN)	D0	D1	D2	D3	D4	D5	D6
				DEFLECTION (microns)						
110	27-Feb-87	18.3	51.22	513.1	419.1	335.3	154.9	76.2	45.7	22.9
130	03-Mar-87	12.8	51.35	622.3	490.2	375.9	167.6	76.2	45.7	22.9
130	12-Jun-87	16.6	51.96	129.5	99.1	81.3	55.9	45.7	35.6	17.8
120	13-Jun-87	25.1	53.24	195.6	152.4	127.0	71.1	53.3	43.2	27.9
120	14-Jun-87	20.4	51.82	355.6	297.2	246.4	119.4	63.5	43.2	25.4
120	15-Jun-87	32.2	50.47	393.7	327.7	269.2	121.9	61.0	43.2	22.9
130	16-Jun-87	32.4	50.07	513.1	416.6	335.3	154.9	66.0	35.6	20.3
140	17-Jun-87	20.2	51.15	464.8	383.5	322.6	157.5	76.2	48.3	22.9
130	18-Jun-87	21.4	51.89	591.8	502.9	424.2	210.8	96.5	45.7	25.4
120	19-Jun-87	21.3	50.68	563.9	475.0	396.2	188.0	83.8	48.3	27.9
140	20-Jun-87	25.6	51.49	581.7	487.7	408.9	198.1	94.0	55.9	30.5
140	21-Jun-87	22.4	50.95	627.4	523.2	439.4	215.9	104.1	66.0	38.1
120	22-Jun-87	21.3	50.68	660.4	561.3	464.8	213.4	99.1	58.4	33.0
140	23-Jun-87	21.1	50.68	688.3	584.2	495.3	246.4	121.9	66.0	38.1
120	24-Jun-87	18.7	50.88	764.5	657.9	553.7	266.7	121.9	71.1	38.1
120	25-Jun-87	17.8	50.74	817.9	708.7	591.8	281.9	127.0	71.1	40.6
120	26-Jun-87	15.2	50.88	815.3	703.6	586.7	284.5	132.1	73.7	40.6
130	27-Jun-87	17.6	49.80	916.9	784.9	662.9	330.2	137.2	58.4	33.0
120	28-Jun-87	20.1	50.74	812.8	701.0	591.8	299.7	144.8	83.8	48.3
130	29-Jun-87	18.8	50.07	916.9	784.9	665.5	325.1	134.6	55.9	27.9
130	30-Jun-87	24.7	48.65	1026.2	861.1	701.0	317.5	119.4	50.8	30.5
130	01-Jul-87	24.7	49.26	1071.9	901.7	721.4	325.1	121.9	50.8	25.4
140	09-Sep-87	7.5	52.23	91.4	73.7	66.0	48.3	43.2	33.0	20.3
140	11-Sep-87	19.0	52.09	302.3	256.5	210.8	101.6	53.3	35.6	25.4
140	12-Sep-87	17.7	50.95	401.3	342.9	289.6	134.6	61.0	38.1	22.9
110	13-Sep-87	15.7	50.47	442.0	381.0	322.6	162.6	76.2	38.1	20.3
140	14-Sep-87	16.9	50.34	419.1	358.1	302.3	149.9	71.1	40.6	22.9
140	15-Sep-87	10.4	52.97	439.4	386.1	330.2	167.6	81.3	45.7	25.4
140	16-Sep-87	11.0	51.89	442.0	386.1	325.1	160.0	76.2	45.7	35.6
140	17-Sep-87	12.6	52.36	482.6	414.0	348.0	172.7	81.3	48.3	33.0
140	18-Sep-87	12.6	51.22	490.2	421.6	353.1	177.8	88.9	48.3	38.1
140	19-Sep-87	11.7	52.09	495.3	426.7	363.2	188.0	83.8	50.8	33.0
140	20-Sep-87	13.3	50.95	492.8	426.7	363.2	182.9	88.9	50.8	38.1
120	21-Sep-87	13.5	51.42	482.6	416.6	363.2	193.0	99.1	55.9	30.5
140	22-Sep-87	14.6	50.74	563.9	485.1	411.5	200.7	91.4	53.3	35.6
120	23-Sep-87	11.4	51.42	551.2	475.0	411.5	223.5	111.8	63.5	33.0
140	24-Sep-87	12.4	51.49	566.4	497.8	429.3	223.5	104.1	58.4	33.0
140	25-Sep-87	10.0	54.86	586.7	523.2	457.2	248.9	121.9	73.7	43.2
140	26-Sep-87	5.6	54.73	574.0	515.6	452.1	261.6	127.0	78.7	38.1
140	27-Sep-87	4.4	55.47	586.7	523.2	462.3	261.6	132.1	78.7	35.6
140	28-Sep-87	8.3	53.24	571.5	515.6	452.1	254.0	127.0	73.7	66.0
140	29-Sep-87	11.8	51.76	602.0	533.4	464.8	254.0	124.5	71.1	43.2
140	30-Sep-87	15.7	51.22	673.1	589.3	508.0	264.2	124.5	73.7	43.2
140	01-Oct-87	12.4	51.01	711.2	624.8	543.6	281.9	134.6	76.2	48.3
140	02-Oct-87	15.6	51.01	716.3	624.8	541.0	292.1	139.7	78.7	48.3
110	03-Oct-87	12.8	50.68	840.7	746.8	645.2	365.8	170.2	71.1	30.5
110	04-Oct-87	6.8	52.30	744.2	673.1	594.4	358.1	182.9	78.7	43.2
110	05-Oct-87	12.2	52.09	772.2	690.9	599.4	353.1	172.7	76.2	30.5
110	06-Oct-87	6.1	51.89	731.5	657.9	584.2	345.4	172.7	78.7	27.9
110	07-Oct-87	12.0	49.53	762.0	675.6	579.1	332.7	157.5	68.6	22.9
130	08-Oct-87	13.3	50.88	891.5	756.9	632.5	330.2	142.2	61.0	43.2
110	09-Oct-87	12.7	50.95	772.2	683.3	594.4	337.8	165.1	71.1	33.0
140	10-Oct-87	11.3	50.88	769.6	680.7	596.9	345.4	182.9	106.7	55.9
140	11-Oct-87	13.8	51.28	739.1	657.9	581.7	340.4	188.0	109.2	45.7
110	13-Oct-87	13.1	51.76	767.1	675.6	589.3	337.8	165.1	71.1	33.0
110	14-Oct-87	11.3	51.55	739.1	655.3	571.5	327.7	160.0	71.1	30.5
110	03-Nov-87	12.6	54.19	729.0	645.2	548.6	315.0	144.8	71.1	27.9

TEST SECTION 2

LOC	DATE	AIR TEMP(C)	LOAD (kN)	DEFLECTION (microns) D0	D1	D2	D3	D4	D5	D6
240	24-Nov-86	10.0	35.38	2677.2	553.7	370.8	182.9	106.7	76.2	35.6
220	27-Feb-87	18.3	37.86	241.3	213.4	182.9	88.9	50.8	33.0	15.2
230	03-Mar-87	12.8	37.79	393.7	322.6	261.6	124.5	68.6	48.3	22.9
240	12-Jun-87	16.6	37.65	88.9	76.2	63.5	43.2	35.6	27.9	17.8
220	13-Jun-87	25.1	39.88	124.5	104.1	88.9	50.8	38.1	35.6	20.3
220	14-Jun-87	20.4	36.37	215.9	188.0	162.6	86.4	48.3	30.5	17.8
230	15-Jun-87	33.0	35.02	279.4	243.8	205.7	104.1	53.3	35.6	20.3
230	16-Jun-87	32.4	35.22	315.0	276.9	236.2	116.8	55.9	38.1	17.8
230	17-Jun-87	20.2	36.64	353.1	309.9	264.2	132.1	63.5	40.6	10.2
220	18-Jun-87	19.9	36.78	348.0	309.9	266.7	132.1	61.0	38.1	22.9
230	19-Jun-87	21.3	37.32	383.5	340.4	292.1	144.8	66.0	40.6	20.3
230	20-Jun-87	25.6	37.05	431.8	383.5	327.7	165.1	73.7	43.2	15.2
220	21-Jun-87	20.4	37.25	480.1	426.7	370.8	198.1	81.3	45.7	22.9
230	22-Jun-87	19.3	36.91	449.6	396.2	342.9	170.2	78.7	45.7	17.8
220	23-Jun-87	20.7	36.57	475.0	419.1	368.3	188.0	78.7	48.3	27.9
230	24-Jun-87	16.6	36.98	482.6	429.3	370.8	190.5	88.9	55.9	22.9
220	25-Jun-87	17.8	37.18	510.5	452.1	393.7	198.1	91.4	53.3	25.4
220	26-Jun-87	15.2	36.98	525.8	454.7	398.8	203.2	91.4	53.3	30.5
220	27-Jun-87	20.4	36.44	520.7	462.3	403.9	213.4	99.1	55.9	27.9
220	28-Jun-87	20.1	37.86	548.6	495.3	431.8	231.1	111.8	63.5	38.1
220	29-Jun-87	20.2	35.83	535.9	480.1	424.2	233.7	114.3	63.5	22.9
220	30-Jun-87	24.7	36.10	622.3	548.6	480.1	254.0	121.9	66.0	33.0
230	01-Jul-87	24.7	35.56	665.5	584.2	495.3	251.5	121.9	73.7	30.5
210	09-Sep-87	12.7	38.33	71.1	58.4	50.8	38.1	27.9	25.4	15.2
210	11-Sep-87	18.6	36.71	124.5	109.2	83.8	48.3	33.0	27.9	15.2
210	12-Sep-87	18.3	35.97	266.7	236.2	208.3	101.6	45.7	35.6	15.2
210	13-Sep-87	15.7	35.90	281.9	248.9	215.9	109.2	50.8	33.0	15.2
240	14-Sep-87	16.9	35.36	276.9	254.0	221.0	111.8	53.3	30.5	12.7
210	15-Sep-87	11.6	36.64	284.5	254.0	221.0	116.8	58.4	35.6	17.8
240	16-Sep-87	11.0	36.78	307.3	276.9	238.8	127.0	61.0	35.6	17.8
240	17-Sep-87	12.6	37.38	325.1	292.1	254.0	132.1	61.0	35.6	15.2
210	18-Sep-87	12.5	37.52	320.0	287.0	248.9	132.1	63.5	38.1	17.8
210	19-Sep-87	12.4	36.91	325.1	289.6	254.0	127.0	61.0	38.1	20.3
210	20-Sep-87	12.7	37.32	337.8	302.3	264.2	139.7	66.0	38.1	17.8
210	21-Sep-87	13.5	36.78	332.7	299.7	264.2	139.7	66.0	38.1	20.3
240	22-Sep-87	14.6	36.24	403.9	358.1	315.0	165.1	73.7	43.2	15.2
240	23-Sep-87	10.7	37.65	414.0	375.9	332.7	188.0	83.8	43.2	17.8
210	24-Sep-87	12.1	37.65	391.2	348.0	307.3	167.6	78.7	45.7	22.9
210	25-Sep-87	10.0	37.79	378.5	342.9	304.8	175.3	83.8	50.8	25.4
210	26-Sep-87	5.6	40.02	388.6	358.1	322.6	190.5	96.5	55.9	22.9
210	27-Sep-87	4.4	38.33	365.8	337.8	304.8	182.9	96.5	53.3	22.9
210	28-Sep-87	8.3	39.21	386.1	353.1	317.5	190.5	101.6	66.0	17.8
240	29-Sep-87	11.8	37.65	419.1	386.1	342.9	198.1	94.0	53.3	27.9
240	30-Sep-87	15.7	36.78	469.9	424.2	375.9	205.7	99.1	53.3	22.9
230	01-Oct-87	12.4	36.84	543.6	475.0	411.5	185.4	91.4	58.4	27.9
210	02-Oct-87	15.6	36.30	469.9	421.6	375.9	215.9	109.2	55.9	22.9
240	03-Oct-87	12.8	36.30	480.1	436.9	391.2	213.4	106.7	58.4	25.4
240	04-Oct-87	6.8	38.73	467.4	431.8	391.2	241.3	129.5	71.1	30.5
210	05-Oct-87	12.2	37.59	459.7	421.6	381.0	236.2	127.0	73.7	33.0
240	06-Oct-87	6.1	39.07	475.0	442.0	401.3	251.5	134.6	73.7	35.6
240	07-Oct-87	12.0	35.70	462.3	424.2	386.1	238.8	129.5	71.1	30.5
240	08-Oct-87	13.3	37.11	500.4	464.8	421.6	254.0	137.2	73.7	33.0
220	09-Oct-87	12.7	37.45	467.4	429.3	388.6	254.0	144.8	81.3	38.1
210	10-Oct-87	11.3	36.30	508.0	459.7	408.9	254.0	139.7	78.7	33.0
240	11-Oct-87	13.8	36.78	502.9	464.8	419.1	256.5	137.2	76.2	27.9
220	13-Oct-87	13.1	37.65	487.7	447.0	406.4	276.9	157.5	88.9	43.2
240	14-Oct-87	11.3	37.45	508.0	475.0	431.8	271.8	149.9	83.8	43.2
240	03-Nov-87	12.6	39.81	495.3	457.2	426.7	254.0	134.6	81.3	38.1
240	24-Nov-86	10.0	51.77	2761.0	1343.7	1064.3	271.8	162.6	114.3	66.0

TEST SECTION 2

LOC	DATE	AIR TEMP(C)	LOAD (kN)	D0	D1	D2	D3	D4	D5	D6
				DEFLECTION (microns)						
220	27-Feb-87	18.3	51.55	518.2	447.0	381.0	203.2	106.7	66.0	33.0
230	03-Mar-87	12.8	51.82	558.8	464.8	373.4	177.8	96.5	66.0	35.6
240	12-Jun-87	16.6	53.38	127.0	104.1	88.9	61.0	48.3	38.1	22.9
220	13-Jun-87	25.1	54.79	167.6	137.2	116.8	71.1	61.0	43.2	35.6
230	14-Jun-87	17.9	52.57	287.0	238.8	203.2	111.8	68.6	50.8	27.9
230	15-Jun-87	33.0	49.80	393.7	340.4	289.6	147.3	73.7	50.8	25.4
230	16-Jun-87	32.4	50.20	444.5	391.2	332.7	165.1	78.7	53.3	27.9
230	17-Jun-87	20.2	52.03	505.5	442.0	378.5	190.5	88.9	55.9	22.9
220	18-Jun-87	19.9	51.82	518.2	459.7	393.7	198.1	91.4	55.9	35.6
230	19-Jun-87	21.3	52.30	553.7	492.8	421.6	208.3	94.0	58.4	30.5
220	20-Jun-87	22.9	51.22	617.2	546.1	469.9	228.6	104.1	66.0	27.9
220	21-Jun-87	20.4	51.82	708.7	627.4	548.6	292.1	119.4	66.0	33.0
230	22-Jun-87	19.3	51.62	662.9	584.2	505.5	254.0	114.3	66.0	33.0
220	23-Jun-87	20.7	51.28	711.2	629.9	553.7	287.0	121.9	68.6	38.1
230	24-Jun-87	16.6	50.81	713.7	627.4	543.6	276.9	132.1	73.7	33.0
230	25-Jun-87	35.7	50.14	764.5	670.6	576.6	292.1	132.1	76.2	33.0
220	26-Jun-87	15.2	50.61	767.1	678.2	591.8	304.8	139.7	78.7	40.6
220	27-Jun-87	20.4	50.27	759.5	680.7	596.9	317.5	149.9	81.3	38.1
230	28-Jun-87	21.4	50.34	784.9	703.6	612.1	330.2	165.1	94.0	43.2
220	29-Jun-87	20.2	50.20	787.4	706.1	627.4	348.0	170.2	91.4	45.7
230	30-Jun-87	24.7	49.39	950.0	835.7	718.8	370.8	180.3	99.1	48.3
230	01-Jul-87	24.7	50.00	970.3	850.9	729.0	370.8	180.3	104.1	50.8
240	09-Sep-87	12.7	54.19	96.5	76.2	63.5	45.7	40.6	33.0	22.9
210	11-Sep-87	18.6	51.35	167.6	137.2	114.3	66.0	48.3	38.1	22.9
240	12-Sep-87	17.7	50.95	348.0	304.8	266.7	139.7	66.0	43.2	25.4
210	13-Sep-87	15.7	50.61	403.9	353.1	307.3	157.5	73.7	45.7	20.3
240	14-Sep-87	16.9	50.14	408.9	373.4	325.1	167.6	76.2	43.2	22.9
210	15-Sep-87	11.6	52.03	419.1	381.0	325.1	170.2	76.2	50.8	22.9
210	16-Sep-87	11.1	53.65	436.9	386.1	335.3	172.7	83.8	50.8	27.9
240	17-Sep-87	12.6	52.70	492.8	444.5	391.2	200.7	91.4	53.3	25.4
240	18-Sep-87	12.6	51.35	505.5	454.7	401.3	210.8	96.5	58.4	25.4
210	19-Sep-87	12.4	51.55	480.1	431.8	381.0	188.0	94.0	53.3	33.0
240	20-Sep-87	13.3	51.28	508.0	457.2	403.9	221.0	106.7	58.4	25.4
210	21-Sep-87	13.5	51.42	500.4	452.1	396.2	213.4	99.1	55.9	27.9
240	22-Sep-87	14.6	50.95	602.0	535.9	475.0	254.0	111.8	61.0	33.0
240	23-Sep-87	10.7	53.17	614.7	558.8	497.8	276.9	127.0	66.0	33.0
210	24-Sep-87	12.1	52.63	574.0	515.6	454.7	251.5	119.4	68.6	35.6
210	25-Sep-87	10.0	52.77	563.9	515.6	457.2	264.2	129.5	73.7	38.1
210	26-Sep-87	5.6	56.48	569.0	520.7	472.4	284.5	144.8	83.8	30.5
210	27-Sep-87	4.4	54.12	541.0	500.4	449.6	274.3	144.8	83.8	35.6
220	28-Sep-87	8.3	55.13	543.6	497.8	452.1	279.4	154.9	81.3	30.5
240	29-Sep-87	11.8	52.03	614.7	566.4	505.5	292.1	142.2	76.2	38.1
240	30-Sep-87	15.7	51.35	693.4	629.9	558.8	309.9	147.3	78.7	38.1
240	01-Oct-87	12.4	50.95	706.1	642.6	574.0	322.6	144.8	83.8	38.1
240	02-Oct-87	15.6	50.95	708.7	642.6	574.0	325.1	144.8	83.8	30.5
240	03-Oct-87	12.8	50.54	711.2	652.8	574.0	304.8	154.9	78.7	33.0
240	04-Oct-87	6.8	54.73	675.6	624.8	571.5	353.1	182.9	106.7	45.7
240	05-Oct-87	13.1	51.42	688.3	637.5	579.1	355.6	190.5	104.1	48.3
240	06-Oct-87	6.1	55.13	690.9	642.6	586.7	368.3	200.7	109.2	58.4
230	07-Oct-87	12.0	49.06	762.0	678.2	594.4	330.2	180.3	99.1	63.5
220	08-Oct-87	13.3	51.49	662.9	607.1	553.7	350.5	205.7	111.8	48.3
210	09-Oct-87	12.7	51.96	693.4	637.5	574.0	358.1	203.2	116.8	58.4
240	10-Oct-87	11.3	50.88	795.0	739.1	665.5	381.0	205.7	111.8	58.4
240	11-Oct-87	13.8	51.01	726.4	673.1	609.6	368.3	198.1	109.2	38.1
240	13-Oct-87	13.1	51.69	736.6	685.8	622.3	388.6	213.4	119.4	66.0
220	14-Oct-87	11.3	51.96	678.2	624.8	574.0	378.5	226.1	127.0	48.3
240	03-Nov-87	12.6	53.31	706.1	650.2	640.1	363.2	193.0	111.8	50.8

TEST SECTION 3

LOC	DATE	AIR TEMP(C)	LOAD (kN)	DEFLECTIONS (microns) D0	D1	D2	D3	D4	D5	D6
340	24-Nov-86	10.0	37.05	1590.0	772.2	320.0	142.2	66.0	50.8	33.0
320	27-Feb-87	18.3	36.44	868.7	645.2	429.3	137.2	71.1	48.3	27.9
340	03-Mar-87	12.8	38.26	828.0	614.7	406.4	129.5	71.1	50.8	30.5
340	12-Jun-87	16.6	38.73	170.2	104.1	50.8	25.4	22.9	20.3	15.2
340	13-Jun-87	22.2	38.26	241.3	154.9	88.9	25.4	27.9	25.4	15.2
310	14-Jun-87	20.4	39.81	375.9	243.8	132.1	38.1	33.0	27.9	17.8
340	15-Jun-87	33.0	36.64	393.7	266.7	160.0	33.0	27.9	22.9	15.2
320	16-Jun-87	32.4	35.83	571.5	416.6	261.6	50.8	33.0	33.0	17.8
320	17-Jun-87	19.0	36.10	769.6	566.4	370.8	83.8	38.1	38.1	22.9
310	18-Jun-87	19.9	36.84	800.1	581.7	381.0	109.2	50.8	40.6	25.4
330	19-Jun-87	21.3	37.45	726.4	556.3	386.1	109.2	48.3	40.6	25.4
330	20-Jun-87	25.6	36.37	726.4	558.8	396.2	114.3	55.9	45.7	27.9
330	21-Jun-87	22.4	36.84	729.0	561.3	408.9	121.9	61.0	45.7	25.4
310	22-Jun-87	21.3	36.30	845.8	652.8	439.4	137.2	68.6	48.3	30.5
310	23-Jun-87	20.7	36.37	896.6	690.9	467.4	154.9	76.2	53.3	33.0
330	24-Jun-87	16.6	36.64	828.0	645.2	467.4	160.0	76.2	53.3	38.1
310	25-Jun-87	17.8	36.30	924.6	731.5	487.7	170.2	94.0	58.4	38.1
310	26-Jun-87	15.2	36.10	914.4	723.9	500.4	182.9	94.0	66.0	40.6
310	27-Jun-87	20.4	35.70	894.1	716.3	500.4	185.4	99.1	63.5	40.6
310	28-Jun-87	20.1	35.97	942.3	754.4	530.9	205.7	109.2	71.1	40.6
330	29-Jun-87	18.8	36.10	891.5	711.2	535.9	210.8	104.1	71.1	33.0
320	30-Jun-87	24.7	35.76	1099.8	911.9	645.2	210.8	101.6	63.5	33.0
330	01-Jul-87	24.7	35.09	965.2	767.1	563.9	233.7	124.5	78.7	50.8
340	09-Sep-87	7.5	37.79	71.1	55.9	33.0	22.9	22.9	17.8	15.2
340	11-Sep-87	19.0	37.72	312.4	210.8	111.8	22.9	22.9	17.8	12.7
340	12-Sep-87	17.7	37.11	411.5	297.2	167.6	22.9	22.9	20.3	22.9
340	13-Sep-87	15.2	37.59	436.9	322.6	198.1	22.9	25.4	20.3	15.2
340	14-Sep-87	16.9	34.95	546.1	434.3	287.0	48.3	27.9	27.9	17.8
340	15-Sep-87	10.4	38.33	701.0	553.7	381.0	76.2	33.0	33.0	17.8
340	16-Sep-87	11.0	36.84	706.1	571.5	396.2	83.8	33.0	40.6	22.9
340	17-Sep-87	12.6	37.32	782.3	632.5	431.8	91.4	38.1	38.1	20.3
340	18-Sep-87	12.6	36.71	787.4	637.5	442.0	94.0	40.6	35.6	22.9
340	19-Sep-87	11.7	37.52	850.9	690.9	485.1	106.7	40.6	38.1	22.9
340	20-Sep-87	13.3	36.03	861.1	703.6	492.8	111.8	50.8	43.2	33.0
310	21-Sep-87	13.5	36.64	690.9	556.3	411.5	127.0	50.8	43.2	35.6
310	22-Sep-87	14.0	37.11	744.2	612.1	457.2	144.8	63.5	45.7	33.0
340	23-Sep-87	10.7	37.05	1033.8	856.0	617.2	165.1	55.9	43.2	25.4
330	24-Sep-87	12.4	36.44	924.6	739.1	525.8	167.6	73.7	50.8	30.5
330	25-Sep-87	10.0	37.72	977.9	795.0	579.1	198.1	86.4	55.9	27.9
340	26-Sep-87	5.6	38.94	1049.0	873.8	650.2	193.0	71.1	55.9	33.0
330	27-Sep-87	4.4	38.40	993.1	830.6	612.1	210.8	96.5	63.5	35.6
340	28-Sep-87	8.3	36.78	1008.4	853.4	635.0	193.0	76.2	53.3	43.2
340	29-Sep-87	11.8	35.97	988.1	825.5	602.0	182.9	76.2	50.8	33.0
310	30-Sep-87	15.7	36.44	835.7	675.6	515.6	198.1	88.9	61.0	43.2
340	01-Oct-87	12.4	35.97	1026.2	868.7	629.9	198.1	83.8	58.4	33.0
340	02-Oct-87	15.6	36.84	1046.5	891.5	655.3	208.3	88.9	55.9	33.0
320	03-Oct-87	12.8	36.98	889.0	731.5	558.8	205.7	94.0	58.4	38.1
330	04-Oct-87	6.8	38.19	1033.8	833.1	622.3	248.9	124.5	78.7	50.8
330	05-Oct-87	13.1	35.76	988.1	835.7	627.4	246.4	137.2	78.7	50.8
340	06-Oct-87	6.1	37.99	1097.3	927.1	708.7	259.1	119.4	76.2	48.3
310	07-Oct-87	12.0	35.76	883.9	731.5	579.1	243.8	119.4	76.2	48.3
330	08-Oct-87	13.3	36.10	1021.1	863.6	647.7	256.5	137.2	83.8	45.7
340	09-Oct-87	12.7	35.70	1051.6	894.1	678.2	256.5	121.9	73.7	50.8
310	10-Oct-87	11.3	35.90	916.9	759.5	596.9	264.2	132.1	83.8	50.8
340	11-Oct-87	13.8	36.10	1010.9	866.1	657.9	251.5	121.9	73.7	48.3
340	13-Oct-87	13.1	35.97	1023.6	873.8	662.9	259.1	127.0	78.7	48.3
330	14-Oct-87	11.3	36.71	1005.8	863.6	655.3	276.9	147.3	91.4	45.7
320	03-Nov-87	12.6	39.21	896.6	756.9	586.7	246.4	127.0	81.3	43.2
340	24-Nov-86	10.0	49.19	2062.5	1168.4	457.2	188.0	83.8	71.1	121.9

TEST SECTION 3

LOC	DATE	AIR TEMP(C)	LOAD (kN)	D0	D1	D2	D3	D4	D5	D6
				DEFLECTIONS (microns)						
320	27-Feb-87	18.3	50.95	1214.1	909.3	624.8	200.7	99.1	68.6	35.6
340	03-Mar-87	12.8	52.63	1127.8	850.9	576.6	190.5	106.7	73.7	43.2
340	12-Jun-87	16.6	53.44	221.0	132.1	68.6	35.6	33.0	27.9	17.8
340	13-Jun-87	22.2	52.84	312.4	203.2	116.8	38.1	38.1	33.0	20.3
340	14-Jun-87	17.9	53.65	408.9	279.4	160.0	50.8	40.6	33.0	22.9
340	15-Jun-87	33.0	51.55	515.6	342.9	203.2	43.2	38.1	30.5	27.9
320	16-Jun-87	32.4	50.20	718.8	502.9	315.0	55.9	40.6	43.2	25.4
330	17-Jun-87	20.2	51.89	889.0	668.0	462.3	121.9	61.0	48.3	33.0
340	18-Jun-87	21.4	52.90	985.5	746.8	525.8	142.2	58.4	48.3	27.9
330	19-Jun-87	21.3	51.96	1021.1	779.8	546.1	154.9	68.6	55.9	33.0
320	20-Jun-87	22.9	51.42	1259.8	955.0	640.1	162.6	68.6	55.9	33.0
340	21-Jun-87	22.4	51.69	1110.0	848.4	602.0	172.7	71.1	58.4	35.6
330	22-Jun-87	19.3	51.15	1089.7	845.8	614.7	198.1	91.4	68.6	43.2
310	23-Jun-87	20.7	50.47	1275.1	990.6	680.7	231.1	111.8	76.2	43.2
330	24-Jun-87	16.6	50.41	1183.6	924.6	680.7	236.2	111.8	76.2	48.3
330	25-Jun-87	35.7	49.26	1183.6	937.3	690.9	246.4	119.4	78.7	50.8
330	26-Jun-87	17.2	49.39	1198.9	947.4	708.7	264.2	134.6	88.9	50.8
310	27-Jun-87	20.4	49.33	1285.2	1036.3	731.5	276.9	144.8	94.0	48.3
310	28-Jun-87	20.1	49.80	1343.7	1082.0	777.2	307.3	162.6	101.6	55.9
310	29-Jun-87	20.2	49.12	1353.8	1112.5	795.0	309.9	165.1	101.6	50.8
310	30-Jun-87	24.7	49.12	1427.5	1148.1	802.6	309.9	172.7	104.1	63.5
310	01-Jul-87	23.2	48.58	1432.6	1160.8	815.3	337.8	182.9	111.8	66.0
320	09-Sep-87	7.5	52.50	71.1	45.7	27.9	20.3	17.8	15.2	10.2
320	11-Sep-87	18.6	50.68	304.8	226.1	127.0	27.9	27.9	25.4	17.8
340	12-Sep-87	17.7	51.35	502.9	365.8	205.7	25.4	33.0	27.9	22.9
320	13-Sep-87	15.7	51.28	485.1	342.9	218.4	40.6	30.5	27.9	17.8
340	14-Sep-87	16.9	49.93	678.2	546.1	363.2	58.4	33.0	38.1	17.8
310	15-Sep-87	11.6	52.36	795.0	607.1	436.9	106.7	40.6	38.1	25.4
320	16-Sep-87	11.1	54.46	835.7	660.4	477.5	127.0	45.7	43.2	27.9
340	17-Sep-87	12.6	52.36	1084.6	858.5	594.4	124.5	40.6	48.3	27.9
330	18-Sep-87	12.6	51.22	1077.0	838.2	576.6	157.5	63.5	55.9	33.0
340	19-Sep-87	11.7	52.03	1170.9	950.0	673.1	149.9	50.8	50.8	27.9
340	20-Sep-87	13.3	50.81	1186.2	970.3	688.3	162.6	55.9	58.4	27.9
320	21-Sep-87	13.5	51.76	983.0	792.5	591.8	175.3	58.4	48.3	35.6
310	22-Sep-87	14.0	51.42	1069.3	876.3	657.9	215.9	86.4	66.0	35.6
310	23-Sep-87	11.4	51.62	1112.5	889.0	678.2	233.7	99.1	71.1	43.2
330	24-Sep-87	12.4	50.41	1305.6	1066.8	772.2	259.1	109.2	73.7	43.2
330	25-Sep-87	10.0	53.44	1399.5	1145.5	848.4	302.3	129.5	86.4	48.3
330	26-Sep-87	5.6	53.51	1424.9	1231.9	856.0	299.7	132.1	86.4	45.7
330	27-Sep-87	4.4	54.12	1427.5	1198.9	889.0	325.1	142.2	91.4	50.8
340	28-Sep-87	8.3	51.35	1412.2	1201.4	901.7	284.5	104.1	73.7	45.7
340	29-Sep-87	11.8	50.41	1402.1	1176.0	871.2	269.2	101.6	71.1	40.6
340	30-Sep-87	15.7	49.87	1419.9	1209.0	899.2	292.1	109.2	73.7	48.3
340	01-Oct-87	12.4	49.66	1455.4	1231.9	911.9	297.2	124.5	78.7	40.6
340	02-Oct-87	15.6	49.73	1483.4	1264.9	944.9	309.9	129.5	81.3	48.3
320	03-Oct-87	12.8	50.74	1272.5	1056.6	812.8	309.9	139.7	83.8	43.2
330	04-Oct-87	6.8	52.36	1452.9	1198.9	904.2	373.4	182.9	111.8	55.9
340	05-Oct-87	13.1	49.80	1511.3	1303.0	988.1	358.1	167.6	99.1	66.0
340	06-Oct-87	6.1	51.96	1539.2	1320.8	1018.5	381.0	175.3	104.1	66.0
340	07-Oct-87	12.0	48.65	1463.0	1252.2	952.5	350.5	162.6	94.0	61.0
330	08-Oct-87	13.3	50.47	1435.1	1224.3	927.1	386.1	195.6	119.4	76.2
340	09-Oct-87	12.7	49.53	1491.0	1277.6	977.9	373.4	180.3	109.2	61.0
330	10-Oct-87	11.3	49.60	1402.1	1196.3	916.9	383.5	205.7	121.9	71.1
330	11-Oct-87	13.8	49.66	1379.2	1168.4	896.6	375.9	200.7	121.9	73.7
330	13-Oct-87	13.1	50.14	1366.5	1148.1	883.9	381.0	203.2	121.9	76.2
330	14-Oct-87	11.3	51.55	1432.6	1231.9	944.9	406.4	215.9	127.0	68.6
330	03-Nov-87	12.6	51.89	1318.3	1115.1	833.1	345.4	182.9	116.8	66.0

TEST SECTION 4

LOC	DATE	AIR TEMP(C)	LOAD (kN)	DEFLECTIONS (microns) D0	D1	D2	D3	D4	D5	D6
430	24-Nov-86	10.0	35.53	1861.8	746.8	391.2	121.9	68.6	48.3	35.6
410	27-Feb-87	18.3	36.37	1165.9	840.7	502.9	147.3	76.2	53.3	33.0
430	03-Mar-87	12.8	38.53	896.6	701.0	490.2	154.9	78.7	53.3	33.0
420	12-Jun-87	16.6	42.04	226.1	162.6	88.9	38.1	27.9	22.9	17.8
440	13-Jun-87	22.2	39.27	335.3	236.2	134.6	43.2	30.5	33.0	20.3
440	14-Jun-87	17.9	41.09	462.3	332.7	193.0	43.2	33.0	27.9	15.2
440	15-Jun-87	33.0	36.17	535.9	381.0	226.1	45.7	38.1	30.5	17.8
410	16-Jun-87	32.4	36.03	589.3	436.9	271.8	43.2	33.0	30.5	17.8
410	17-Jun-87	19.0	36.44	795.0	622.3	419.1	91.4	33.0	33.0	20.3
410	18-Jun-87	19.9	36.98	823.0	642.6	439.4	104.1	43.2	35.6	22.9
410	19-Jun-87	21.3	36.84	873.8	696.0	472.4	109.2	38.1	35.6	22.9
430	20-Jun-87	25.6	37.45	1046.5	782.3	508.0	127.0	48.3	38.1	22.9
430	21-Jun-87	22.4	36.71	1054.1	800.1	525.8	137.2	55.9	43.2	25.4
440	22-Jun-87	19.3	36.24	1176.0	957.6	683.3	177.8	73.7	53.3	35.6
440	23-Jun-87	21.1	35.70	1176.0	977.9	698.5	188.0	76.2	53.3	40.6
440	24-Jun-87	16.6	36.03	1237.0	1016.0	736.6	208.3	88.9	58.4	38.1
440	25-Jun-87	20.7	35.43	1254.8	1023.6	734.1	210.8	81.3	58.4	45.7
410	26-Jun-87	15.2	36.17	1077.0	899.2	655.3	200.7	81.3	53.3	33.0
440	27-Jun-87	17.6	35.56	1348.7	1140.5	845.8	264.2	99.1	71.1	50.8
440	28-Jun-87	21.4	35.29	1323.3	1120.1	828.0	261.6	104.1	66.0	53.3
440	29-Jun-87	18.8	36.37	1361.4	1160.8	861.1	276.9	116.8	71.1	45.7
410	30-Jun-87	24.7	35.56	1145.5	944.9	690.9	233.7	106.7	63.5	40.6
410	01-Jul-87	23.2	34.68	1140.5	985.5	716.3	246.4	114.3	66.0	40.6
430	09-Sep-87	7.5	37.99	114.3	119.4	76.2	43.2	38.1	30.5	22.9
430	11-Sep-87	19.0	37.59	312.4	241.3	147.3	27.9	22.9	22.9	15.2
430	12-Sep-87	17.7	37.05	406.4	309.9	195.6	33.0	22.9	22.9	15.2
430	13-Sep-87	15.2	38.73	447.0	358.1	238.8	35.6	25.4	30.5	15.2
430	14-Sep-87	16.9	35.63	541.0	414.0	274.3	45.7	22.9	25.4	17.8
410	15-Sep-87	11.6	36.37	754.4	596.9	401.3	88.9	30.5	35.6	22.9
430	16-Sep-87	11.0	37.18	772.2	612.1	439.4	99.1	33.0	33.0	22.9
410	17-Sep-87	14.2	36.44	825.5	645.2	431.8	101.6	33.0	30.5	17.8
420	18-Sep-87	12.5	37.65	1077.0	901.7	670.6	175.3	50.8	43.2	33.0
410	19-Sep-87	12.4	36.91	906.8	718.8	490.2	119.4	38.1	35.6	22.9
430	20-Sep-87	13.3	36.03	840.7	690.9	505.5	132.1	48.3	33.0	33.0
410	21-Sep-87	13.5	36.44	944.9	769.6	530.9	132.1	48.3	40.6	27.9
420	22-Sep-87	14.0	35.56	1231.9	1046.5	769.6	223.5	73.7	48.3	25.4
420	23-Sep-87	11.4	36.64	1249.7	1071.9	792.5	236.2	83.8	50.8	43.2
430	24-Sep-87	12.4	36.10	990.6	833.1	619.8	182.9	61.0	40.6	30.5
420	25-Sep-87	10.0	38.19	1297.9	1125.2	863.6	284.5	99.1	61.0	33.0
430	26-Sep-87	5.6	38.53	1046.5	906.8	701.0	231.1	81.3	53.3	35.6
430	27-Sep-87	4.4	40.08	1079.5	927.1	721.4	248.9	88.9	53.3	55.9
440	28-Sep-87	8.3	41.43	1300.5	1117.6	899.2	355.6	139.7	71.1	50.8
430	29-Sep-87	11.8	35.90	1038.9	886.5	673.1	228.6	86.4	50.8	33.0
430	30-Sep-87	15.7	35.63	1071.9	916.9	690.9	231.1	88.9	50.8	43.2
430	01-Oct-87	12.4	35.90	1102.4	937.3	706.1	246.4	96.5	55.9	38.1
430	02-Oct-87	15.6	36.17	1115.1	965.2	739.1	259.1	106.7	58.4	27.9
430	03-Oct-87	12.8	35.70	1127.8	960.1	734.1	264.2	109.2	58.4	38.1
430	04-Oct-87	6.8	39.00	1150.6	993.1	782.3	297.2	127.0	66.0	43.2
440	05-Oct-87	13.1	38.67	1341.1	1165.9	927.1	383.5	165.1	88.9	45.7
430	06-Oct-87	6.1	37.59	1158.2	1008.4	800.1	315.0	137.2	73.7	48.3
430	07-Oct-87	12.0	35.16	1084.6	947.4	741.7	289.6	127.0	68.6	66.0
430	08-Oct-87	13.3	36.03	1153.2	995.7	784.9	315.0	139.7	76.2	55.9
440	09-Oct-87	12.7	37.25	1303.0	1122.7	886.5	358.1	160.0	91.4	66.0
430	10-Oct-87	11.3	35.56	1143.0	993.1	774.7	299.7	139.7	76.2	48.3
440	11-Oct-87	13.8	39.41	1287.8	1120.1	883.9	358.1	160.0	94.0	63.5
440	13-Oct-87	13.1	40.29	1287.8	1120.1	886.5	360.7	167.6	94.0	68.6
440	14-Oct-87	11.3	41.36	1356.4	1168.4	909.3	363.2	160.0	99.1	76.2
440	03-Nov-87	12.6	42.71	1214.1	1059.2	815.3	325.1	142.2	91.4	58.4

TEST SECTION 4

LOC	DATE	AIR TEMP(C)	LOAD (kN)	D0	D1	D2	D3	D4	D5	D6
				DEFLECTIONS (microns)						
410	24-Nov-86	10.0	47.52	2865.1	1010.9	492.8	193.0	81.3	61.0	45.7
410	27-Feb-87	18.3	50.88	1572.3	1168.4	746.8	221.0	114.3	76.2	43.2
430	03-Mar-87	12.8	52.84	1249.7	980.4	690.9	223.5	109.2	73.7	48.3
440	12-Jun-87	16.6	58.23	231.1	205.7	132.1	55.9	43.2	38.1	22.9
430	13-Jun-87	22.2	52.97	393.7	228.6	111.8	40.6	38.1	33.0	22.9
440	14-Jun-87	17.9	53.85	581.7	414.0	238.8	55.9	45.7	38.1	27.9
440	15-Jun-87	33.0	51.42	693.4	485.1	287.0	61.0	48.3	40.6	22.9
410	16-Jun-87	32.4	50.41	734.1	530.9	330.2	53.3	40.6	38.1	22.9
440	17-Jun-87	20.2	52.43	1219.2	950.0	650.2	144.8	58.4	55.9	38.1
440	18-Jun-87	21.4	52.36	1348.7	1071.9	751.8	177.8	68.6	58.4	40.6
440	19-Jun-87	21.3	51.62	1529.1	1247.1	868.7	208.3	76.2	61.0	43.2
430	20-Jun-87	25.6	51.55	1430.0	1082.0	708.7	177.8	61.0	50.8	30.5
430	21-Jun-87	22.4	50.81	1473.2	1127.8	756.9	193.0	71.1	61.0	33.0
440	22-Jun-87	19.3	49.60	1686.6	1374.1	988.1	259.1	94.0	71.1	45.7
440	23-Jun-87	21.1	49.06	1714.5	1424.9	1033.8	284.5	109.2	76.2	50.8
440	24-Jun-87	16.6	49.06	1790.7	1480.8	1089.7	315.0	121.9	83.8	50.8
440	25-Jun-87	20.7	48.79	1831.3	1501.1	1099.8	325.1	127.0	83.8	50.8
440	26-Jun-87	17.2	48.45	1861.8	1534.2	1127.8	340.4	139.7	94.0	55.9
440	27-Jun-87	17.6	47.98	1930.4	1643.4	1239.5	381.0	132.1	91.4	61.0
440	28-Jun-87	21.4	47.78	1899.9	1620.5	1211.6	386.1	152.4	94.0	63.5
440	29-Jun-87	18.8	47.91	1968.5	1691.6	1277.6	416.6	175.3	104.1	66.0
410	30-Jun-87	24.7	48.92	1645.9	1374.1	1016.0	348.0	157.5	88.9	55.9
410	01-Jul-87	23.2	48.11	1651.0	1417.3	1054.1	368.3	167.6	94.0	55.9
430	09-Sep-87	12.7	53.78	157.5	127.0	63.5	33.0	30.5	22.9	17.8
430	11-Sep-87	19.0	52.23	391.2	302.3	182.9	38.1	27.9	27.9	17.8
430	12-Sep-87	17.7	51.89	508.0	386.1	241.3	40.6	30.5	33.0	22.9
430	13-Sep-87	15.2	52.63	558.8	444.5	287.0	45.7	30.5	33.0	15.2
430	14-Sep-87	16.9	49.80	688.3	528.3	353.1	58.4	27.9	35.6	25.4
410	15-Sep-87	11.6	52.36	965.2	769.6	510.5	106.7	35.6	43.2	33.0
430	16-Sep-87	11.0	53.04	1005.8	812.8	579.1	127.0	35.6	43.2	33.0
410	17-Sep-87	14.2	51.62	1135.4	906.8	609.6	139.7	38.1	40.6	25.4
420	18-Sep-87	12.5	51.62	1539.2	1303.0	977.9	254.0	58.4	50.8	43.2
410	19-Sep-87	12.4	51.35	1264.9	1010.9	693.4	170.2	45.7	45.7	27.9
430	20-Sep-87	13.3	50.61	1206.5	993.1	726.4	190.5	48.3	43.2	48.3
420	21-Sep-87	13.5	49.33	1681.5	1412.2	1082.0	299.7	96.5	71.1	43.2
430	22-Sep-87	[illegible]	[illegible]	[illegible]	[illegible]	810.3	221.0	63.5	48.3	35.6
420	23-Sep-87	11.4	48.92	1816.1	1562.1	1173.5	363.2	116.8	76.2	58.4
430	24-Sep-87	12.4	50.20	1430.0	1209.0	906.8	276.9	83.8	53.3	40.6
430	25-Sep-87	10.0	53.44	1536.7	1300.5	1016.0	340.4	104.1	68.6	55.9
430	26-Sep-87	5.6	52.57	1491.0	1310.6	1023.6	358.1	121.9	71.1	48.3
430	27-Sep-87	4.4	53.58	1529.1	1325.9	1023.6	373.4	129.5	76.2	68.6
430	28-Sep-87	8.3	51.15	1491.0	1282.7	1000.8	353.1	124.5	71.1	48.3
430	29-Sep-87	11.8	50.14	1501.1	1292.9	990.6	342.9	121.9	68.6	50.8
430	30-Sep-87	15.7	49.46	1562.1	1336.0	1028.7	358.1	132.1	81.3	50.8
430	01-Oct-87	12.4	49.87	1569.7	1353.8	1038.9	373.4	139.7	76.2	50.8
430	02-Oct-87	15.6	48.85	1607.8	1394.5	1082.0	391.2	154.9	83.8	48.3
430	03-Oct-87	12.8	49.33	1602.7	1384.3	1069.3	401.3	157.5	83.8	63.5
430	04-Oct-87	6.8	52.30	1630.7	1450.3	1135.4	447.0	185.4	96.5	58.4
430	05-Oct-87	13.1	49.53	1612.9	1407.2	1115.1	439.4	182.9	96.5	53.3
430	06-Oct-87	6.1	51.96	1635.8	1432.6	1155.7	467.4	203.2	106.7	66.0
430	07-Oct-87	12.0	48.58	1559.6	1366.5	1074.4	426.7	185.4	94.0	76.2
420	08-Oct-87	13.3	49.06	1953.3	1737.4	1384.3	523.2	233.7	129.5	73.7
430	09-Oct-87	12.7	49.53	1587.5	1404.6	1082.0	449.6	203.2	109.2	66.0
430	10-Oct-87	11.3	49.06	1625.6	1414.8	1110.0	439.4	198.1	106.7	71.1
430	11-Oct-87	13.8	49.46	1572.3	1391.9	1094.7	442.0	200.7	109.2	68.6
440	13-Oct-87	13.1	53.44	1846.6	1612.9	1287.8	533.4	233.7	132.1	83.8
440	14-Oct-87	11.3	54.46	1922.8	1666.2	1313.2	541.0	236.2	137.2	99.1
440	03-Nov-87	12.6	54.79	1737.4	1526.5	1186.2	477.5	208.3	129.5	[illegible]

REPORT DOCUMENTATION PAGE

Form Approved
OMB No. 0704-0188

1. AGENCY USE ONLY (Leave blank)

2. REPORT DATE
November 1990

3. REPORT TYPE AND DATES COVERED

4. TITLE AND SUBTITLE
Predicting the Behavior of Asphalt Concrete Pavements in Seasonal Frost Areas Using Nondestructive Techniques

5. FUNDING NUMBERS
PR: 4A762784AT42
WU: BS/006

6. AUTHORS
Vincent C. Janoo and Richard L. Berg

7. PERFORMING ORGANIZATION NAME(S) AND ADDRESS(ES)
U.S. Army Cold Regions Research and Engineering Laboratory
72 Lyme Road
Hanover, New Hampshire 03755-1290

8. PERFORMING ORGANIZATION REPORT NUMBER
CRREL Report 90-10

9. SPONSORING/MONITORING AGENCY NAME(S) AND ADDRESS(ES)
U.S. Army
Office of the Chief of Engineers
Washington, D.C. 20314-1000

U.S. Department of Transportation
Federal Aviation Administration
Research and Development Service
Washington, D.C. 20591

10. SPONSORING/MONITORING AGENCY REPORT NUMBER
DOT/FAA/RD-90/33

11. SUPPLEMENTARY NOTES

12a. DISTRIBUTION/AVAILABILITY STATEMENT
Approved for public release; distribution is unlimited.

Available from NTIS, Springfield, Virginia 22161.

12b. DISTRIBUTION CODE

13. ABSTRACT (*Maximum 200 words*)

Four different pavement test sections were subjected to freeze–thaw cycling in CRREL's Frost Effects Research Facility (FERF). The test sections, each 610 cm in length, consisted of 1) 15.2 cm of asphalt concrete pavement over a clay subgrade, 2) 15.2 cm of asphalt concrete over 10.2 cm of crushed gravel over a clay subgrade, 3) 5.1 cm of asphalt concrete over 17.8 cm of crushed gravel over 20.3 cm of clean sand over a clay subgrade and 4) 5.1 cm of asphalt concrete over 25.4 cm of crushed gravel over 12.7 cm of clean sand over a clay subgrade. Thermocouples were imbedded throughout the pavement structure and subgrade. During the thawing periods, deflection measurements were made at four locations in each test section using a Dynatest Falling Weight Deflectometer (FWD). The results of the deflection measurements are presented here. An analysis was done to quantify the subgrade strength based solely on FWD measurements. It was also shown that a relationship existed between thaw depth and FWD measurement in the subgrade.

14. SUBJECT TERMS
Airfields, Laboratory tests, Roads, Frost heave, Pavement, Cold tolerance

15. NUMBER OF PAGES
64

16. PRICE CODE

17. SECURITY CLASSIFICATION OF REPORT	18. SECURITY CLASSIFICATION OF THIS PAGE	19. SECURITY CLASSIFICATION OF ABSTRACT	20. LIMITATION OF ABSTRACT
UNCLASSIFIED	UNCLASSIFIED	UNCLASSIFIED	UL

NSN 7540-01-280-5500

Standard Form 298 (Rev. 2-89)
Prescribed by ANSI Std. Z39-18
298-102

☆ U. S. GOVERNMENT PRINTING OFFICE: 1990--500-063--22053